Analysis of Tramadol and its Metabolites in Rat Skeletal Tissues following Acute and Repeated Dose Patterns using High Performance Liquid Chromatography Tandem Mass Spectrometry

By

Christian L. Buckingham

A thesis submitted in partial fulfillment

of the requirements for the degree of

Master of Science (MSc) in Chemical Sciences

The Faculty of Graduate Studies

Laurentian University

Sudbury, Ontario, Canada

P3E 2C6

THESIS DEFENCE COMMITTEE/COMITÉ DE SOUTENANCE DE THÈSE
Laurentian Université/Université Laurentienne
Faculty of Graduate Studies/Faculté des études supérieures

Title of Thesis Titre de la thèse	Analysis of Tramadol and its Metabolites in Rat Skeletal Tissues following Acute and Repeated Dose Patterns using High Performance Liquid Chromatography Tandem Mass Spectrometry
Name of Candidate Nom du candidat	Buckingham, Christian
Degree Diplôme	Master of Science
Department/Program Département/Programme	Chemical Sciences
Date of Defence Date de la soutenance	October 15, 2020

APPROVED/APPROUVÉ

Thesis Examiners/Examinateurs de thèse:

Dr. James Watterson
(Supervisor/Directeur(trice) de thèse)

Dr. Gustavo Arteca
(Committee member/Membre du comité)

Dr. Joy Gray-Munro
(Committee member/Membre du comité)

Dr. Theresa Stotesbury
(External Examiner/Examinateur externe)

Approved for the Faculty of Graduate Studies
Approuvé pour la Faculté des études supérieures
Dr. Serge Demers
Monsieur Serge Demers
Acting Dean, Faculty of Graduate Studies
Doyen Intérimaire, Faculté des études supérieures

ACCESSIBILITY CLAUSE AND PERMISSION TO USE

Abstract

The use of skeletal elements for the viable analysis of drugs of abuse has seen increased prevalence in the past 10 years. Advancements in the analytical methods used, including solid phase extraction and mass spectrometry, have allowed for increased sensitivity and selectivity. Previous studies have focused on the influence of dose-death interval, microclimate, differential patterns of exposure, and the influence of body position. In this work, the opioid analgesic tramadol was investigated for its pharmacological behaviour when administered as part of three dosage patterns to male Sprague Dawley rats. The three exposure patterns consisted of an acute low (n = 4, 1 doses, 30 mg/kg) group, a repeated high survived group (n = 5, 3 doses, 30 mg/kg) and a repeated high overdosed group (n = 11, 3 doses, 30 mg/kg). Drug free rats (n = 4) served as negative controls. Following euthanasia by CO_2 asphyxiation, animals were decomposed to skeleton outdoors over the summer of 2019 in Sudbury, Ontario. Bones were sorted by animal and skeletal element (skull, vertebrae, ribs, pelvis, femur, tibia/fibula), then washed and ground to powder before undergoing dynamic methanolic extraction. Semi-quantitative analysis of tramadol and four of its metabolites – O-desmethyltramadol, N-desmethyltramadol, N,O-didesmethyltramadol and tramadol N-oxide – was conducted using high-performance liquid chromatography coupled with tandem mass spectrometry (HPLC-MS/MS) in positive ion mode. Analyte levels were expressed as a mass-normalized response ratio (RR/m) in order to account for the exact mass of bone used. Method validation for the analysis of tramadol and its metabolites was investigated in accordance with the Scientific Working Group of Toxicologists (SWGTOX) standards of practice, with all criteria except for dilution integrity successfully met at a limit of detection and limit of quantitation of 1 ng/mL. The effect of exposure pattern on analyte level and analyte level ratio was assessed using the Kruskal-Wallis test for significant differences ($P < 0.05$).

A total of 315 pairwise comparisons were performed to assess significant differences, with the ratio of tramadol to N-desmethyltramadol determined to be the metric most commonly able to identify these differences in 91% of tests. Additionally, the effect of skeletal element on analyte level and analyte level ratio was also assessed, with a total of 675 pairwise comparisons. Skeletal element was determined to be a significant factor in all cases. This data suggests that both skeletal element and dose pattern are important measures to evaluate with respect to the analysis of drugs of abuse in bone tissues. Furthermore, different metrics, including analyte level and analyte level ratios, may be useful for discriminating between these different dosing patterns.

KEY WORDS: Tramadol, tandem mass spectrometry, skeletal tissues, forensic toxicology

Acknowledgements

First and foremost, I would like to thank my supervisor Dr. James Watterson for his support over the last two years. It was Dr. Watterson who inspired me to study forensic toxicology midway through my undergraduate degree, and I have never regretted it since. This work would not be possible without his patience, guidance, and knowledge. Furthermore, James's ability to make his students laugh in even the most trying of times is a testament to his ability as a mentor, professor and scientist.

I would also like to thank the members of my supervisory committee, Drs. Joy Gray-Munro and Gustavo Arteca. Their constructive feedback through this process has proven invaluable to the successful completion of this project.

I would also like to thank the Natural Sciences and Engineering Research Council of Canada for their financial support.

I wish to also extend my heartfelt thanks to my colleagues in Dr. Watterson's lab. Kirk Unger, Joshua Cassidy, Lauren Somers, Eric Robidas, Camilla Figueroa and Sam Cooper have all been a joy to work with and I wish them all the best going forward. Particular thanks go to Heather Dufour, whose experience and technical expertise has benefitted me in indescribable ways.

Lastly, I wish to thank my friends and family, without whom I would not be here. For brevity's sake I will not mention you all by name, but there truly are no words that can adequately describe how much you all mean to me.

And to Joshua, *amor aeternus.*

Table of Contents

List of Tables

List of Figures

Acronyms and Abbreviation

ACN – acetonitrile
ACU L – acute low
APCI – atmospheric pressure ionization
BTE – bone tissue matrix
CI – chemical ionization
CID – collision induced dissociation
CV – coefficient of variation
DDI – dose-death interval
EI – electron impact
ESI – electrospray ionization
ELISA – enzyme-linked immunosorbent assay
FA – formic acid
FEM – femora
FID – flame ionization detector
FPIA – fluorescence polarization immunoassay
GC – gas chromatography
HRMS – high-resolution mass spectrometry
IS – internal standard
KW – Kruskal-Wallis
LC – liquid chromatography
LLE – liquid-liquid extraction
LOD – limit of detection
LOQ – limit of quantitation
MeOH – methanol
MPA – mobile phase A
MPB – mobile phase B
MRM – multiple reaction monitoring
MS – mass spectrometry
MS/MS – tandem mass spectrometry
m/z – mass to charge ratio
NDMT – N-desmethyltramadol
NODMT – N,O-didesmethyltramadol
NPD – nitrogen phosphorus detection
OD – overdose
ODMT – O-desmethyltramadol
PEL – pelvic girdle
PES – post-extraction spike
QQQ – triple quadrupole
QTOF – quadrupole time of flight
R^2 – correlation coefficient
REP H – repeated high
RIB – ribs
RR – response ratio
RR/m – mass-normalized response ratio
SIM – selected ion monitoring
SKU – skull
SURV – survived
SWGTOX – Scientific Working Group for Forensic Toxicologists
THC - tetrahydrocannabinol
TIB/FIB – tibia/fibula
TOF – time of flight
TRAM – tramadol
TNO – tramadol-N-oxide
UPLC – ultra-performance liquid chromatography
VRT – vertebrae

Chapter 1: Introduction

1.1 Overview of Opioids and the Opioid Crisis

Opioids are a class of drug used commonly for pain relief.[1] They were originally designed to simulate the effects produced by morphine.[2] Morphine was first isolated in the early 1800s from *Papaver somniferum*, commonly known as the opium poppy plant.[3] Morphine is a key ingredient in the synthesis of other prevalent painkillers, such as hydromorphone, oxymorphone and heroin.[4] As such, many opioids share many structural similarities with morphine. Opioids that are derived from morphine are called semi-synthetic opioids, since they are not found naturally, but instead are derived from a naturally occurring substance. Extended use of opioids can lead to physical dependence, which results in symptoms of withdrawal if the use of these substances is discontinued. Aside from pain relief, many opioids also have euphoric effects, which can attract recreational use.[5] The building of tolerance to the effects of opioids can occur in repeat users, meaning that users may need to take higher doses of these drugs in order to achieve the same effect.[6] It is this combination of physical dependence and the building of tolerance that contribute to the addictive nature of opioids.[7] Opioid addiction is treated by replacing the opioid in question with an alternative opioid which tends to have more moderate effects but is longer acting. Methadone or buprenorphine are both commonly used for this purpose.[8]

In 2017, there were over 70 000 drug overdose deaths in the United States. Of those, approximately two thirds involved an opioid.[9] While it has been reported that there has been a decrease in the total number of opioid deaths,[10] there has been a 10% increase in the number of overdose deaths attributed to synthetic opioid use from 2017 to 2018.[9,11] In Canada, there were approximately 2 800 opioid related deaths in 2016. This exceeds the number of deaths recorded at the peak of the HIV crisis in the 1990s.[12] It is this increase in synthetic opioid use that has led to

many labelling it as a crisis or epidemic.[13] In particular, novel synthetic opioids such as fentanyl and fentanyl analogues have contributed greatly to the recent surge in synthetic opioid use, and have been described as an emerging public health threat. One of the greatest challenges facing law enforcement agencies is controlling and scheduling these substances, a time consuming process which illicit drug manufacturers are able to outpace given the fast rate of production.[14] The increased potency of these novel synthetic opioids also allows them to serve as powerful adulterants of other substances, where users may not be aware of their presence, often resulting in fatality.[15] Additionally, these substances tend to have vastly increased potency when compared to traditional opioids such as morphine. This can make them undetectable by conventional presumptive test kits, where the analytical threshold cannot detect such small concentrations of these substances.[16] While traditional semi-synthetic opioids are derived from morphine, many novel synthetic opioids have wide variability in their chemical structures which can further complicate detection, due to limited cross-reactivity with conventional test kits.[17] Some substances, such as AH-7921, MT-45, and U-47700, have chemical structures that are completely unique, and as such share little to no cross reactivity with immunoassay kits designed to detect fentanyl analogues.[18] While tramadol is not seen as prevalently as many novel synthetic opioids in cases resulting in death via overdose, it is still very much of forensic relevance. In a study of American opioid overdose cases in 2018, tramadol overdose was attributed to suicide approximately 75% of the time.[19] One study investigated the use of various analgesics in self-poisoning cases, and found that tramadol is one of the most common drugs in suicidal overdose.[20] It is also important to note that in Canada, tramadol was only labelled a Schedule I substance in 2019, and up until that time was used commonly as a prescription painkiller. It is also commonly used in veterinary medicine.[21]

1.2 Pharmacokinetic and Pharmacodynamic Properties of Tramadol Hydrochloride

Tramadol hydrochloride, (1RS,2RS)-2-[(dimethylamino)methyl]-1-(3-methoxyphenyl)-cyclohexanol hydrochloride, is a centrally acting analgesic that shares structural similarities with codeine and morphine. Originally synthesized in 1962, it first became available for treatment of pain in Germany in 1977.[22] Traditionally administered orally, as either a capsule or drop form, tramadol tends to be absorbed rapidly by the body, with a lag time (the time before absorption begins) of approximately 0.2[23] to 0.5 hours,[24] depending on pharmaceutical form. Plasma concentrations of tramadol have been reported to peak within 1.2[23] to 1.9[24] hours after administration, again dependent on form of administration. Plasma concentration has been shown to increase linearly over a dose range of 50-400 mg.[25] Oral bioavailability (the fraction of an administered drug that reaches circulation) has been measured at 70% following a single dose, with the extent of oral absorption of tramadol almost at 100%.[24] Tramadol also tends to be distributed rapidly throughout the tissues, with an initial phase having a half-life of approximately 6 minutes, followed by a slower phase with a half-life of approximately 1.7 hours. Tramadol has also been shown to possess high tissue affinity, with plasma protein binding at about 20%.[26] In rodent models, tramadol has been shown to distribute preferentially into the lungs, spleen, liver, kidneys and brain.[27] Tramadol tends to reach peak concentration in the brain within 10 minutes of oral administration, with concentrations of its major active metabolite O-desmethyltramadol peaking after about 20-60 minutes. Some studies have shown that there is a preferential brain versus plasma distribution of tramadol over its active metabolite in rodent models.[28] In humans, approximately 90% of tramadol is excreted via the kidneys.[29] In one study, tramadol was shown to have an average half-life of approximately 5-6 hours in blood.[23]

Tramadol primarily undergoes N- and O-demethylation. Conjugation of O-demethylation compounds has also been described extensively. Tramadol is metabolised much more rapidly in animals than in humans, with approximately 1% excreted unchanged in the urine in animals versus 25-30% in humans. However, the main metabolites are the same regardless of species. In all species, O-desmethyltramadol and its conjugates, N-O-didesmethyltramadol and its conjugates, and N-desmethyltramadol are the main metabolites. All other metabolites have only been reported in minor quantities.[30] Another metabolite of particular interest is the N-oxide, which has also been identified as a prodrug (a compound that is only pharmacologically active after being metabolised) for tramadol.[31] While tramadol N-oxide has not been reported to have any direct pharmacodynamic effects, it has produced dose-related pain relief in rodent models. It was found that tramadol concentrations were approximately the same after administration of either tramadol or tramadol N-oxide. This suggests that tramadol N-oxide undergoes complete conversion to tramadol. This implies that tramadol N-oxide could offer an extended duration of action and a lower initial plasma concentration, which may help alleviate the possible adverse effects of tramadol.[31] The structure of tramadol and the four of its metabolites relevant to this study are shown in Figure 1.1.

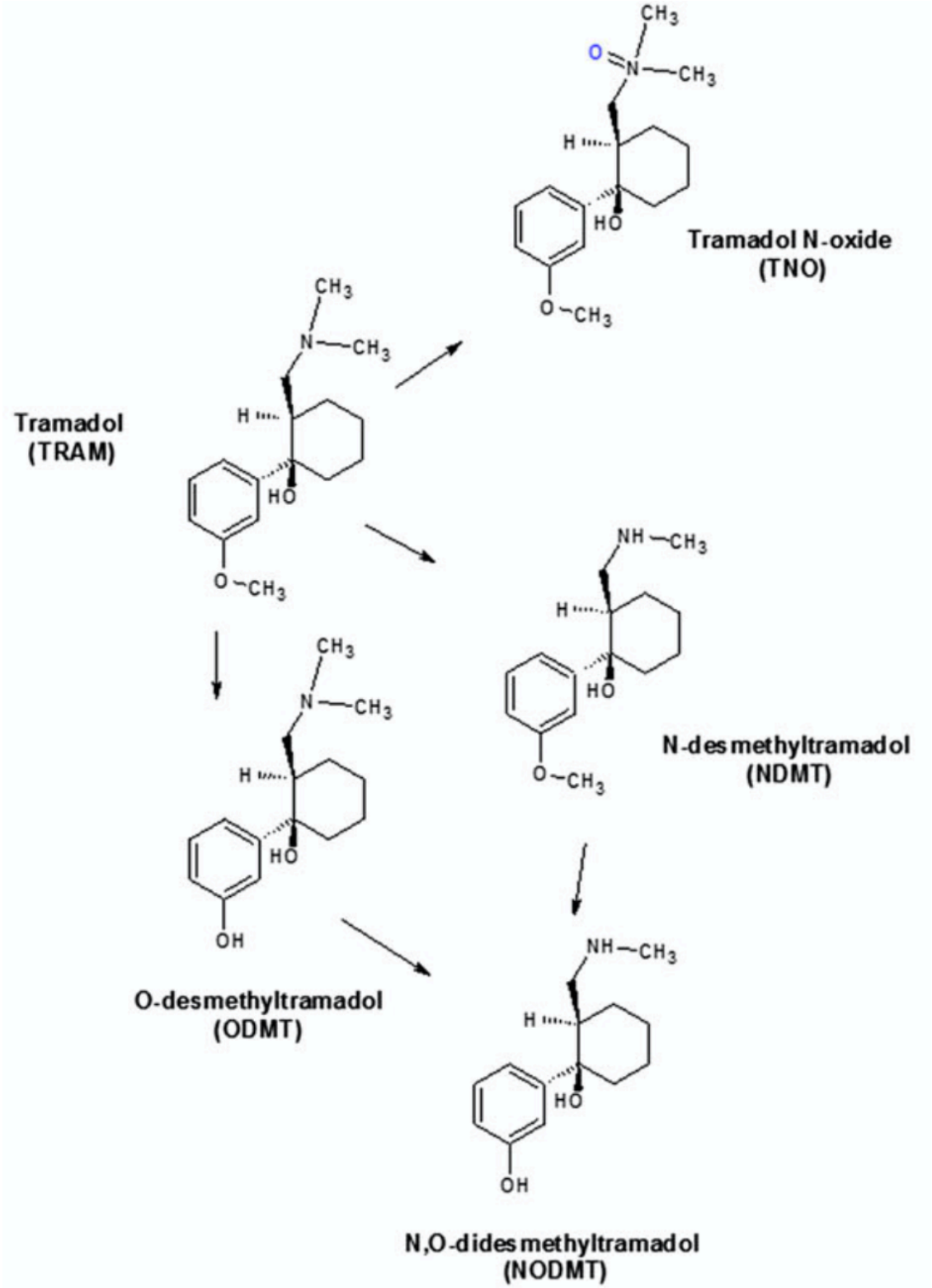

Figure 1.1 Chemical structures of tramadol and four of its metabolites.[87]

Numerous investigations have shown that the O-demethylation of tramadol is catalyzed by CYP2D6, an enzyme from the family of cytochrome P450, located in the liver. [32] With respect to the N-demethylation of tramadol, it is primarily catalyzed by CYP2B6 and CYP3A4. Further demethylation products such as N,O-didesmethyltramadol would be catalyzed by the appropriate enzyme depending on whether it is metabolizing O-desmethyltramadol or N-desmethyltramadol.[33] Tramadol differs from many opioids in that it is chiral. Both O- and N-demethylation have been demonstrated to be stereoselective in humans. The O-demethylation of tramadol is twice as likely for the (-)-enantiomer than for the (+)-enantiomer. Conversely, the N-demethylation of tramadol is preferential for the (+)-enantiomer.[32] Given that O-demethylation is the dominant metabolic pathway in humans, higher concentrations in the plasma of the (+)-enantiomer of tramadol can be expected. However, several studies have shown that at high concentrations, N-desmethyltramadol formation is predominant.[33] The metabolic pathway of tramadol is shown in Figure 1.2.

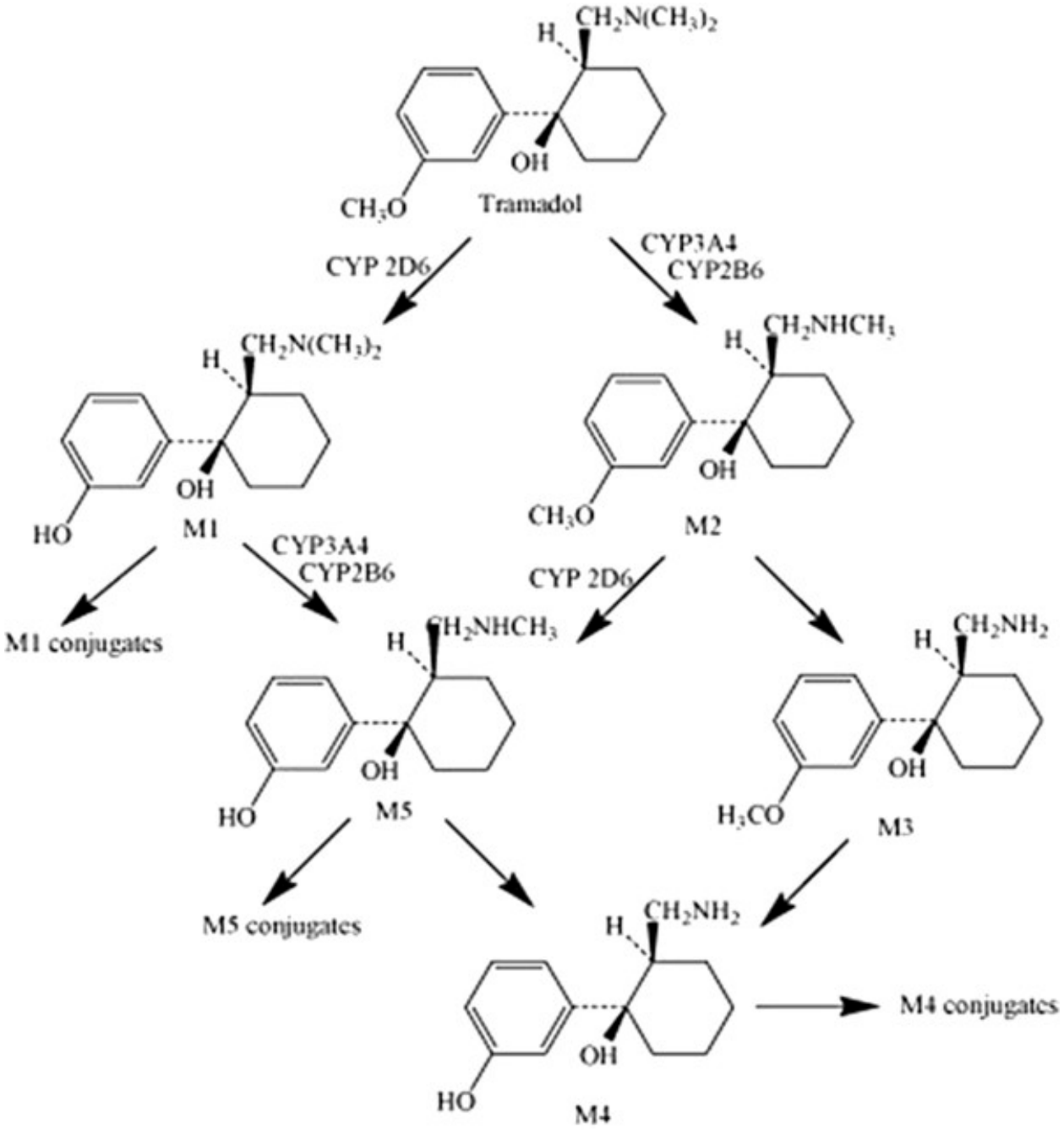

Figure 1.2 Metabolic pathway of tramadol. M1 corresponds to O-desmethyltramadol, M2 to N-desmethyltramadol, M3 to N,N-didesmethyltramadol, M4 to O,N,N-tridesmethyltramadol, and M5 to N,O-didesmethyltramadol.[34]

Tramadol has a relatively weak affinity for the opioid μ receptor when compared to other common opioids (approximately 10-fold less than codeine and 6 000-fold less than morphine).[35] The μ opioid receptor is primarily located in the brain and spinal cord and is most commonly associated with pain relief. Additionally, tramadol has no affinity for the δ and κ opioid receptors. This suggests that tramadol's affinity for the opioid receptors does not seem to be the primary contribution to its analgesic effect. In fact, O-desmethyltramadol binds with approximately 300-fold higher affinity than the parent metabolite. This indicates that the O-desmethyltramadol, the primary and only active metabolite, contributes greatly to tramadol's analgesic effect.[36] Tramadol is unique among many other opioids in that it inhibits the neuronal reuptake of both norepinephrine and serotonin.[37] Studies have shown that the (+)-enantiomer of tramadol inhibits the neuronal reuptake of serotonin[38], while the (-)-enantiomer of tramadol is a more potent blocker of norepinephrine reuptake.[39] These findings have all led to the hypothesis that given tramadol's relative lack of affinity for opioid receptors, its antinociception (pain relief) in animals is driven by a multimodal mechanism.[40] O-desmethyltramadol acts as a more potent μ opioid receptor agonist, the (+)-enantiomers inhibits serotonin reuptake and (-)-tramadol inhibits norepinephrine reuptake. This hypothesis supports the finding that the racemate of tramadol is superior in terms of its pain relief ability to either enantiomer alone.[41]

Tramadol's pain relief effects have been found to peak at around 3 hours and last for up to 6 hours. Given the proposed hypothesis on how tramadol's analgesia functions, the opioid antagonist naloxone, used to block the effects of many opioids, is only partly successful in antagonising tramadol-induced analgesia.[42] Furthermore, given tramadol's many differences from other opioids, its influence on respiration is comparatively small. It is unlikely to produce clinically relevant respiratory depression at the recommended dosage. In fact, overdose of tramadol is more

often associated with neurological toxicity. The most common symptoms of tramadol overdose are lethargy, nausea, agitation and seizures.[43]

1.3 The Importance of Alternative Matrices in Forensic Toxicology

A primary role of the forensic toxicologist is to assist in the determination of the cause of death through analysis of xenobiotics present in various biological samples. These samples include a wide array of biological samples, such as blood, urine and hair. These samples are analyzed for the presence of drugs or other compounds that may be relevant to the case file. Blood is the preferred substrate for toxicological analysis because the effects of any given drug are most easily correlated with its blood concentration. Other tissues are difficult to directly relate drug concentration to drug effect, given that there can be wide variability in drug distribution patterns between blood and various tissues.[44] Furthermore, there may be cases where blood is not easily obtainable for analysis, or is unsuitable (e.g., in cases of long delays between exposure and sampling). These situations can include cases where a body has experienced significant decomposition. In these cases, analysis of blood is difficult given the wide array of by-products produced throughout the decomposition process, which can interfere with most instrumentation. It is for this reason that analysis of alternative matrices may be preferable. Some studies have investigated using vitreous humour or cerebrospinal fluid to detect ethanol and heroin metabolites.[45,46] These matrices are of scientific interest due to their relative protection from microbial action that is active during decomposition. However, as putrefaction progresses the cells undergo lysis and tissues dissolve allowing the various bodily fluids to become mixed. This means that as decomposition progresses, it becomes increasingly difficult to determine antemortem drug concentrations.[47]

Hair and bone tissues present an interesting alternative to liquid matrices, as they are better protected from the effects of decomposition. In fact, it is distinctly possible that these substances may be the only samples still viable for analysis in the case of advanced decomposition. However, these matrices are comparatively less understood, and experiments involving them are limited in that it is difficult to design control into analyses of human post-mortem tissues. The vast majority of controlled studies in bone are reliant on animal models, in which various drugs may have different pharmacokinetic and/or pharmacodynamic properties, limiting the direct applicability of the studies to human subjects. While detection of a given compound of interest is a crucial first step, this type of qualitative information is not useful for creation of models for estimation of dose pattern or time of exposure. It is for this reason that studies need to involve closely controlled experimental conditions where factors such as dose, dose pattern, and dose-death-interval can be closely monitored.[44]

Until recently, reports on drug concentration in human bone tissue was focused on individual case reports, where the authors may not have necessarily been interested in the specific bone elements that were sampled. One of the first published studies that focused on quantitative determination of various drugs used femoral bone and bone marrow obtained from a series of postmortem investigations.[48] However, this study was limited in that they rejected samples originating from bodies that experienced significant decomposition. Given that blood is the preferred matrix for sampling except in cases of extreme decomposition, sampling of skeletal elements when blood is available is not necessarily of toxicological relevance. There exist other complications with respect to the toxicological analysis of skeletal tissues after death. For example, there is a general lack of understanding of the stability of various drugs in bone tissues. Studies have shown that, method dependent, not all drugs are detectable in skeletal tissues even when they

are detectable in blood samples taken from the same subject.[49] It is possible that the analytical methods used to quantify/identify these substances in these studies possessed insufficient analytical sensitivity, and that current instrumentation would be able to detect drugs at much lower concentrations in skeletal tissues. Another complication with skeletonized remains is the inability to accurately determine, or calibrate for, analyte recovery. In other words, it is impossible to tell if you have successfully extracted the entirety of the drug or drugs of interest. Since bone tissue is a solid, heterogeneous tissue, a sample needs to undergo significant processing in order to maximize the surface area required for extraction. This extraction step generally involves an organic solvent, such as methanol, which is able to diffuse into the matrix and extract out the drugs. If the bone sample is not processed into sufficiently small fragments, incomplete diffusion of the solvent into the tissue is likely. In this case, it is difficult for an appropriate internal standard to accurately correct for matrix effects.[44]

It is important, when discussing the behaviour of drugs in skeletal tissues, to understand the physiological nature of bone and marrow. There are two main types of bone: cortical (compact) bone and cancellous (spongy) bone. Spongy bone tends to be rich in marrow, a semi-solid tissue that produces billions of blood cells per day. It is bone marrow that fills the porous empty space found in cancellous bone. The various bones within the skeleton are made up of different amounts of these two types of tissues (Figure 1.1). It is this proportion that heavily influences the extent to which various drugs are able to partition into these skeletal tissues. Long bones, such as the femur, tend to have their shafts (diaphyses) primarily made up of cortical bone, while their ends (epiphyses) are made up of primarily cancellous bone. Regardless of the type of bone tissue, all bones are highly vascularized. Long bones are covered in a periosteum, which is a thick membranous sheath that serves as a protective outer layer. This sheath is rich in osteoblasts, which

are cells that promote bone formation. Long bones also possess a cavity within their diaphyses called the medullary cavity. This medullary cavity is filled with red or yellow marrow, which has a very high lipid content. Yellow marrow differs from conventional red marrow in that its function is more connective than hematopoietic (production of blood cells). Given the high lipid content found in the diaphysis of long bones, the more lipophilic a drug, the more likely it is that it will partition into these tissues.

An important consideration, when it comes to the study of drug distribution in bone, is the relationship between the amount of drug in skeletal tissue versus the concentration of drug in blood. There is a tendency to focus research on developing a quantitative model that can assign a blood concentration to a given measurement of drug in skeletal tissues. However, there has been no significant evidence presented in the literature to date that this is feasible with current methodologies.[50] This relationship is further complicated by a variety of variables, including the doth-death interval and post-mortem distribution/diffusion. As stated previously, the inability to determine the extent of drug recovery from bone tissues is a large impediment to the development of a quantitative relationship.

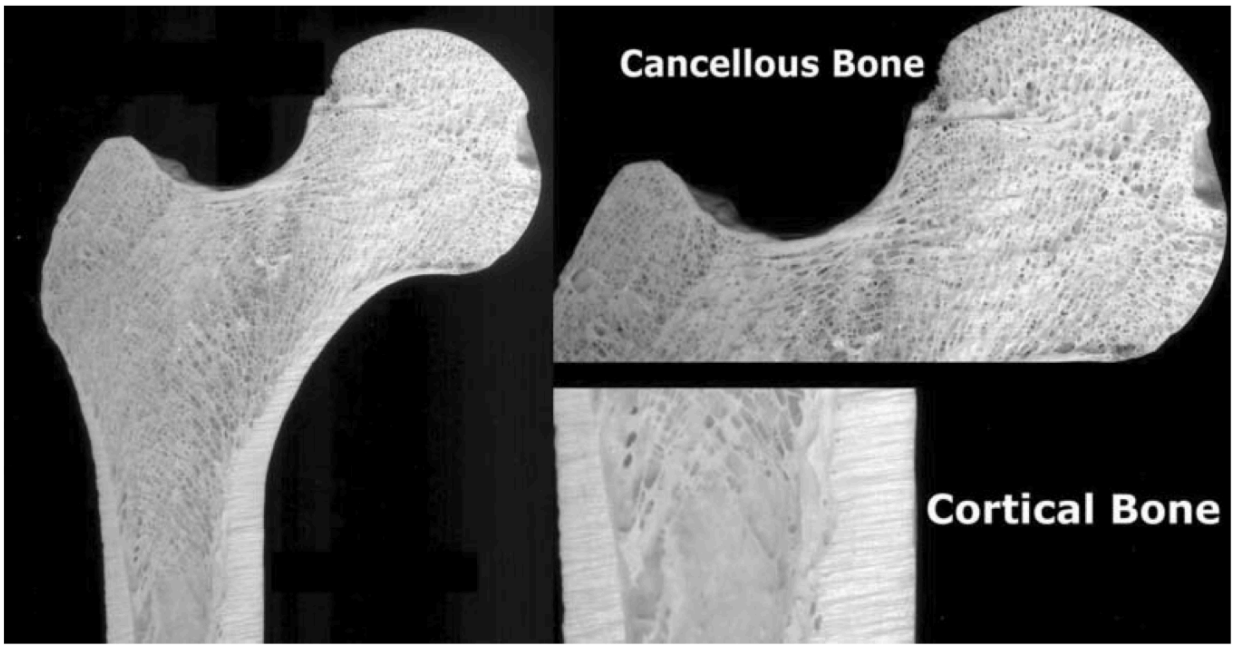

Figure 1.3 Proximal segment of a human femur. Expanded images show cancellous portion (upper) and cortical portion (lower).[44]

1.4 Past and Present Trends and Methodologies in the Analysis of Drugs of Abuse in Bone

Past studies have made substantial progress in documenting the behaviour of various drugs of abuse in a wide variety of experimental conditions and using a wide array of instrumentation. A study from 2001 utilized fluorescence polarization immunoassay (FPIA) and gas chromatography with a flame ionization detector (GC-FID) to determine that there was a loss of 54% morphine concentration when a piece of drug-positive bone was buried for a year.[51] Another study detected citalopram in the bones of an individual who suffered acute intoxication. However, the instrumentation used (gas chromatography with nitrogen phosphorus detection (GC-NPD)), followed by qualitative confirmation using electron impact gas chromatography/mass spectrometry (EI-GC/MS)) was unable to detect the citalopram that also appeared in the toxicological analysis of the individual's blood post-mortem.[52] Triazolam has been detected in a study of the skeletal remains of two individuals buried underground for 4 years using gas chromatography/mass spectrometry (GC/MS) in negative ion chemical ionization mode.[53] A quantitative ELISA (enzyme-linked immunosorbent assay) kit was used to detect a variety of benzodiazepines in bone tissues.[54] One study used a rodent model to quantitatively compare heroin levels following both acute and chronic doses. The study utilized liquid-liquid extraction (LLE) followed by GC/MS to analyze the levels of two heroin metabolites, 6-acetylmorphine and morphine. The study confirmed what has been mentioned previously, that there does not seem to be any strong correlation between blood and bone drug concentrations.[55] Methamphetamine and amphetamine were both detected in the skeletonized remains of a body that had been buried for 5 years. Analysis was carried out using gas chromatography coupled to chemical ionization mass spectrometry (GC/CI-MS).[56] Pentobarbital levels in bone marrow obtained from the femur were compared to heart blood concentrations in a 1985 study that utilized gas chromatography. The

study found that there were approximately equal concentrations of pentobarbital in both matrices.[57] One author examined human rib and sternum samples to detect a variety of drugs, including amobarbital and glutethimide using GC/MS.[58] Another study dosed rabbits with ethanol before sacrificing them and storing them for almost a month. Animals stored at low temperatures showed consistent ethanol levels until three weeks after sacrifice, at which point levels began to drop. When compared to control animals, this study showcased the effect of microclimate with respect to skeletal drug concentrations postmortem.[59] A different study used rabbits exposed to a repeated dosage of nortriptyline. Bone marrow was gradually collected over the 48 hours following the animals' sacrifice. This study also attempted to discern a relationship between bone marrow and blood drug concentrations, finding that there was no significant change in the ratio of nortriptyline concentrations in blood and bone over the first 24 hours.[60] A study from our laboratory also investigated the sensitivity of a qualitative ELISA screen coupled to a liquid chromatography tandem mass spectrometry (LC-MS/MS) quantitative analysis. The study focused on the dose death interval and its effect on ketamine concentration in skeletal tissues and found that both the specific tissue type and the DDI may influence the sensitivity of detection.[61] The studies mentioned above showcase a variety of comparatively early studies focused on the behaviour of drugs of abuse in bone. They covered assorted amphetamines, opiates, benzodiazepines, barbiturates, alcohols and tricyclic antidepressants. The instrumentation was predominately focused on immunoassays and gas chromatography/mass spectrometry.

With the development of new technologies and the changing prevalence of various drugs, the standards of practice utilized in forensic toxicology has likewise continued to shift. A recent study used ultra-performance liquid chromatography quadrupole time-of-flight mass spectrometry (UPLC-QTOFMS) to determine differences between acute and repeated exposures of

dextromethorphan in rat skeletons. The study also looked at the influence of skeletal element with respect to drug and metabolite distribution.[62] Another study looked at the distribution of amitriptyline and citalopram, along with their respective metabolites, in skeletal tissues. The study utilized a combination of solid-phase extraction and ultra-high performance liquid chromatography to determine whether significant differences exist between drug levels in skeletal elements.[63] A group of Greek researchers developed a method using liquid chromatography tandem mass spectrometry (LC-MS/MS) for the detection and quantification of over 25 drugs of abuse, including cocaine, venlafaxine, methamphetamine, and carboxy-THC (a metabolite of Δ^9-THC).[64] Another group performed a bone distribution study of clofazimine in bone marrow using reverse phase liquid chromatography.[65] A case report from 2013 utilized LC-MS/MS to determine that a skeleton found in a river possessed diazepam levels to support the proposition that the individual was a chronic user of diazepam.[66] A Belgian study detected methadone in the skeletal issues of rats following chronic exposure using LC-MS/MS.[67] Another study showcased the detection of a variety of drugs of abuse, including tramadol, in a human skeleton using high resolution mass spectrometry (HRMS).[68] These studies showcase the wide range of methodologies used to detect and analyse forensically relevant compounds.

1.4.1 Immunoassay and Presumptive Testing

The immunoassay that has been used predominately in the past were ELISA (enzyme-linked immunosorbent assay) kits. The exact mechanism of an ELISA kit differs according to the manufacturer and according to the substance being screened for. Generally, ELISA kits detect a drug of interest through competitive binding. Haptens, which are small drug molecules, are introduced in a fixed volume of sample. These haptens then compete with a fixed quantity of

enzyme-labelled drug for binding sites on immobilized antibodies. At equilibrium, there is a distribution of both drug and labelled drug bound to these antibodies. This relative distribution is determined by the drug concentration in the original sample. Lastly, an enzyme substrate is added in order to produce a colour change, which can be measured spectroscopically. This spectroscopic response is inversely related to the amount of unlabelled drug in the sample, which allows for semi-quantitative analysis.[69] Immunoassay kits are useful tools in forensic toxicology, as they are of low cost compared to other methods and are fairly simple to use, requiring only small volumes. Additionally, they can be easily automated, enabling high-throughput and fast turnover of samples. There are limitations associated with immunoassays, including susceptibility to matrix effects and poor selectivity of compounds. Closely related compounds may be undetectable, while different classes of drugs may have compatible ligands that can bind to the enzyme substrate. Therefore, they are considered to be well suited for presumptive testing purposes, but they require further confirmatory tests with equal or greater sensitivity.

1.4.2 Chromatography

Chromatography remains the standard of practice in the field of forensic toxicology and has done so for many years. Chromatography is the separation of compounds through differential interaction between a stationary and a mobile phase. For example, gas chromatography is a form of column chromatography, in which an inert carrier gas serves as the mobile phase which moves substances through the column towards the detector. The time required for a substance to pass through the column and reach the detector is called the retention time. Ideally, a given compound should be in equilibrium between the mobile phase and the solid phase, which is the coating on the interior of the column. When this occurs, it is the difference in affinity that a substance has for each phase that allows a mixture to be chromatographically separated. This, in large part, is what

measures column efficiency. An inefficient chromatographic system is one that is unable to resolve the substances in a mixture, such that the detector registers a peak that corresponds to multiple analytes. This peak is expressed graphically. An efficient column that is able to pull all the constituents in a mixture apart will yield multiple, thin peaks. Additionally, it is ideal for these peaks to be sufficiently separated such that the signal from one substance's peak does not carry over into a different substance's peak. The ability of a chromatographic method to separate the components of a mixture is called the resolution.

In gas chromatography, an extract is volatilized within the injection port, at which point it begins to move through the column. An inert carrier gas serves as the mobile phase, and separation is achieved dependent on the boiling point of the mixture and any intermolecular interactions that may occur with the stationary phase. The temperature of the column is a key factor that can be used to adjust the retention times of the various components within the mixture. While gas chromatography is an extremely powerful tool, it does possess some limitations that can render it ineffectual for analysis of certain compounds. Primarily, gas chromatography is most effective at separating volatile, non-thermally labile compounds.[70] Compounds bearing hydroxyl groups and non-tertiary amines often must be derivatized before analysis by gas chromatography, in order to increase volatility and minimize hydrogen bonding interactions that can distort peak shape, and decrease resolution. One of the most common detectors used in conjunction with gas chromatography is a flame ionization detector. Simply, compounds that are eluted from the column are ionized by a small hydrogen flame, at which point the ions formed during combustion are collected by an electrode. This detector is limited in that it is not particularly selective for the compounds that it detects. Furthermore, it also does not produce any spectral information.[71] It is

because of these limitations that the coupling of gas chromatography with mass spectrometry was introduced as a very convenient, and popular, approach to separating and characterizing analytes.

As can be seen from a review of the literature, in the last five years the instrumentation most commonly used by forensic toxicologists has changed drastically. Whereas GC-MS was the industry standard, LC-MS (including LC-MS/MS and LC-HRMS) is quickly emerging as one of the most useful tools available to analysts. While the basic principles of chromatography and mass spectrometry apply to both GC-MS and LC-MS, LC-MS functions in a different manner. Liquid chromatography takes place in a liquid mobile phase, rather than a gaseous one, and as such the column is operated via a pump. The ability of analytes to partition between the stationary and mobile phases is based upon their relative solubility between their two phases, and as such, the composition of the mobile phase is an important factor to control in addition to temperature. The mobile phase in liquid chromatography is ofttimes a mixture of two solutions, and the relative proportion of these two solutions at any given time throughout the run can heavily influence the resolution of a given method. Adjustment of the proportions of mobile phase solvents throughout the chromatographic run is called gradient elution. Liquid chromatography is also more universally applicable than gas chromatography, as analytes do not need to be volatile or thermally labile when the mobile phase is a liquid. A common detector used in liquid chromatography applications is a fixed wavelength diode array detector. These detectors record the absorption spectra of column eluent passing through it, similar in function to a spectrophotometer. This kind of detector also avoids the limitations of detectors in gas chromatography by being nearly universal, as it is not only compatible with combustible analytes. Liquid chromatography also rarely requires the derivatization of compounds, as compounds simply need to be soluble within the mobile phase to be analyzed.

Like gas chromatography, liquid chromatography is frequently coupled with mass spectrometry to increase its analytical prowess. Mass spectrometry functions the same regardless of what it is coupled to but will involve different ionization methods, done at atmospheric pressure. Two common ionization methods in LC-MS are electrospray ionization (ESI) and atmospheric pressure ionization (APCI). In ESI, the liquid phase is passed through a stainless-steel capillary whose tip has a large applied voltage (~kV), in the presence of a heated desolvation gas (typically N_2), at a high flowrate. This configuration results in the liquid eluent being converted to a charged aerosol. According to the most popular model, as the droplets move towards the mass selector, they gradually evaporate, and as they do, the charge is ultimately passed directly to the solute (ideally, the analyte). This "soft" ionization process is much less energetic than what is observed with electron impact ionization in GC-MS, resulting in much less fragmentation. Following mass selection (e.g., by quadrupole(s), ion traps, time-of-flight), the ions reach the detector, and are counted. The count is represented as an intensity of a given mass to charge ratio, similar to GC-MS. APCI works somewhat similarly to electrospray ionization, except that instead of the eluent being ionized immediately after exiting the column and the stainless steel capillary (which is heated but does not have an applied voltage), the aspirate is ionized via a corona discharge as it approaches the mass selector.[72]

1.4.3 Mass Spectrometry

Mass spectrometry consists of the ionization and fragmentation of compounds, followed by the sorting and detection of these ionized fragments according to their mass to charge ratio. Mass spectrometry can be used on its own but is frequently coupled to a separatory technique such as chromatography. Ionization in GC-MS usually involves either chemical or electron impact, both

of which occur under high vacuum (typically, $\leq 10^{-4}$ torr). As separated compounds exit the column, they are ionized under these high vacuum conditions. Chemical ionization involves a generated electron beam which is used to bombard the molecules of a reagent gas, such as methane or ammonia, that undergo some intermolecular collisions, resulting in new reaction products, which, in turn, have reduced energies. These ionized reaction products then collide with the analyte molecules that have eluted from the column, leading to the fragmentation of the analytes. These ionized analytes tend to undergo less fragmentation than the ions produced in electron impact ionization, wherein the electron beam directly bombards the analyte molecules. The identity of the predominant ion, and the pattern of fragmentation characteristic of each compound, contributes to what is used to identify a given compound in mass spectrometry.

The mass spectrum generated by this process is a plot of intensity versus the mass to charge ratio (m/z). Intensity is a unitless measurement, with the most predominant m/z ratio being assigned, via signal normalization, a ratio of 100%. The fragment ion that is assigned that value is termed the "base peak". All other fragment ion intensities are measured relative to that intensity measurement, creating the mass spectrum. Spectral libraries have been developed in order to compare the spectra of unknown analytes with those of known reference standards. Comparison of an unknown compound to these spectral libraries is an important part of forensic toxicology investigations. A combination of chromatograms and mass spectra can be used for quantitative work, as the signal of a given set of ions at a given retention time is concentration dependent. A limitation of gas chromatography mass spectrometry is that it can tend to introduce a lot of background noise in the spectra, given the extensive fragmentation of analytes. This can be partially avoided by operating instruments in what is called selected ion monitoring (SIM) mode. SIM involves monitoring the intensity of only certain ions of a particular mass to charge ratio,

which greatly increases the selectivity. The reduction of background noise also tends to increase the sensitivity of the instrument, however it offers much less spectral information compared to full scan mode, where all ions produced through ionization are logged by the detector.[70]

Once ionized, the analyte molecules (as well as any eluted matrix components) are able to undergo gas-phase interactions (typically, pair collisions), potentially leading to further fragmentation. Fragmentation resulting from collisions with other molecules is called collision-induced dissociation (CID). CID can be both advantageous and disadvantageous, as further fragmentation can increase the instruments ability to distinguish between different substances but if not controlled, can also increase the amount of background noise. There is a wide variety of mass selection configurations, but those most commonly used in LC-MS are the quadrupole and time-of-flight (TOF) mechanisms. A quadrupole is made up of four rods arranged parallel to each other, with each opposing pair of rods being connected electrically. This creates an electric potential with the rods, through which molecules may pass dependent on their mass to charge ratio. By varying the potential applied to the quadrupole, the selective passage of ions is possible. Ions that do not have the appropriate mass to charge ratio will collide with the rods and will fail to reach the detector. Quadrupoles can also be used in sequence. This is one form of tandem mass spectrometry. Tandem mass spectrometry can also refer to any subsequent sequence of mass analyzers but is most commonly applied to a triple-quadrupole setup. In a triple quadrupole, the first and third quadrupoles function as described previously, but the second quadrupole differs in that it contains an inert collision gas (typically, Ar or N_2). This collision gas promotes collision induced dissociation. As such, the third quadrupole's applied voltage selectively filters out the fragments created in the second quadrupole. Mass spectrometers that operate in this way possess what is called selected reaction monitoring, in addition to full scan and selected ion monitoring

modes. This form of tandem mass spectrometry has vastly increased sensitivity and selectivity but requires knowledge of the substances being analyzed in order to instruct the instrument which mass to charge ratios to filter for. This makes tandem mass spectrometry a powerful tool for the confirmation of the presence of analytes but requires complex method development for use as a screening tool. Another common mass analyzer used in LC-MS application is time-of-flight (TOF). In TOF instrumentation, ions are accelerated by a voltage pulse into an area where there is no electric potential applied called the drift tube. This means that all ions, regardless of mass, possess the same kinetic energy (under the assumption that the ions have identical charges, as ions with a higher charge experience increased acceleration). As such, the time that it takes to reach the detector is directly dependent on their masses, as this is what will determine their velocities. For example, lighter ions will reach the detector faster than heavier ions so long as they are accelerated by the same voltage pulse. Many TOF mass analyzers also possess a reflectron, a region which uses localized electric fields to "reflect" the ions trajectories. This increases the distance that ions travel before reaching the detector, without impacting the overall size of the instrument. TOF mass analyzers originally tended to have lower sensitivity than quadrupoles but can be more advantageous as a result of the large mass ranges that they are able to process. This makes them better suited for screening than quadrupoles. Modern TOF mass analyzer that are equipped with reflectron technology are now extremely sensitive as a result of the background signal reduction that is possible due to the very high mass resolution, and are now part of what is commonly known as high resolution mass spectrometry.[70]

High resolution mass spectrometry (HR/MS) is quickly becoming the gold standard for qualitative and quantitative analysis in forensic toxicology. One form of HRMS is quadrupole-time-of-flight (QTOF) MS, which combines the screening power and high mass resolution of TOF

instrumentation with the increased sensitivity and selectivity of tandem quadrupole technology. Given the increased mass resolution, HRMS can discriminate between compounds with very similar molecular masses, with an accuracy of approximately 0.001 atomic mass units or less. This allows tentative identification based on the exact mass to charge ratio, rather than on a specific fragmentation pattern that must be compared to spectral libraries.[73]

One feature of TOF MS is the inability to direct the TOF mass analyzer to detect ions in a targeted manner, to the exclusion of ions that are deemed to be irrelevant or uninteresting. The multitude of modes in which HRMS can operate is incredibly useful for toxicology laboratories but compiles a vast amount of data from each run. This data can then be retrospectively mined at a later date and has been used recently to investigate samples processed in the past to further elucidate toxicological information. For example, in the case where commercially manufactured drug standards may not be available, an initial presumption may be sufficient based on the assigned molecular formula until such a time as a drug standard is made available. This technology also allows for the elimination of toxicologically irrelevant compounds that reduces the possible number of false positive matches.[74]

Unfortunately, high resolution mass spectrometry is not without its disadvantages. One is that spectral libraries are rarely transferable between different types of instruments. Existing spectral libraries would need to be recompiled for these new instruments, a time consuming and expensive process, and one which requires strict LC method control. Another disadvantage of high-resolution mass spectrometry is its prohibitive cost. While most instruments used in the forensic toxicology laboratory are expensive, LC-MS is especially expensive, and HRMS even more so. This increased cost can be outside the operational budget of many forensic toxicology laboratories. Many laboratories still make use of GC-MS, as they may not be able to afford even a single quadrupole

LC-MS. Another disadvantage of HRMS is that instruments tend to have a smaller dynamic range and are unable to accurately measure samples at high concentrations. These high concentrations tend to rapidly saturate the detector, requiring modified sample preparations to dilute samples to an appropriate concentration.[75]

1.5 Important Considerations in the Analysis of Skeletal Tissues

Given the lack of understanding of the precise quantitative relationship between the level of drug in blood compared to bone, conclusions reached from the analysis of drug and bone need to be tempered with caution. There are a wide variety of factors that need to be considered when it comes to dosing, sample preparation, instrumentation, and experimental design. Furthermore, there is an overall lack of research that has been done to date on drug in bone, and analytical procedures have yet to be standardized. To date, there has also been no documented comparisons of different sample preparation methods. A wide variety of external factors have been shown to influence the behaviour of drug in bone, including insect activity,[76] body position,[77] bone type,[78] microclimate,[79] dose-death interval[80] and dosage pattern.[81] Our laboratory has focused on attempting to understand these various factors for several drugs of abuse, including but not limited to, ketamine,[77] diazepam,[82] fentanyl,[83] amitriptyline,[63] colchicine,[84] tramadol[85] and dextromethorphan.[79]

As mentioned previously, there is a lack of standardized practices in the field of forensic toxicology. Most laboratories will have their own operational procedures which they adhere to, but there are very few collaborative efforts to standardize how toxicological analyses is done for all laboratories. This highlights the importance of method validation. Method validation is the process of performing a set of experiments that reliably estimates the efficacy and reliability of a

given method. It is also performed when an existing validated method is modified.[86] Groups such as the Scientific Working Group for Forensic Toxicology have published guidelines for all toxicologists to practice in order to ensure that a method is capable of successfully performing at the level of its intended use. Additionally, method validation identifies a method's limitations under normal operating conditions. These operating conditions are meant to simulate the day-to-day work that a practicing forensic toxicologist may need to do.

1.6 Objective of Study

The objective of this study was two-fold. The first objective was to develop a method for the sensitive detection of tramadol and five of its metabolites in rat skeletal tissues using LC-MS. This is similar to previous work from our laboratory which has successfully developed methods for the detection of tramadol using GC/MS[85] and LC/QTOF-MS.[87] A simplified sample preparation approach was developed which involved dynamic methanolic extraction of analytes followed by a modified solid-phase extraction protocol. The second objective was to compare differences in tramadol and metabolite levels in the skeletal remains of rats that underwent different tramadol dosing patterns. To this purpose, various metrics were assessed, in order to determine if there were significant differences in analyte levels or in analyte level ratios between exposure patterns. This builds on previous work done that assessed if significant differences exist in tramadol levels between acute and repeated exposure patterns.[85] Previous studies have only studied tramadol and its primary metabolite, O-desmethyltramadol, while this present study builds on the study which used UPLC-QTOF-MS to expand the number of metabolites analyzed from one to four. The levels of N-desmethyltramadol, N,O-didesmethyltramadol, and tramadol N-oxide were analyzed for this purpose, the ratios between all five analyte levels were computed and

compared across dosing patterns. Finally, this work resulted in a unique and unanticipated opportunity to assess tramadol and metabolite levels in animals that suffered a fatal overdose after exposure.

Chapter 2: Methods and Materials

2.1 Reagents and Reference Standards

TRAM, ODMT, NDMT, NODMT and TNO reference standards were purchased from Toronto Research Chemicals (Toronto, ON) as solids and dissolved to a concentration of 40 µg/mL in methanol. The internal standards TRAM-d6, ODMT-d6, NDMT-d3 and NODMT-d3 were purchased from Toronto Research Chemicals (Toronto, ON) as solids and dissolved to a concentration of 4 µg/mL in methanol. LC/MS grade ammonium formate and formic acid were purchased from Fisher Scientific (Nepean, ON). All solvents, including methanol, water and acetonitrile were Omni-Solv® LCMS brand and were purchased from EMD Chemicals (Gibbstown, NJ).

2.2 Drug Administration and Bone Preparation

Male Sprague Dawley rats (n = 52), used as part of three studies, were purchased from Charles River Laboratories (Saint Constant, QC). The rats were housed at the Laurentian University Animal Care Facility and treated in accordance with the Laurentian University Animal Care Committee guidelines. For this study, animals were divided into two groups (ACU L, n = 4; REP H, n = 16). Animals in the ACU L group received one dose of TRAM (30 mg/kg) via intraperitoneal administration and were euthanized by CO_2 asphyxiation one hour after dosing. Animals in the REP H group received three doses of TRAM (30 mg/kg) via intraperitoneal administration, with each dose administered 45 minutes apart. However, 11 of the 16 animals in the REP H group died within one hour of the last dose (REP H OD). Subsequently the remaining 5 animals were euthanized one hour after the last dose (REP H SURV). Four animals served as drug-free negative controls. Following euthanasia, all animals were placed outdoors in Sudbury,

Ontario in July 2019, under wire mesh, to decompose to skeleton with full exposure to various weather conditions (sunlight, precipitation, etc.) for approximately 3 weeks.

Bones collected for analysis included vertebrae (VRT), femora (FEM), pelvic girdles (PEL), tibiae and fibulae (TIB/FIB), ribs (RIB), and skulls (SKU). Following collection, bones were separated according to animal (ex: ACUL) and skeletal element (ex: VRT). Bones were then rinsed sequentially with water (2 mL), methanol (2 mL) and acetone (2 mL). Bones were left to air-dry for at least 48 hours and then were ground to powder using a domestic coffee grinder for 45 seconds.

2.3 Plate Comparison Study

Two 96-well sample preparation plates were assessed for their suitability in this study. The first plate was a Waters Oasis® PRiME MCX microelution (2 mg, 30 µm), and the second was a Waters Ostro® Protein Precipitation & Phospholipid Removal Plate (25 mg). The procedure for the first plate was more time consuming and labour intensive. Samples were acidified with phosphoric acid before being loaded onto the plate. The plate was then washed with 5% formic acid in water, then washed again with methanol. After these washes, the plate was then dried under high vacuum for 10 minutes. The collection plate was then changed, and the sample was eluted with 50 µL of 5% ammonium hydroxide in acetonitrile. This results in a five-fold theoretical magnification of the original samples concentrations (e.g. 10 ng/mL pre-extraction, 50 ng/mL post-extraction). The procedure for the second plate was much simpler. Samples were diluted with a 1:1 methanol:acetonitrile mixture in order to obtain a 1:5 dilution (e.g. 10 ng/mL pre-extraction, 1 ng/mL post-extraction). Samples were then eluted under low vacuum. This simplified extraction

does not require switching of the collection plate, as substances which can complicate analysis, such as phospholipids, are absorbed by the plate while the desired analytes pass through.

2.4 Extraction Solvent Study

A comparison of various extraction solvents for use with the Ostro® Plate was also performed. Four compositions of extraction solvent were prepared: 1:1 (v/v) methanol:acetonitrile, 1:1 methanol:acidified acetonitrile (0.1% formic acid), pure acetonitrile, and acidified acetonitrile (0.1% formic acid).

2.5 Analyte Extraction

Analyte extraction from ground bone was done by dynamic methanolic extracting using a Tissuelyzer® apparatus (Qiagen, Germantown, MD, USA). Bone samples (0.1g, n = 3) from a given animal and skeletal element was combined with 950 μL of methanol and 50 μL of the appropriate internal standard (IS) in 2 mL screw-cap vials and agitated at 30 cycles/s for 30 min, which was determined to be the optimal extraction time of tramadol from skeletal tissues in a prior study.[87] Prior to SPE, 200 μL of the extract was diluted with 800 μL acidified acetonitrile:water (1:1 v/v) to obtain a 1:5 sample dilution. Diluted samples were loaded onto an Ostro® plate and allowed to flow by way of a vacuum pump. Filtered samples were then transferred to 1.5 mL autosampler vials with silanized micro-inserts.

2.6 Instrumental Analysis

Analysis of prepared extracts (2 μL) was performed using an Acquity® H-Class UPLC coupled to a TQS Micro triple quadrupole mass spectrometer (Waters Corp, Milford, MA). The

column used for analysis was an Acquity® HSS C18 column (150mm x 2.1mm, 1.7µm particle size, Waters Corp, Milford, MA). Gradient elution was used with a flow rate of 0.4 mL/min. The column was maintained at a temperature of 50°C. Mobile phase A consisted of 5 mM ammonium formate with 0.1% formic acid in water (pH 3.0). Mobile phase B consisted of 0.1% formic acid in acetonitrile. Initial mobile phase were 90% A for 1 min, followed by a linear decrease to 80% over 2 min, then decreasing to 75% A for 1 min, followed by a decrease to 50% over 2 min, then decreasing to 25% over 0.5 min, followed by a decrease to 10% A over 1.5 min, then an increase to 90% A over 1 min, and then maintaining that condition for 1 min, giving a total runtime of 10 min (Table 2.1).

The QQQ-MS was operated in positive electrospray ionization mode, using a capillary voltage of 1.00 kV and sampling cone voltage of 25 V. The source temperature was 50°C, and the desolvation gas temperature was 500°C with a flow rate of 1000 L/hr.

Positive identification of a given target analyte required a retention time within 0.02 min of the corresponding reference standard, and precursor-product ion ratios within 20% of those of the corresponding reference standards (Table 2.2).

Table 2.1 Mobile phase gradient elution parameters for analysis of tramadol and metabolites by UPLC-MS/MS

Time Window (min)	Mobile Phase A (%)	Mobile phase B (%)
0 - 1	90	10
1 - 3	90 → 80	10 → 20
3 - 4	80 → 75	20 → 25
4 - 6	75 → 50	25 → 50
6 - 6.5	50 → 25	50 → 75
6.5 - 8	25 → 10	75 → 90
8 - 9	10 → 90	90 → 10
9 - 10	90	10

Table 2.2 Analytes, and corresponding internal standards, retention time and precursor and product mass-to-charge-ratio values for multiple reaction monitoring (MRM).

Analyte	**Precursor Ion $[M + H]^+$ (m/z)**	**Product Ion $[M + H]^+$ (m/z)**	**Retention time (min)**	**Internal Standard**
TRAM	264.2	58.1	5.24	TRAM-d6
TNO	280.1	58.1	5.51	N/A
ODMT	250.2	58.1	3.40	ODMT-d6
NDMT	250.2	44.0	5.31	NDMT-d3
NODMT	236.1	44.0	3.54	NODMT-d3

2.7 Statistical Analysis

XLSTAT®:PC 2018.1-49531 (Addinsoft, New York, NY) in conjunction with MS Excel® 2016 (Microsoft Corp., Redmond, WA) was used for all statistical analyses with the critical value set to 0.05 (e.g., $P < 0.05$). Kruskal-Wallis (KW) analysis was used to compare all analyte levels and analyte level ratios across different groups (ex: ACU L vs. REP H OD vs. REP H SURV).

2.8 Expression of analyte levels – mass-normalized response ratios

Previous work has been done in describing a semi-quantitative approach to expressing drug concentration in bone.[62] Reporting analyte levels as a mass-normalized response ratio (RR/m), allows for one to mostly account for the inability to determine or calibrate for analyte recovery from bone tissues. RR/m is defined as the ratio of the response ratio (RR, the ratio of analyte response to the corresponding IS response) of a given analyte to the mass of bone sampled.

$$Response\ Ratio = \frac{Analyte\ peak\ area}{IS\ peak\ area}$$

$$Mass\ Normalized\ Response\ Ratio = \frac{Response\ Ratio\ of\ analyte}{mass\ of\ bone\ analyzed}$$

2.9 Method Validation

The method used in this study was adapted from a previously published study.[87] As such, it was re-validated according to SWGTOX guidelines.[86] It should be noted that while SWGTOX was disbanded in 2014, it passed ownership of all of its publications to the Toxicology Subcommittee of the Organization of Scientific Area Committees (OSAC), which is in turn administrated by the National Institute of Standards and Technology (NIST). While the original

document has been updated, the method validation requirements have remained the same for the purpose of this study.[88] The criteria evaluated included selectivity, concentration dependence, carryover, limit of detection (LOD), limit of quantitation (LOQ), bias, precision, matrix effects, recovery, dilution integrity and stability. Drug-free bone tissue was sonicated in phosphate buffer saline (PB6, pH 6.0, 0.1 M) after decomposition outdoors to create the bone tissue matrix (BTE). Calibrators were prepared in 1 mL of BTE in the range of 1-500 ng/mL in triplicate.

Selectivity was determined by evaluating the presence of interfering substances that may be present in the sample. Blank BTE, without the addition of any analyte or internal standards was analyzed at the beginning of each run. Additionally, extracts were spiked with IS at low, medium and high concentrations to determine whether any non-labelled compounds were present that could interfere with analyte MRM analyses. Likewise, extracts spiked with analyte, but with no IS, were also analyzed to determine whether any compounds were present that could interfere with IS MRM analyses.

The concentration dependence was evaluated using seven calibrants over the working range of 1-500 ng/mL (1, 2, 5, 25, 50, 250, 500 ng/mL). Each of these calibrants was run in triplicate over five separate runs. These calibrants were used to generate a standard curve that describes the mathematical relationship between sample concentration and instrumental response. Analyte carryover into a subsequent sample was evaluated by running blank BTE after calibrants of a high analyte concentration. Carryover was determined to be negligible if no analyte signal above the LOD was present in these blank matrix samples.

The LOD refers to the lowest concentration of a given analyte in a sample that can be reliably distinguished from blank matrix. The LOQ is defined as the lowest concentration that can

be evaluated with acceptable bias and precision. Both the LOD and the LOQ were determined using samples fortified with analyte and were run in triplicate over three separate runs.

Bias, or accuracy, refers to the closeness of agreement between a concentration determined from a given instrumental response and the known concentration of the same sample. Bias was measured in triplicate over three separate runs and was measured at low (5 ng/mL), medium (50 ng/mL), and high (250 ng/mL) concentrations.

$$Bias\ (\%)\ at\ concentration\ x = \left(\frac{Average\ of\ Calculated\ Concentration_x - Nominal\ Concentration_x}{Nominal\ Concentration_x}\right) * 100\%$$

Precision studies were run concurrently to bias studies and evaluated the closeness of agreement in the instrumental response between multiple samples of the same concentration. Precision was measured as the coefficient of variation (CV, %) at a given concentration, for both within-run and between-run samples.

$$Within\ run\ CV\ (\%)\ at\ concentration\ x = \frac{standard\ deviation\ of\ response\ ratio\ of\ a\ single\ run\ of\ samples_x}{mean\ response\ ratio\ of\ a\ single\ run\ of\ samples} * 100$$

$$Between\ run\ CV\ (\%)\ at\ concentration\ x = \frac{standard\ deviation\ of\ grand\ mean\ of\ response\ ratio_x}{grand\ mean\ of\ response\ ratio_x} * 100\%$$

Matrix effects can include ionization suppression or enhancement, which are alterations of an instruments signal due to the presence of co-eluting compounds. This is a common complication

in LC-MS applications, and was measured here by preparation and comparison of two different sets of samples. The first set was composed of neat standards prepared at low and high concentrations, each of which was run several times to determine an average instrument response. The second set of samples was composed of blank BTE that underwent the SPE procedure used in this study. After extraction, each sample was fortified with analyte at either low or high concentrations (post-extraction spikes, PES). The mean response of each analyte in each set at a given concentration level was then compared to numerically represent ionization enhancement/suppression as a percentage as follows:

$$Matrix\ effects = \left(\frac{Mean\ Response\ PES}{Mean\ Response\ Neats} - 1\right) * 100\%$$

Recovery was measured by comparing the average response obtained from neat standards to the average response obtained from extracted samples, at low and high concentrations. Recovery was represented as a percentage and describes the amount of analyte lost during the extraction process.

$$Recovery\ at\ concentration\ x = \frac{Mean\ Response\ of\ Extracts_x}{Mean\ Response\ of\ PES_x} * 100\%$$

Dilution integrity studies measures the degree to which dilution of a sample affects the observed bias and precision. Studies involve replicating bias and precision studies at common dilution factors, such as 1:5 and 1:10.

Analyte stability experiments are designed to measure the change in instrument response when processed samples sit in the instrument autosampler for extended periods of time before analysis, as may occur with a large batch of samples. The study was composed of samples at low

and high concentrations being stored on the autosampler, which is kept refrigerated at 4°C. Samples were run every 12 hours for 36 hours, and the response at each time interval was compared to the signal at time zero. Samples were considered to no longer be stable when the average response changed by ± 10%.

The acceptance parameters for method validation are outlined in Table 2.3.

Table 2.3 Summary of method validation parameters and their respective acceptance criteria.

Parameter	Description	Acceptance Criteria
Bias	Accuracy of a measurement/degree of agreement between actual and theoretical	Must not exceed ± 20%
Calibration Model	Mathematical relationship between analyte concentration and instrument response	1-500 ng/mL with preferred linear model
Carryover	Appearance of unintended analyte signal	Carryover after highest calibrator (500 ng/mL) does not exceed 10% of signal of lowest calibrator (1 ng/mL)
Selectivity	Exclusion of non-targeted compounds	No interferences from matrix or internal standards
Matrix Effects	Alteration of signal due to co-elution of matrix components	<25% suppression/enhancement and <15% CV
Limit of Detection (LOD)	Lowest concentration that can be differentiated from a blank sample	Administratively defined as lowest calibrator (1 ng/mL)
Limit of Quantitation (LOQ)	Lowest concentration that can be reliably measured	Administratively defined as lowest calibrator (1 ng/mL)
Precision	Closeness of agreement between multiple samplings	% CV within-run AND between-run must not exceed 20%
Dilution Integrity	Bias and precision are not affected when analyte is diluted	Bias and precision criteria must be met with diluted samples
Stability	Analytes resistance to chemical change	Evaluate length of time that samples stored on autosampler remains stable
Recovery	Determine the degree to which extraction influences signal response	***N/A***

Chapter 3: Results

The order of the results presented in this section is the same as the order in which the studies were performed. First, a sample preparation plate comparison study was performed to assess differences in the precision, matrix effects and recovery of each plate. Second, an extraction and diluent solvent comparison study to assess differences in the precision of each composition. Third, a full suite of quantitative method validation experiments was performed, in accordance with SWGTOX guidelines.[86] Fourth, the comparison of analyte levels and analyte level ratios from rats dosed with each of the three exposure patterns. And lastly, a comparison of the relative distribution of each analyte level and analyte level ratio in the various skeletal elements collected.

3.1 Plate Comparison

The plate comparison study was completed to assess the performance of each of the two extraction plates. Precision, matrix effects, and recovery were calculated for all drugs at low, medium, and high concentrations on both plates.

Precision (Figure 3.1) was measured as the calculated coefficient of variation (CV, %) in RR for all analytes on both plates, each at three different concentrations. Most analytes had acceptable precision (CV < 20%) at all concentrations for both plates. TNO had the poorest precision for both plates, with the MCX plate extraction having calculated CV values in excess of 20% at medium and high concentrations. The MCX plate also had a calculated CV in excess of 20% for TRAM at the high concentration greater than 20%. The Ostro® plate extraction also had a higher calculated CV values for TNO at all concentrations in comparison to the MCX plate, but the calculated precision fell within the acceptable 20% limit at all concentrations.

Matrix effects fell within the acceptable 25% window for all analytes at all concentrations across both plates (Figure 3.2). Matrix effects were consistently calculated as positive on the MCX extraction plate, indicating that ionization enhancement was occurring with this method. Conversely, matrix effects were consistently calculated to be negative using the Ostro® extraction, indicating that ionization suppression was occurring with this method. Additionally, matrix effects were at their lowest at the medium concentration for all analytes, regardless of the plate used.

Recovery ranged widely between analytes, concentrations, and the extraction plate used (Figure 3.3). The MCX plate yielded greater recovery for TRAM, ODMT and NDMT at all concentrations tested than the Ostro® plate. Conversely, the Ostro® plate yielded greater recovery for TNO and NODMT than the MCX plate. The calculated recovery of the Ostro® plate decreased as the concentration increased for all analytes. This trend was less apparent in the MCX extraction plate however it was shown that recovery increased with the concentration for the analytes TNO and NODMT.

These studies showcased that the performance of the MCX and Ostro® extraction plates were comparable. The MCX plate yields a theoretical five-fold enhancement in sample concentration, which can be useful for highly potent analytes found at very low concentrations. However, this signal enhancement can also be incompatible with an instruments linear dynamic range when samples are at a high concentration. Given that both extraction plates have their advantages and disadvantages, it was decided that the Ostro® extraction would be more suitable for the purposes of this study. Tramadol is not a particularly potent drug, so detection at minute concentrations is not necessary. Additionally, the simplified procedure, faster throughput, and comparatively low cost are important advantages of the technology.

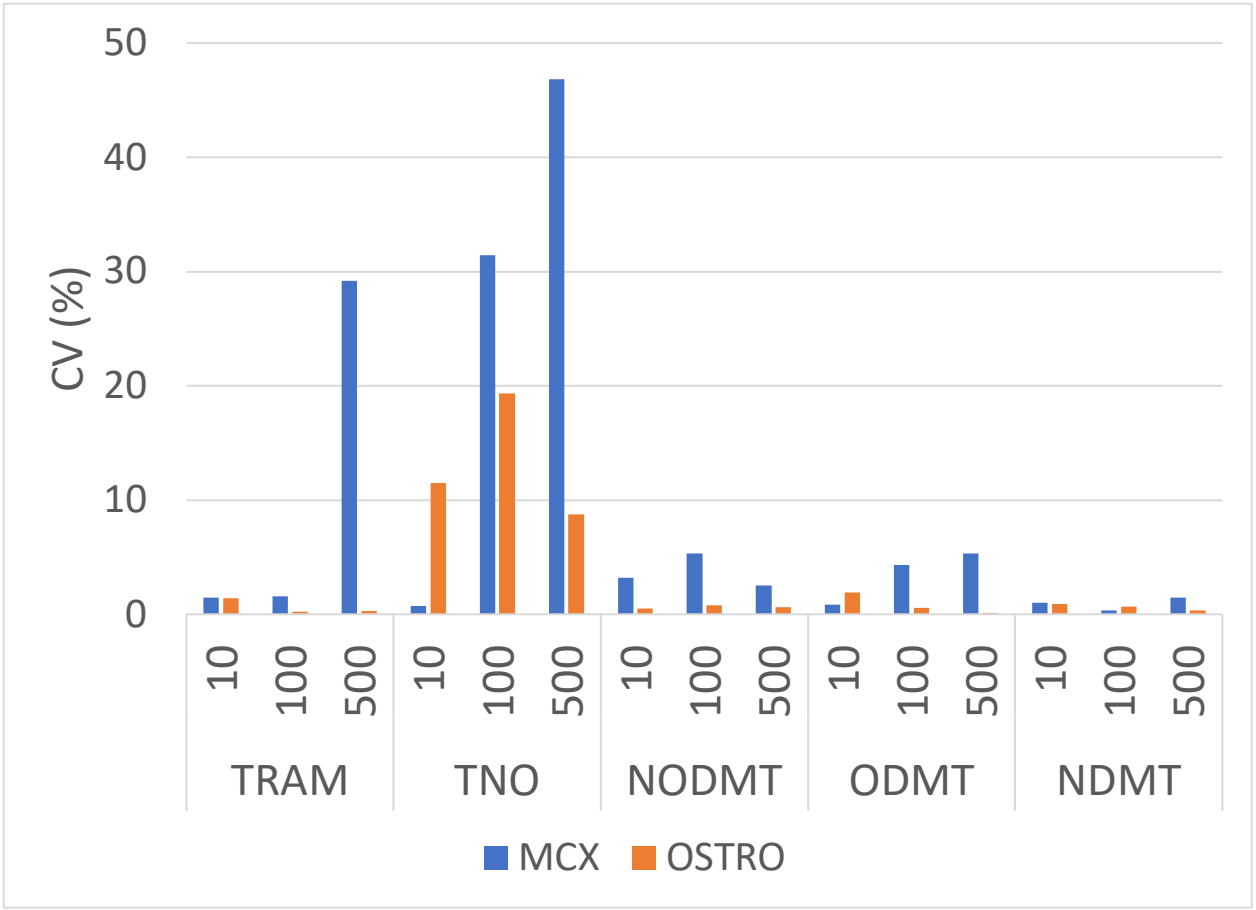

Figure 3.1 Calculated coefficient of variation (CV, %) of each analyte using both plates. Samples were run at low (10 ng/mL), medium (100 ng/mL), and high (500 ng/mL) concentrations.

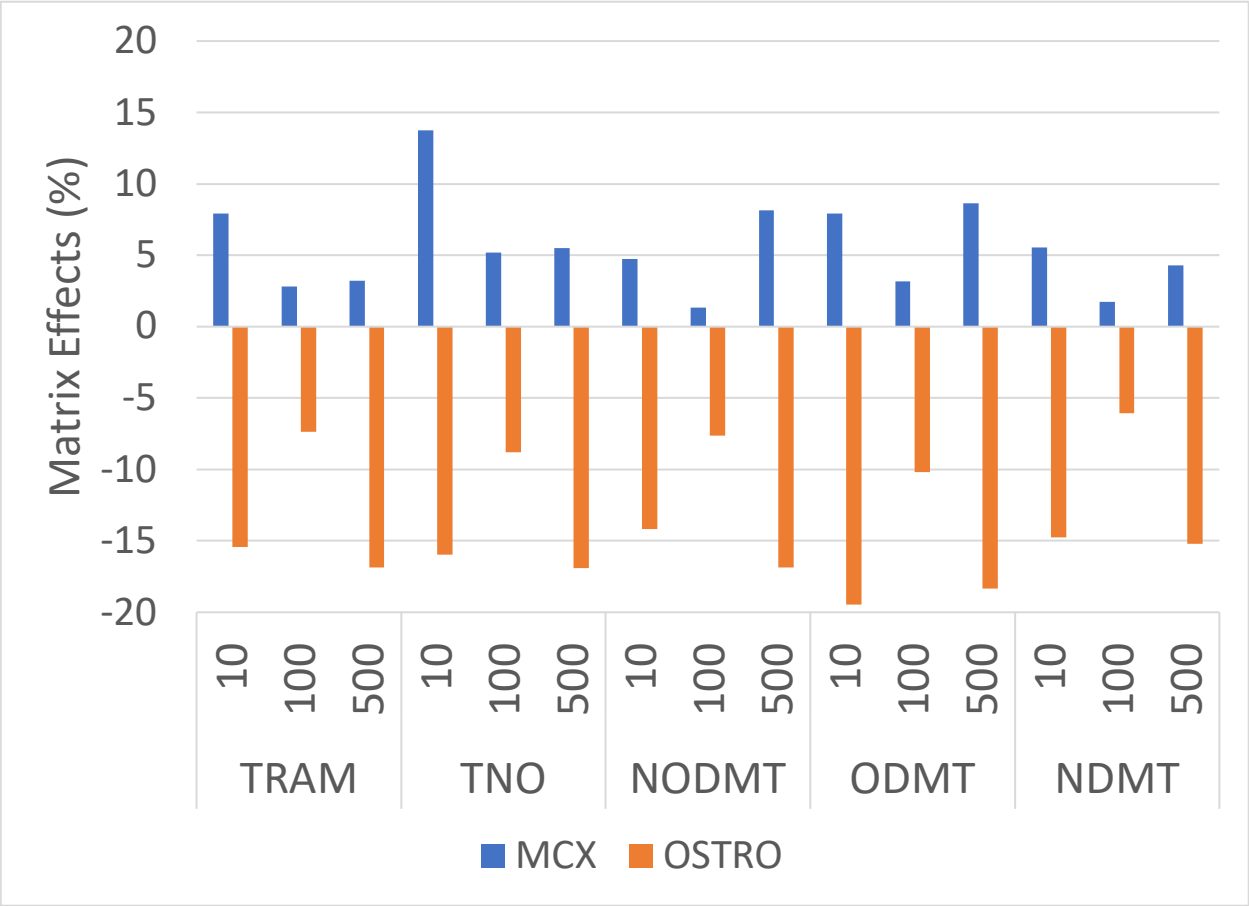

Figure 3.2 Calculated matrix effects (%) for each analyte across both extraction plates. Samples were run at low (10 ng/mL), medium (100 ng/mL), and high (500 ng/mL) concentrations.

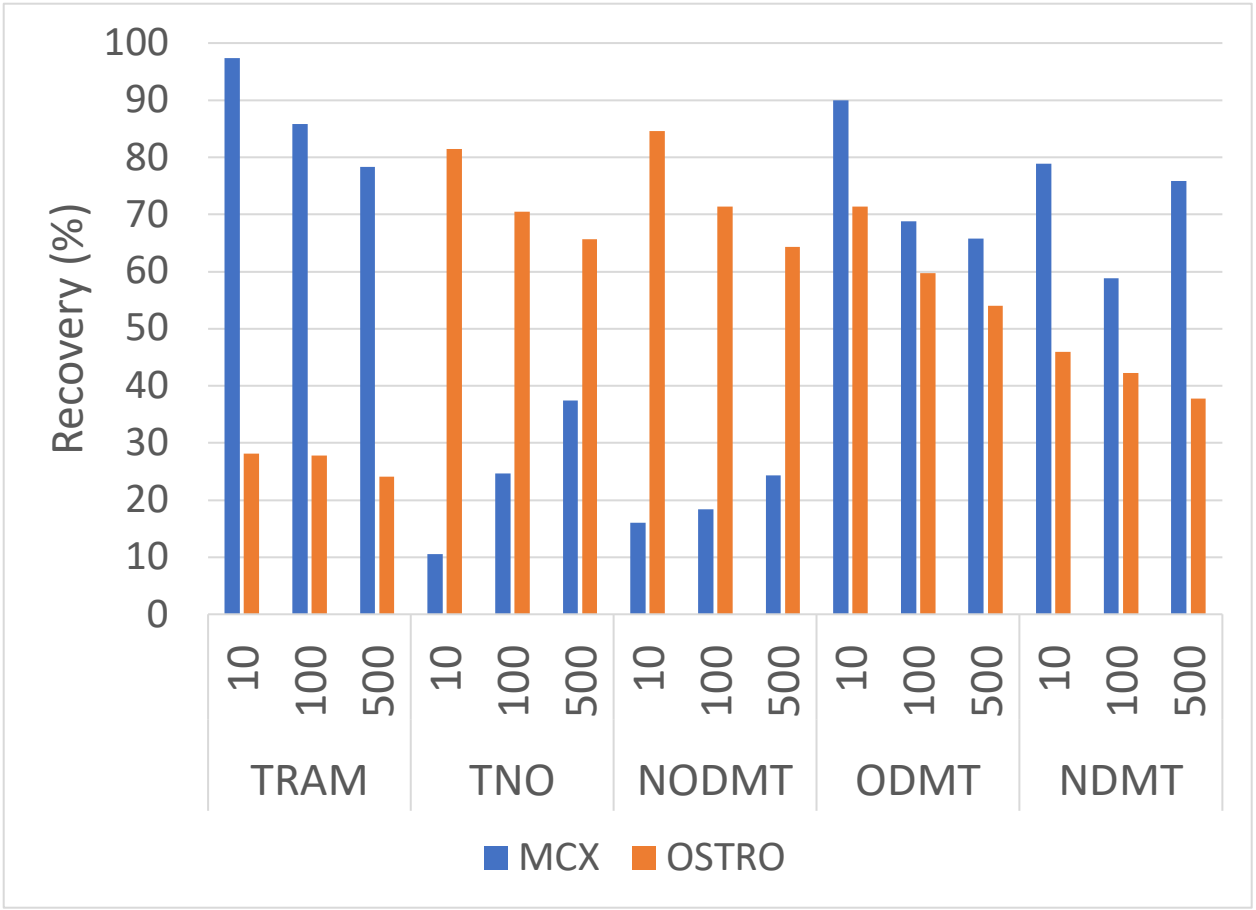

Figure 3.3 Calculated recovery (%) for each analyte across both extraction plates. Samples were run at low (10 ng/mL), medium (100 ng/mL), and high (500 ng/mL) concentrations.

3.2 Extraction and Diluent Solvent Comparison

The results of the extraction solvent comparison study are shown in Figure 3.4. Four different extraction solvent compositions were evaluated for their precision across the five analytes. Samples were made up in each of three different media: BTE, water and methanol. No significant trends were observed in the data. However, of the four extraction solvents, 50:50 (v/v) MeOH:ACN (0.1% FA) was the only one that had CVs lower than 20% in all groups. Pure ACN and acidified ACN (0.1% FA) had the lowest precision in most samples, while 50:50 MeOH:ACN had low precision in only one instance (NODMT in water).

Given the data obtained in this study, 50:50 MeOH:ACN (0.1%) was determined to be the optimal extraction solvent composition for the analysis of tramadol and metabolites.

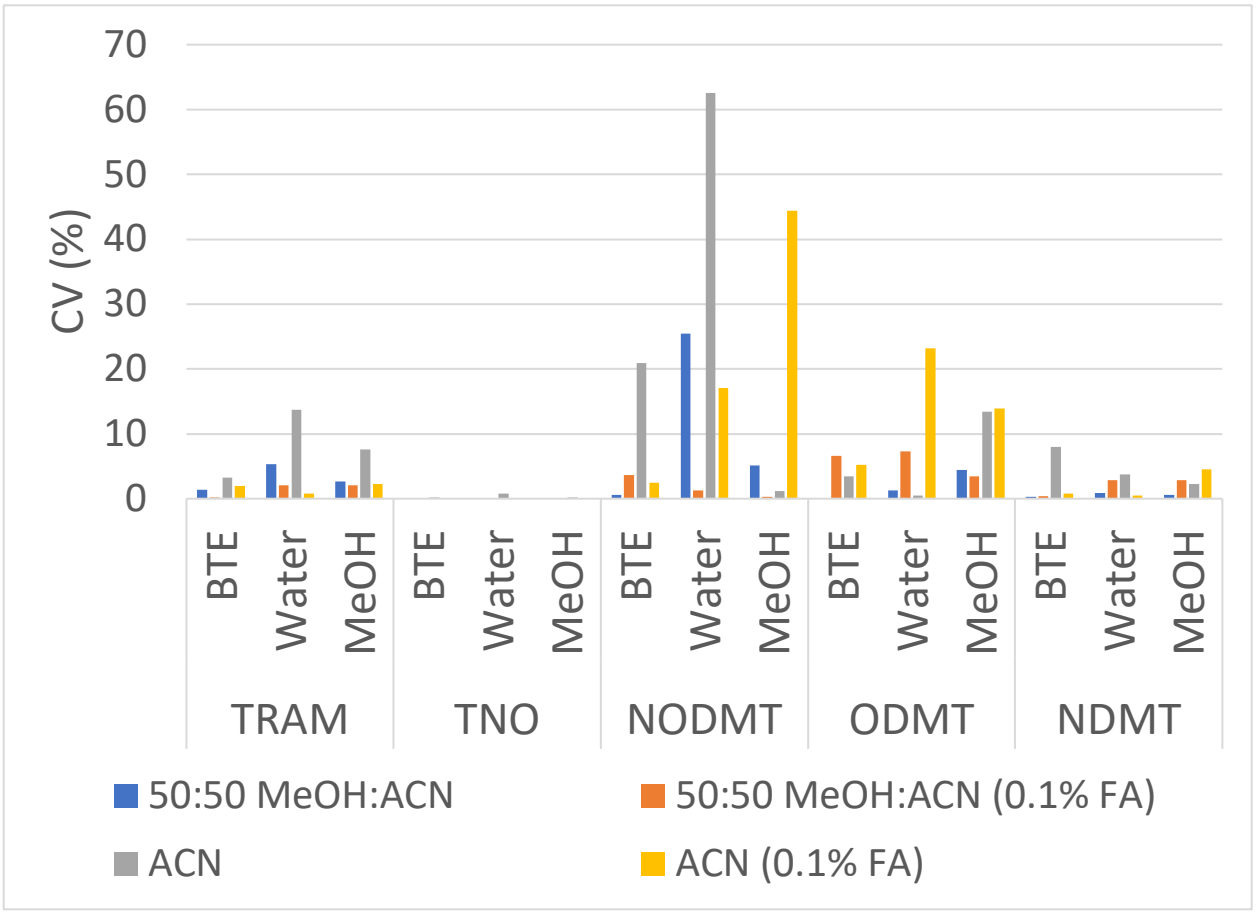

Figure 3.4 Calculated coefficient of variation (CV, %) of three different extraction solvents for use with Waters Ostro® extraction plate. Extraction solvents were used to dilute samples made up in three different media: BTE, water, and methanol. Samples were run in duplicate at a concentration of 250 ng/mL.

3.3 Method Validation – Ostro® Plate Extraction with 0.1% formic acid in 1:1 methanol:acetonitrile as Diluent Solvent

Several studies were performed to assess the reliability and the reproducibility of the method. Studies assessed selectivity, concentration dependence, carryover, limit of detection (LOD), limit of quantitation (LOQ), bias, precision, matrix effects, recovery, dilution integrity and stability.

Selectivity studies showed no interferences from endogenous compounds in any of the three samples run. Additionally, no interference was detected from non-labelled compounds in samples containing only the deuterated internal standards. Likewise, no interference was detected from labelled compounds in samples containing only the analytes investigated.

Standard curves created from analytes over the range of 1-500 ng/mL showed a strong linear trend, with correlation coefficients (R^2) > 0.98 for all analytes, using $1/x^2$ curve weighting. The standard curve for TRAM is shown in Figure 3.5. The LOD and LOQ were both administratively defined as the lowest calibrator, 1 ng/mL. No carryover was observed above the LOD in blank samples run after high concentration calibrants. The LOD was administratively defined as the lowest calibrator, in this case, 1 ng/mL. Likewise, the LOQ was also administratively defined as the lowest calibrator, at 1 ng/mL.

Bias was calculated from calibrants (5, 50, 250 ng/mL) that were run in triplicate over five separate runs. Initial calculations using the linear regression model from Figure 3.6 yielded bias values in excess of the acceptable ± 20% limit. Therefore, the linear model was changed to a weighted linear model, with the observational weights set as $1/x^2$. Using this modified model, the calculated bias fell within the acceptable ± 20% limit for all analytes at all concentrations assayed (Figure 3.6).

Precision was calculated for both within-run and between-run samples. Samples were run in triplicate across five separate runs and samples were made at low, medium, and high concentrations. Precision fell within the acceptable ± 20% window in all cases. The range of coefficients of variation (CV, %) calculated is shown in Table 3.1.

Matrix effects were calculated to be lower than the ± 25% limit in all cases (Figure 3.7). All calculated values were positive, indicating that ionization enhancement was occurring. Additionally, matrix effects were greater at low concentrations than at high concentrations for all analytes. Recovery was also calculated for tramadol and its metabolites at both low and high concentrations (Figure 3.8). In all cases, recovery was greater than 100%, and was higher at low concentrations than at high. Values ranged from 101 to 171%.

The results from the dilution integrity study are shown in Table 3.2. Samples were diluted to both 1:5 and 1:10 ratios, where bias and precision studies were repeated. Values varied widely for all analytes, with some concentrations/dilution ratios exceeding the acceptable ± 20% window. Precision calculations, for both within-run and between-run, showed acceptable results in most cases, whereas bias experiments failed in the majority of cases. This indicates that this method is not suitable for the quantitative evaluation of tramadol and its metabolites in diluted samples, and no such approach was taken in analysis of bone samples from the rats used in this study.

The results of the processed sample stability study are shown in Figures 3.9. All analytes, at both low and high concentrations, displayed a change in average response within the acceptable 20% window. Additionally, the change in average response ratio over the 36 hour period are presented in Figure 3.10. At both low and high concentrations, the change in average response ratio fell within the acceptable 20% window for all analytes. The lack of clear trends in both sets

of data may be indicative of random variation in response within a sample, rather than being indicative of instability or evaporative losses.

These results showcase that this method is suitable for the semi-quantitative analysis of tramadol and five of its metabolites in skeletal tissues. The method successfully met the criteria as laid out by SWGTOX, and also showcased favorable recovery for all of these analytes. The only limitation of this method is that it did not meet the acceptable criteria for the dilution integrity studies. As such, it is not reliable for quantification of these analytes in diluted samples. A summary of the results of the method validation studies is shown in Table 3.2.

Table 3.1 Calculated coefficients of variation (CV, %) of TRAM and metabolites, determined both for within-run and between-run. Samples were run in triplicate over five separate runs at low, medium, and high concentrations.

Drug	Within-Run Precision (CV, %)	Between-Run Precision (CV, %)
TRAM	0.05 – 2.75	2.77 – 5.82
TNO	0.11 – 3.69	1.80 – 7.65
NODMT	0.11 – 4.23	1.62 – 6.28
ODMT	0.07 – 3.70	5.47 – 9.31
NDMT	0.15 – 5.67	4.61 – 7.63

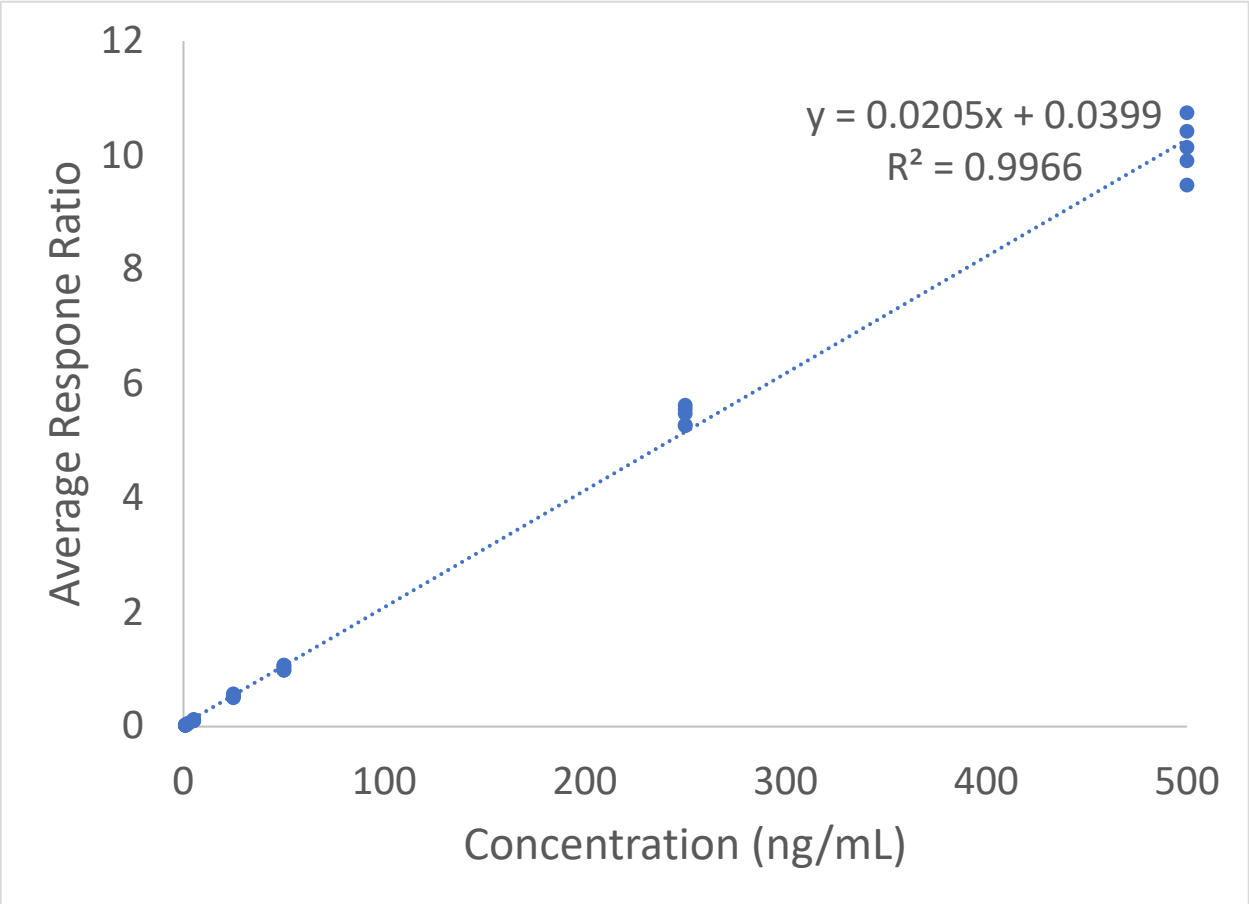

Figure 3.5 Standard curve for TRAM over the range of 1-500 ng/mL. Samples were run in triplicate over five separate runs, at concentrations of 1, 2, 5, 25, 50, 250, and 500 ng/mL.

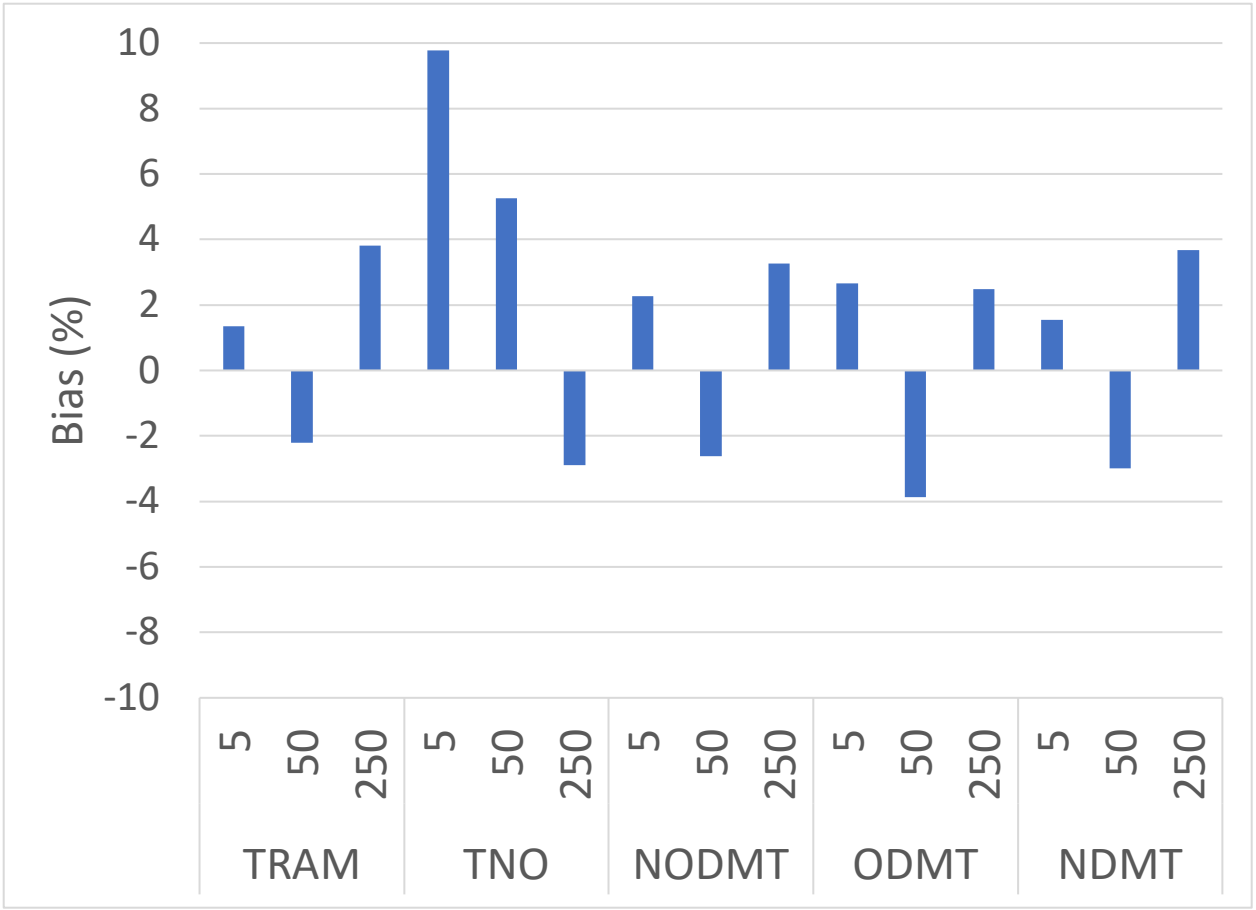

Figure 3.6 Calculated bias (%) for TRAM and its metabolites. Samples were run in triplicate over five different runs at low, medium and high concentrations (5, 50, 250 ng/mL). A weighted linear regression model was used to calculate bias, as the non-weighted model lost linearity at low concentrations. At these concentrations, bias exceeded the acceptable ± 20% limit. With the weighted model, bias was acceptable for all calibrants and at all concentrations.

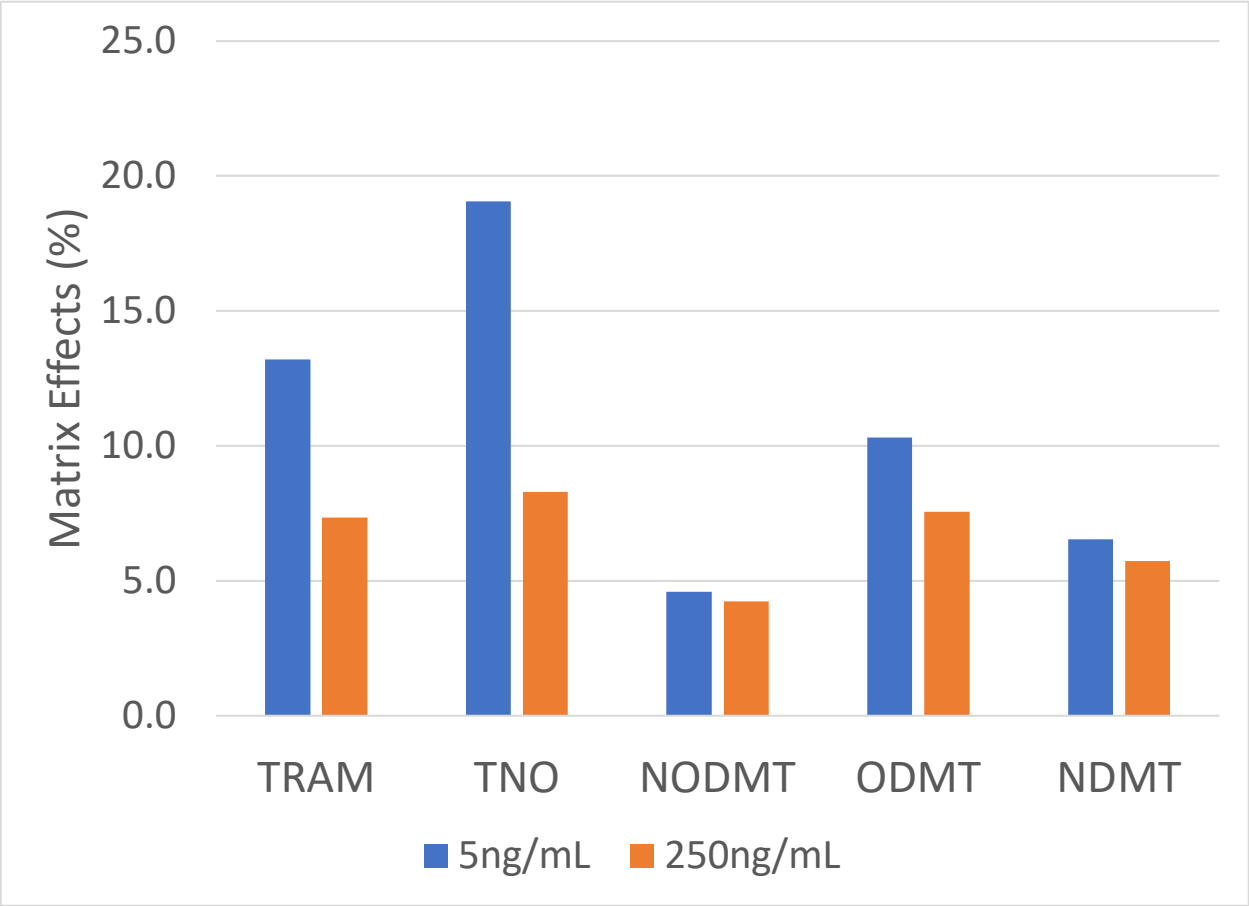

Figure 3.7 Calculated matrix effects for tramadol and its metabolites, at low (5 ng/mL) and high (250 ng/mL) concentrations.

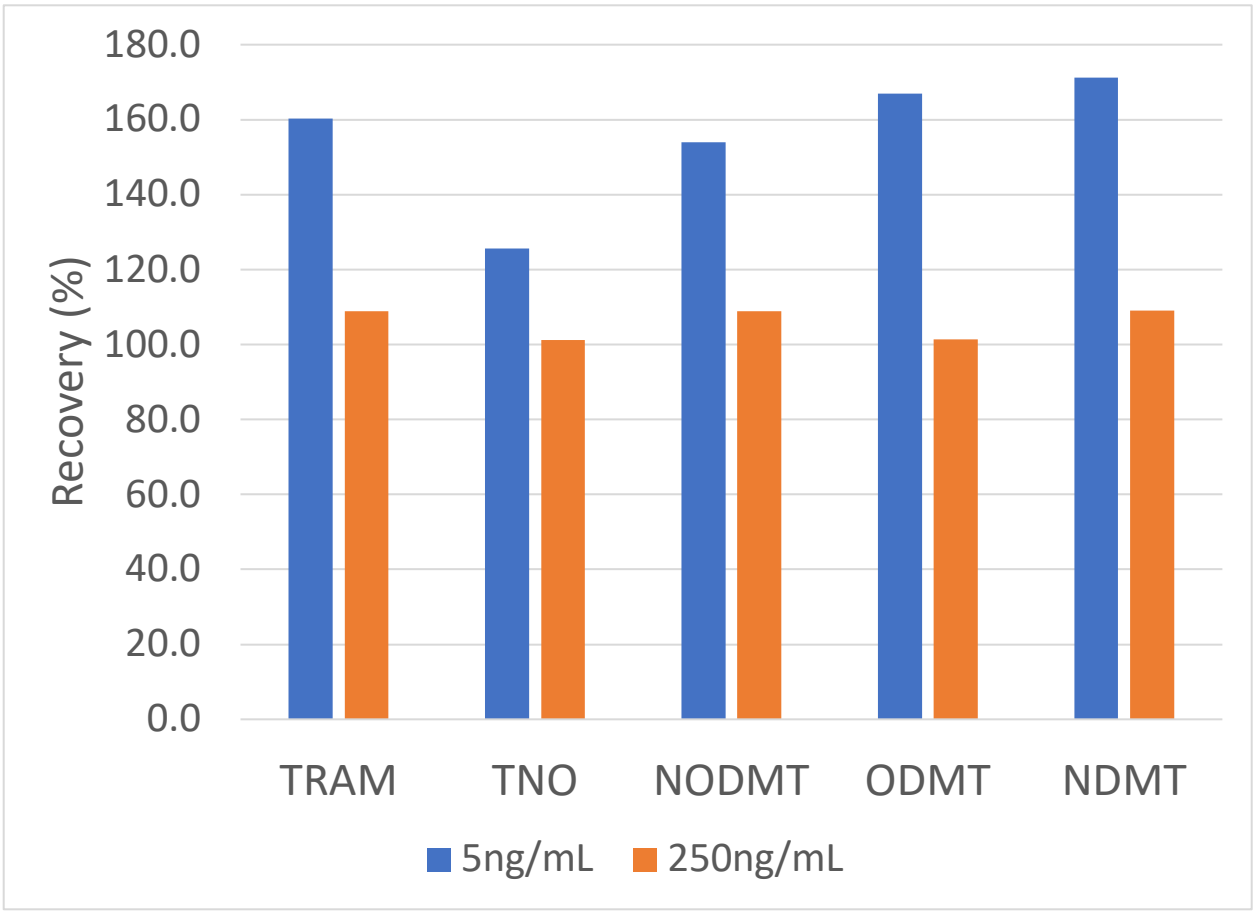

Figure 3.8 Calculated recovery for tramadol and its metabolites, at low (5 ng/mL) and high (250 ng/mL) concentrations.

Table 3.2 Calculated bias and precision at common dilution factors. Values that are both bolded and italicized fell outside of the acceptable ± 20% acceptance window.

	Drug	**5 ng/mL (1:5)**	**5 ng/mL (1:10)**	**100 ng/mL (1:5)**	**100 ng/mL (1:10)**	**250 ng/mL (1:5)**	**250 ng/mL (1:10)**
Bias (%)	TRAM	-13.76	***122.33***	***-29.04***	***-34.50***	***-22.32***	***-24.91***
	TNO	-7.52	-4.56	-16.65	***-24.83***	-8.51	-11.65
	NODMT	-18.08	-2.63	***-35.74***	***-42.68***	***-22.35***	***-26.05***
	ODMT	-10.91	***21.24***	***-59.17***	***-62.33***	***-35.07***	***-38.20***
	NDMT	***-21.61***	-1.76	***-58.02***	***-61.54***	***-31.40***	***-33.39***
Within-run Precision (%)	TRAM	***25.23***	***97.91***	13.91	6.17	***38.75***	17.74
	TNO	4.88	19.11	1.90	1.28	0.78	1.81
	NODMT	5.87	13.28	1.95	1.91	0.09	1.89
	ODMT	6.34	7.87	6.45	5.29	0.45	10.48
	NDMT	2.52	13.85	2.49	2.78	1.02	1.57
Between-run Precision (%)	TRAM	***25.25***	***27.58***	5.48	3.21	8.23	11.51
	TNO	8.80	0.88	8.48	4.32	7.89	7.31
	NODMT	7.74	0.66	6.04	3.48	7.13	10.06
	ODMT	14.22	1.23	7.90	2.33	14.10	***21.30***
	NDMT	14.71	1.46	3.62	2.31	11.44	16.41

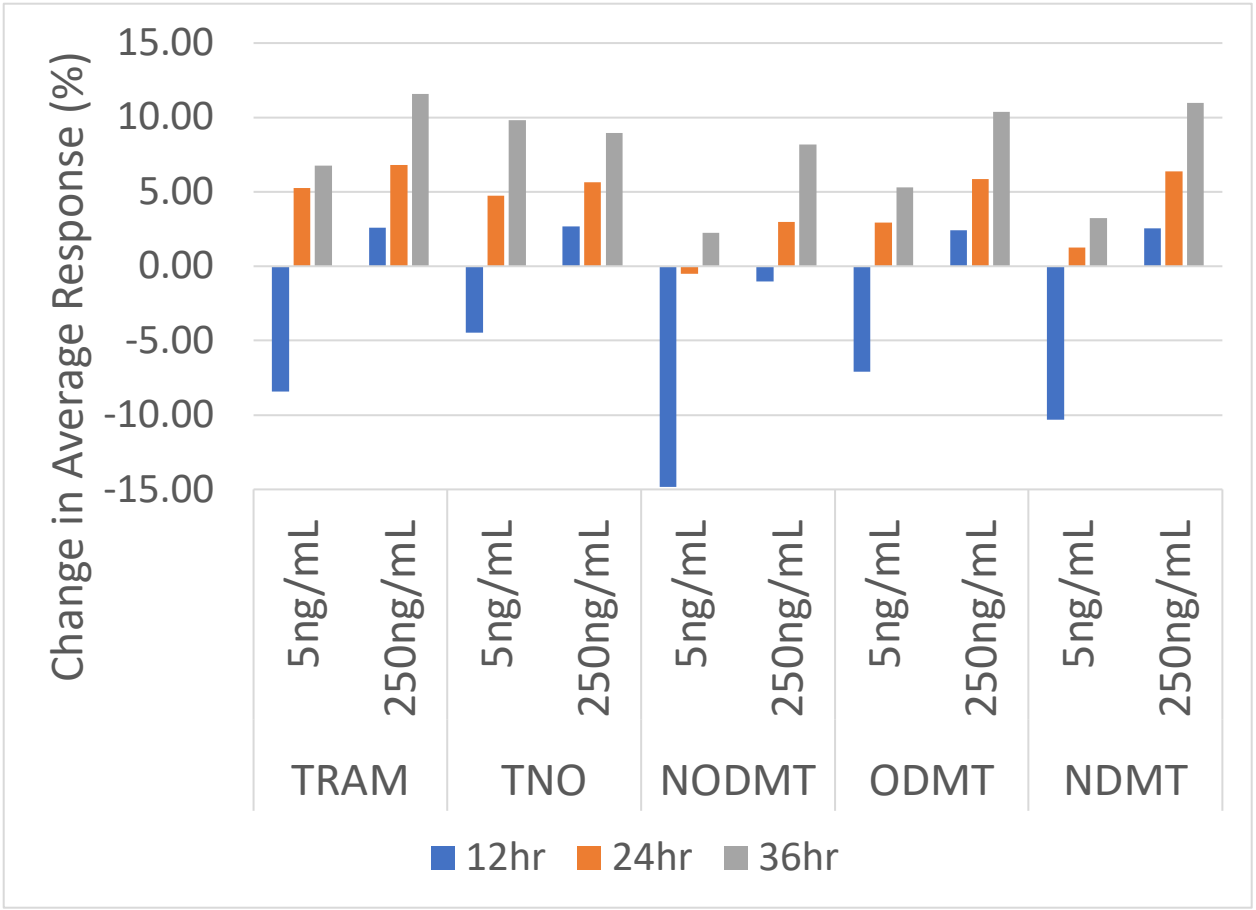

Figure 3.9 Results of processed stability study measured as the change in average response. The acceptable change in average response across the time period assayed is 20%. All analytes, at both low and high concentrations, showcased acceptable results over the course of the 36 hour time period tested.

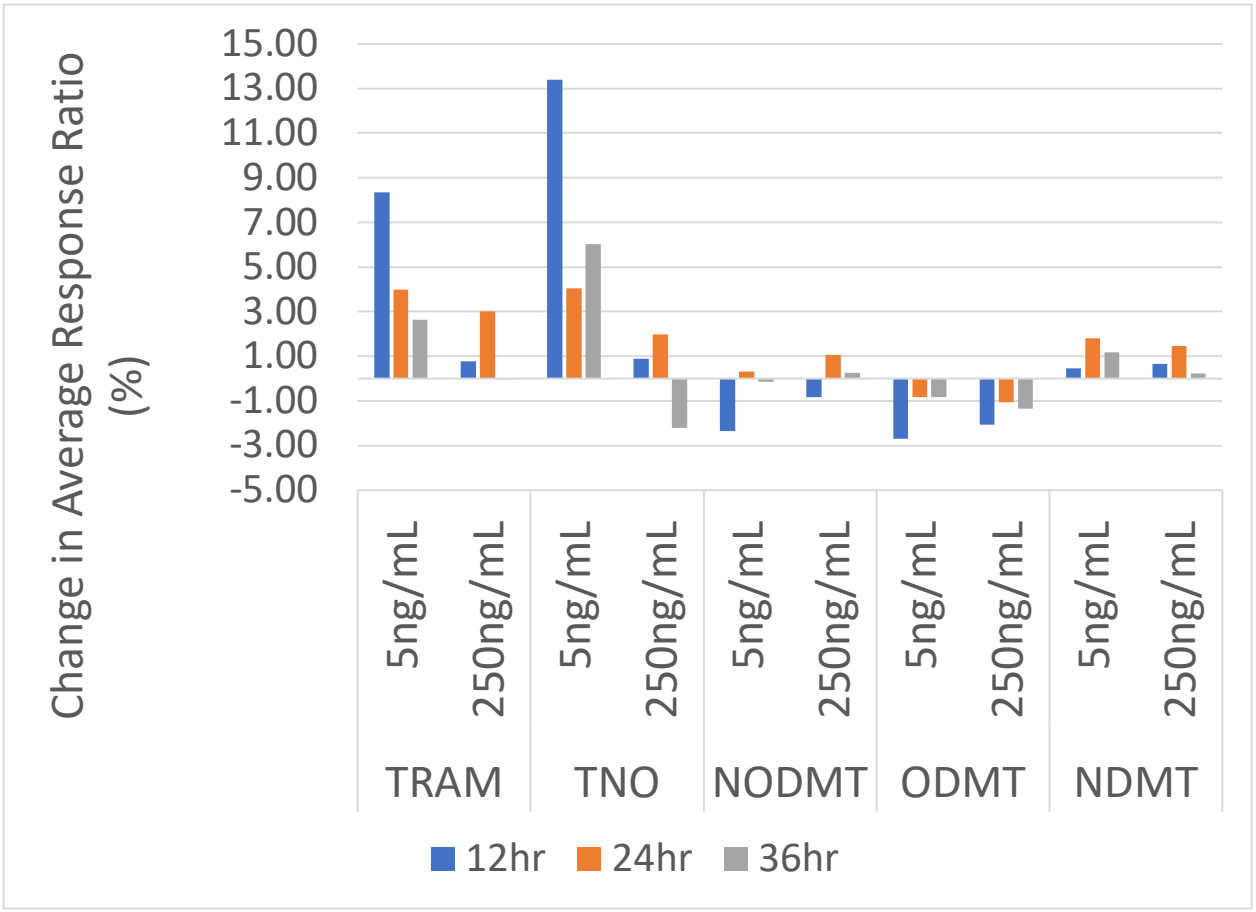

Figure 3.10 Results of processed stability study measured as the change in average response ratio. The acceptable change in average response ratio is 20%. All analytes, at both low and high concentrations, showcased acceptable results over the course of the 36 hour time period tested.

Table 3.3 Summary of method validation results. All parameters showcased acceptable results except for the results from the dilution integrity studies.

Parameter	**Result**	
Bias	Acceptable for all calibrants and analytes	✅
Calibration Model	Linear model has strong R^2	✅
Carryover	No carryover above LOQ	✅
Selectivity	No interferences from internal standards or other analytes	✅
Matrix Effects	Matrix effects within acceptable range (± 25%)	✅
Limit of Detection (LOD)	Administratively determined as lowest calibrator (1 ng/mL)	✅
Limit of Quantitation (LOQ)	Administratively determined as lowest calibrator (1 ng/mL)	✅
Precision	Precision within acceptable limit (20%) for both between-run and within-run	✅
Dilution Integrity	Bias unacceptable at all concentrations; precision acceptable for most concentrations/drugs	❌
Stability	Processed sample stability acceptable over 36 hour period	✅
Recovery	Recovery > 50% at both low and high concentrations	✅

3.4 Comparison of Measures Across Exposure Patterns

The Kruskal-Wallis (KW) test was used for comparison of analyte levels across exposure patterns. Tests were performed for each individual skeletal element, as well as for pooled skeletal elements. Analyte level varied significantly ($P < 0.05$) for all analytes across the three exposure patterns for each of the six skeletal elements examined. Additionally, analyte levels differed significantly for all analytes across the three exposure patterns in pooled skeletal tissues. A total of 35 KW tests were performed. The distribution of mean RR/m values for TRAM and for ODMT in pooled skeletal elements across the three exposure patterns is shown in Figure 3.11 and Figure 3.12, respectively.

The KW test was also used for comparison of analyte level ratios across exposure patterns. Individual skeletal elements were tested for differences, in addition to pooled skeletal elements. A total of 70 KW tests were performed for this purpose. Analyte level ratios varied significantly ($P < 0.05$) in 62 out of 70 tests. The distribution of mean ratio of response (RR/m)/(RR/m) for TRAM/ODMT and for ODMT/NDMT in pooled skeletal elements across the three exposure patterns is shown in Figure 3.13 and Figure 3.14, respectively.

It should be noted that similar plots were made comparing each of the 15 metrics across the three exposure patterns in each of the six skeletal elements collected, in addition to pooled bone tissue. For brevity, only four of these plots are included in this report, as the results are summarized in Tables 3.4 and 3.5 later in this section.

The critical *P* values for comparison of exposure patterns are shown in Appendix I.

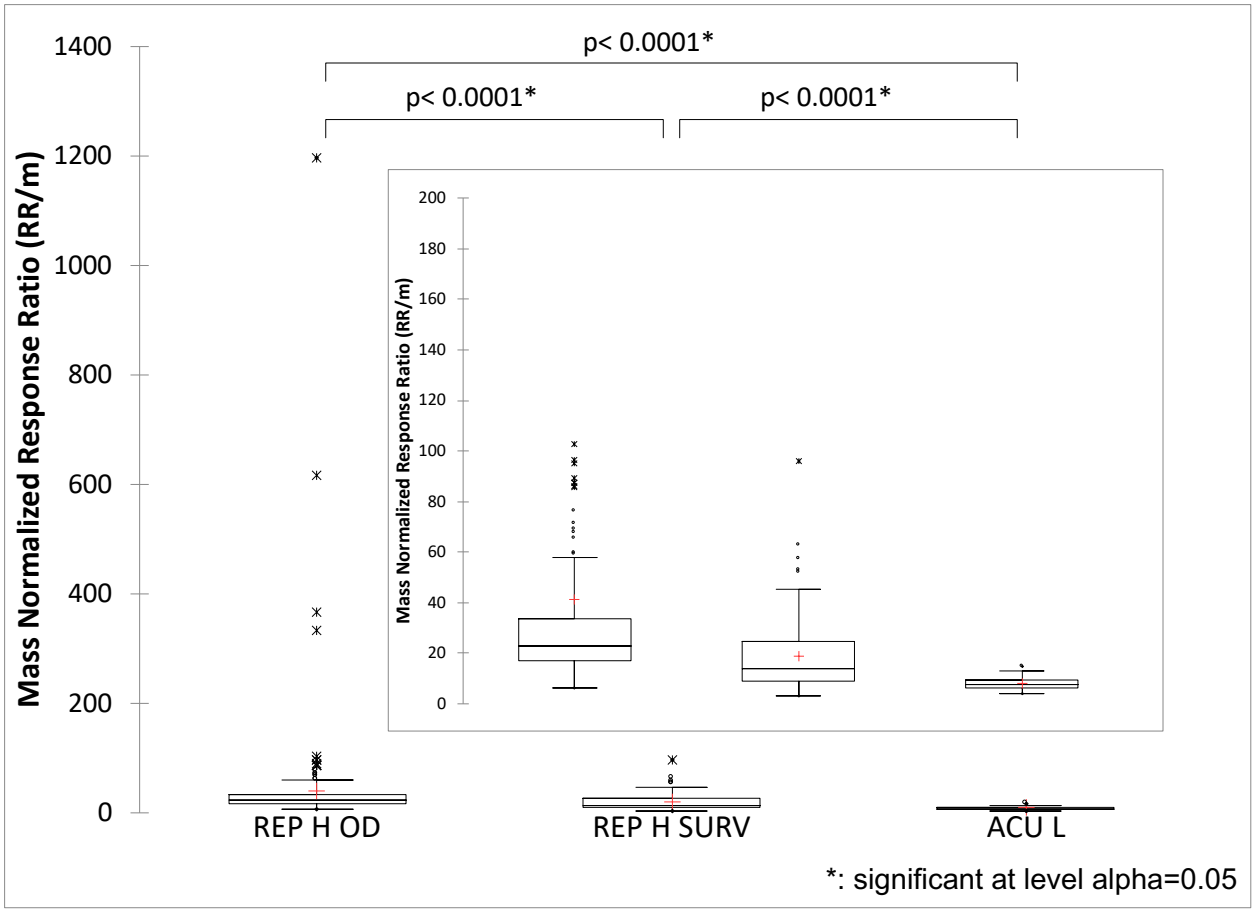

Figure 3.11 Pooled TRAM analyte levels for three exposure patterns in pooled skeletal elements, with expanded view showing shortened y-axis to remove extreme outliers present in the REP H OD group.

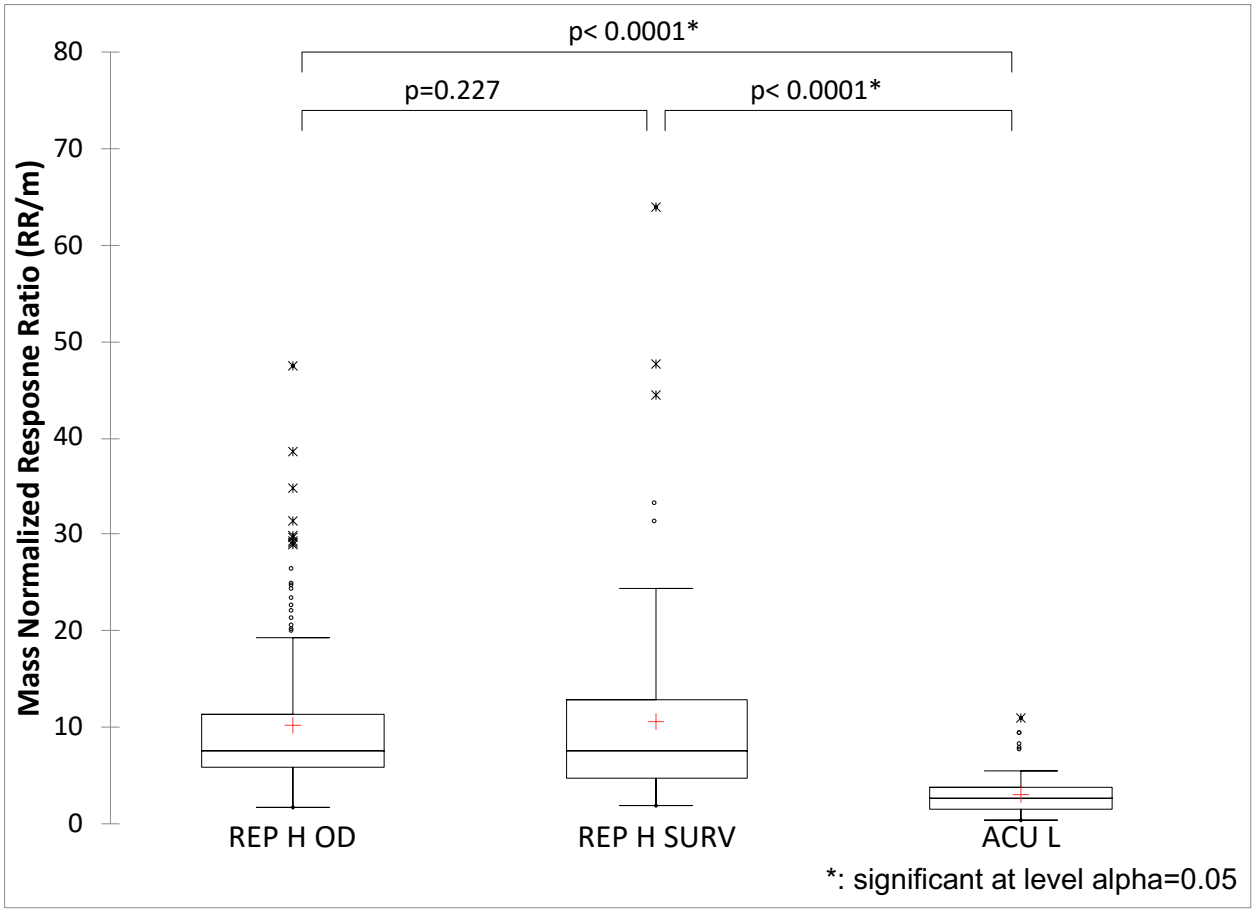

Figure 3.12 Pooled ODMT analyte levels for three exposure patterns in pooled skeletal elements.

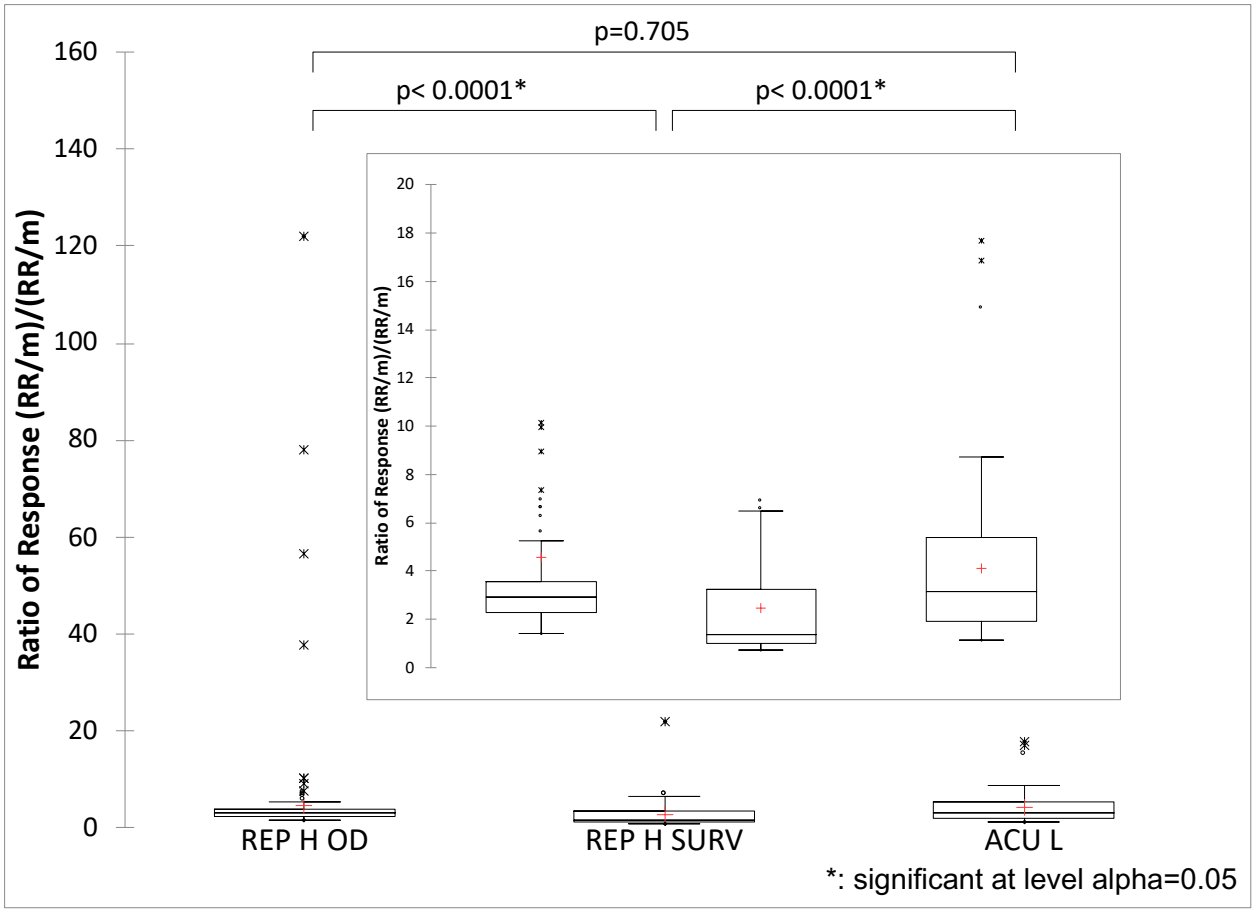

Figure 3.13 Pooled TRAM/ODMT analyte level ratios for three exposure patterns in pooled skeletal elements, with expanded view showing shortened y-axis to remove extreme outliers present in REP H OD group.

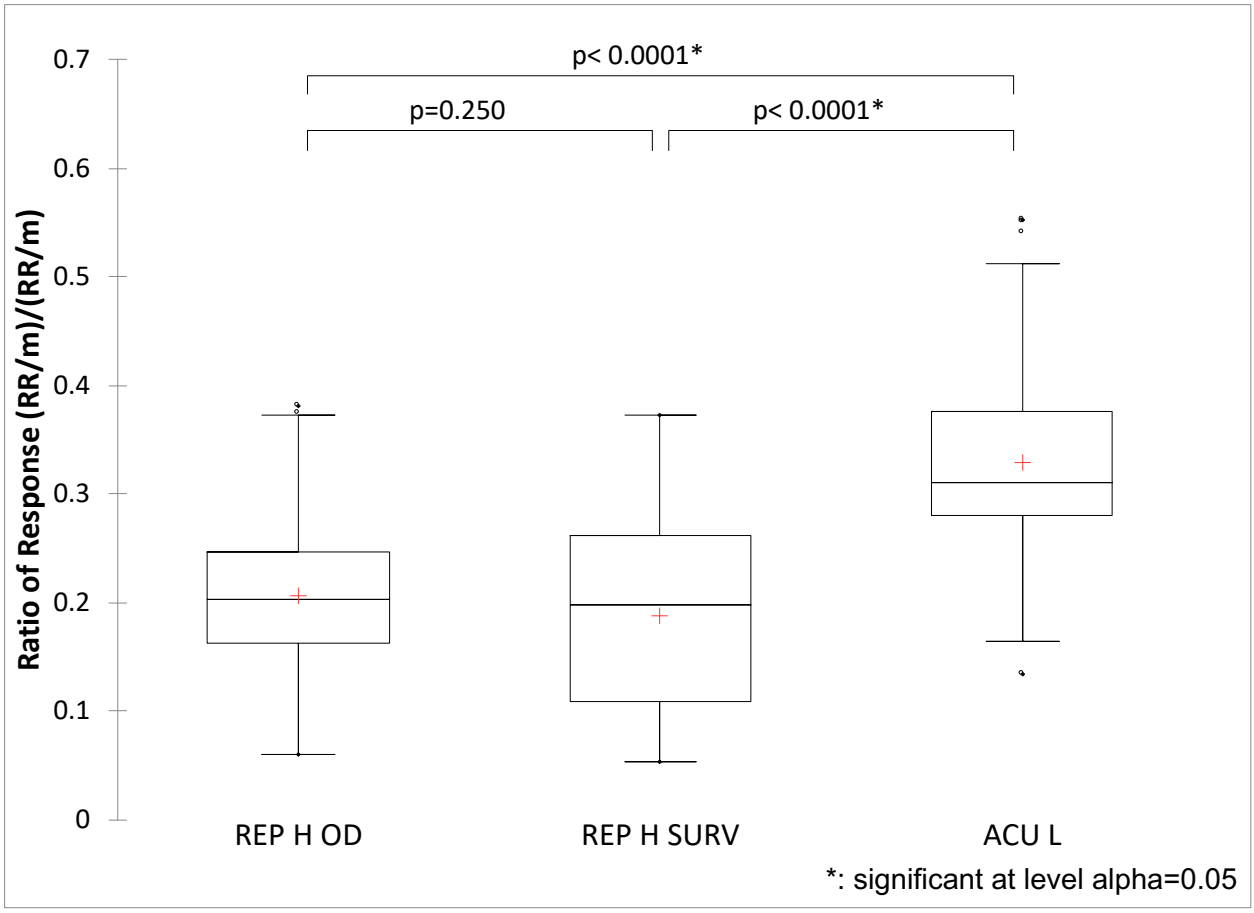

Figure 3.14 Pooled ODMT/NDMT analyte level ratios for three exposure patterns in pooled skeletal elements.

3.5 Summary of Significant Differences across Exposure Patterns

This experiment involved the comparison of 15 different metrics (5 analyte levels and 10 analyte level ratios), measured in six different skeletal elements, with data obtained from animals that underwent one of three exposure patterns. Comparing these various measures leads to an abundance of data that must be sifted through in order to identify useful information. As such, it is important to establish a measure that can provide an immediate glimpse into the results of a study such as this. Previous work in our laboratory has investigated the value of assigning a frequency of significance (F_{sig}), in order to concisely summarize the results obtained in a study such as this.[62] Within each of the six skeletal elements, three pairwise comparisons were generated for each of the 15 metrics to yield a total of 270 pairwise comparisons. Additionally, three pairwise comparisons were generated for each of the 15 metrics in pooled samples, yielding a grand total of 315 pairwise comparisons. F_{sig} values calculated may be combined to create a F_{sig} *score*, which is defined as the percentage of comparisons from a specific metric that yielded significant differences. The F_{sig} and F_{sig} *score* values are shown in Table 3.5.

Table 3.4 Fraction (F_{sig}) of comparisons (across skeletal elements) with significant differences by the KW test ($P < 0.05$).

Measure	REPHOD vs REPHSURV	REPHOD vs ACUL	REPHSURV vs ACUL	F_{sig}
TRAM/NDMT	6/6	4/6	6/6	16/18
TRAM	4/6	6/6	3/6	13/18
NDMT	1/6	6/6	6/6	13/18
ODMT	0/6	6/6	6/6	12/18
TNO	0/6	6/6	6/6	12/18
TRAM/TNO	1/6	5/6	6/6	12/18
ODMT/NDMT	0/6	6/6	6/6	12/18
NDMT/NODMT	0/6	6/6	6/6	12/18
NODMT	0/6	6/6	6/6	12/18
ODMT/NODMT	0/6	5/6	5/6	10/18
NODMT/TNO	1/6	5/6	3/6	9/18
NDMT/TNO	4/6	3/6	2/6	9/18
TRAM/ODMT	5/6	0/6	4/6	9/18
TRAM/NODMT	5/6	0/6	2/6	7/18
ODMT/TNO	0/6	3/6	3/6	6/18

Table 3.5 Scores of comparisons (across skeletal elements and with data pooled by exposure pattern) with significant differences by the KW test ($P < 0.05$).

Measure	F_{sig} (across skeletal elements)	F_{sig} (pooled by exposure pattern)	Total F_{sig} score (%)
TRAM/NDMT	16/18	3/3	90
TRAM	13/18	3/3	76
TNO	12/18	3/3	71
TRAM/TNO	12/18	3/3	71
NDMT	13/18	2/3	71
ODMT	12/18	2/3	67
ODMT/NDMT	12/18	2/3	67
NDMT/NODMT	12/18	2/3	67
NODMT	12/18	2/3	67
NODMT/TNO	9/18	3/3	57
ODMT/NODMT	10/18	2/3	57
NDMT/TNO	9/18	2/3	52
TRAM/ODMT	9/18	2/3	52
ODMT/TNO	6/18	3/3	43
TRAM/NODMT	7/18	2/3	43

3.4 Comparison of Measures Across Skeletal Elements

The Kruskal-Wallis (KW) test was used for comparison of analyte levels across skeletal elements, within each exposure pattern, for a total of 15 KW tests. In all cases (15/15), skeletal element was determined to be a significant factor on analyte level within the different exposure patterns. Differences between analyte level ratios were also tested for using the KW test. A total of 30 KW tests were used to compare analyte level ratios across skeletal elements (within a given exposure pattern). As with the analyte levels, in all cases (30/30) skeletal element was determined to be a significant factor on the analyte level ratio within a given exposure pattern. For the 45 KW tests mentioned above, 15 pairwise comparisons were performed for each of the 15 metrics within each of the three exposure patterns, for a grand total of 675 pairwise comparisons. The *P* values for these comparisons are presented in Appendix II.

The mean mass normalized response ratio for each of the five analytes in pooled skeletal elements across the three exposure patterns are shown in Figure 3.15. Additionally, the mean ratio of response for each of the ten analyte ratios in pooled skeletal elements across the three exposure patterns are shown in Figure 3.16.

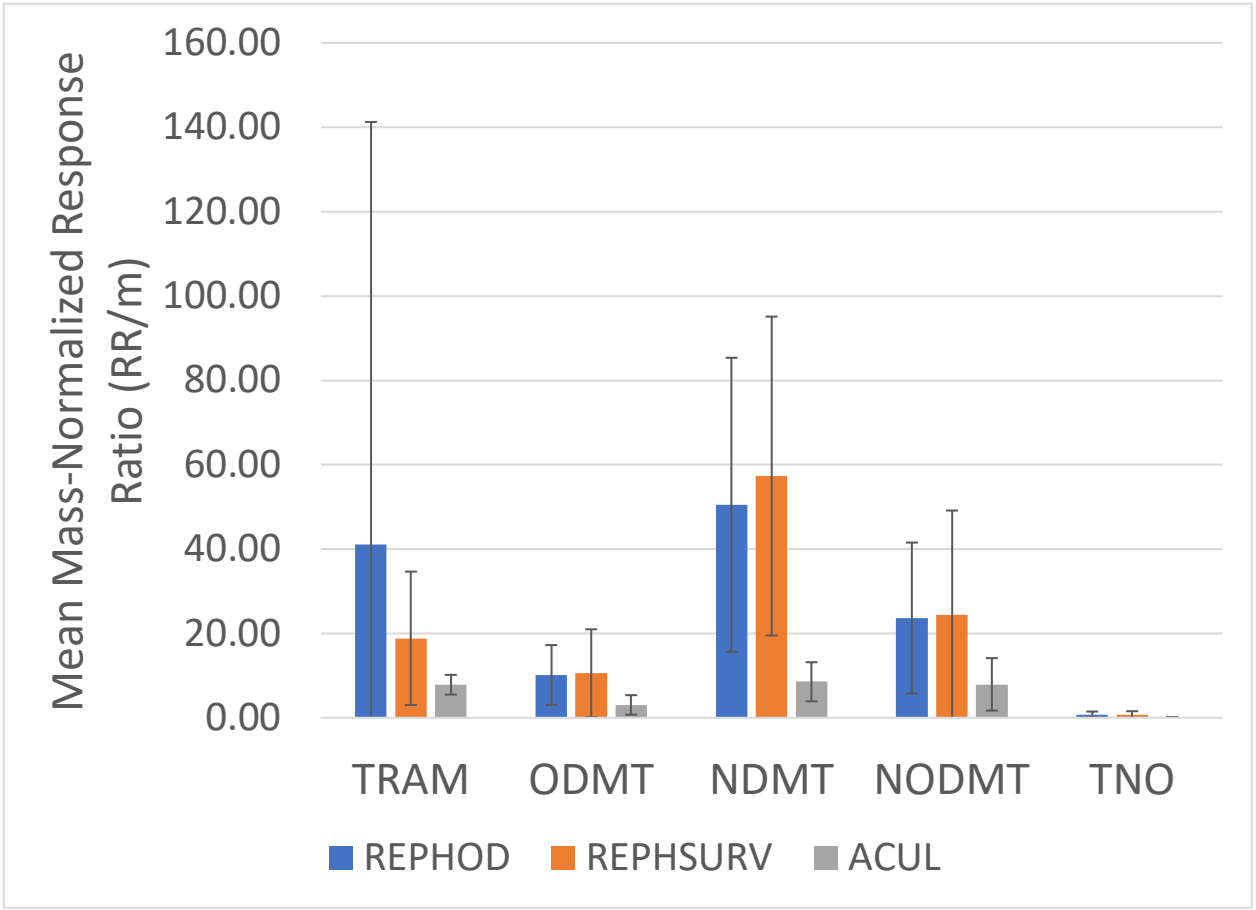

Figure 3.15 Mean (± SD) mass-normalized response ratio of TRAM and its metabolites in pooled skeletal elements for each of the three exposure patterns.

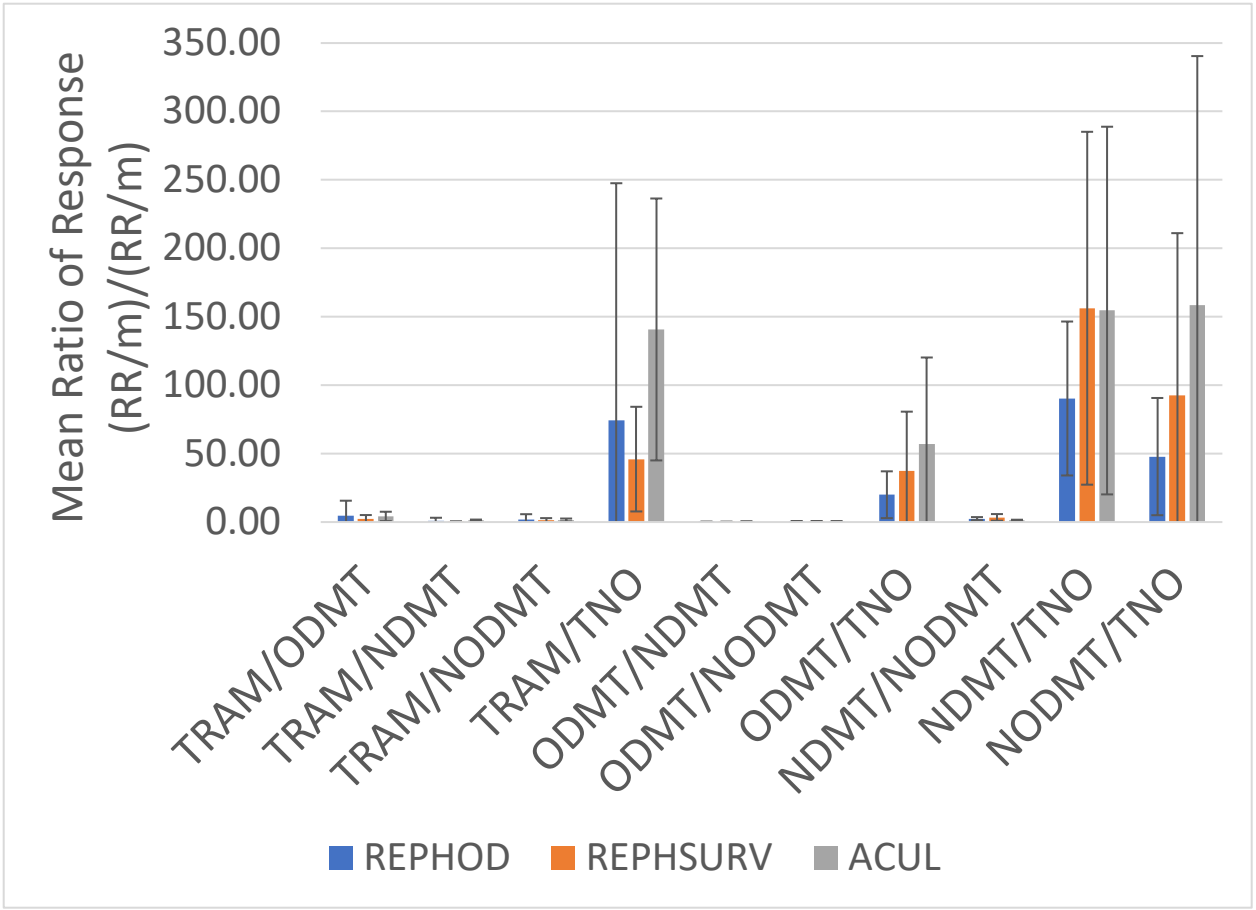

Figure 3.16 Mean (± SD) ratio of response of analyte ratio in pooled skeletal elements for each of the three exposure patterns.

Chapter 4: Discussion

The HPLC-MS/MS method described in this work was specifically developed for the analysis of tramadol and its metabolites in skeletal elements that underwent different exposure patterns. However, the simple sample preparation procedure when combined with the analytical sensitivity and selectivity of HPLC-MS/MS allows for this method to be adapted to a wide range of studies. For example, an experimental design focused on the effects of microclimate or dose death interval on the distribution of tramadol and its metabolites could be easily adapted from this work.

As has been mentioned previously in this text, there exists several issues with utilizing skeletal tissues as an appropriate matrix for analysis. We can account for many of these complications by representing our data as a mass-normalized response ratio (RR/m). This allows us to make comparisons in the instrumental response between samples that differed in the exact mass of bone used. Additionally, as bone samples are ground in such a way as to completely mix both the compact and cancellous portions, the different properties of these two types of bone can be mostly disregarded with respect to replicate sampling from a given bone.

It is important to note that by its nature, tandem mass spectrometry is primarily suited for applications in which an analyte of interest is already suspected of being present in a given sample, as the analyst is required to program the instrument with the molecular information required to successfully recognize a specific compound. While this method may not be suitable for the screening of a wide range of forensically relevant compounds (assuming that a spectral library is not present), the inherently high selectivity and sensitivity of HPLC-MS/MS allows for the successful detection and quantification of compounds at very low concentrations. As such, it remains a valuable analytical tool.

The purpose of this study was threefold. First, the goal was to develop and successfully validate a methodology for the semi-quantitative analysis of tramadol and four of its metabolites using HPLC-MS/MS. This study is based on a previously published study that developed a method for the semi-quantitative analysis of tramadol using UPLC-qTOF-MS.[87] As part of the method validation procedure, a comparison was made of two solid phase extraction plates. This comparison included the measurement of precision, matrix effects, and recovery. As highlighted earlier in this paper, the results from the plate comparison showcased the suitability of the OSTRO® plate for this study. However, it should be noted that the OSTRO® plate had overall lower recovery than that of the MCX plate (< 30% vs. > 70%). This can raise possible issues in cases where a drug may be present in a sample in extremely low concentrations. However, for the purpose of this study, all analytes were detected even at low concentrations (1 ng/mL, the LOD), and as such the lower recovery is acceptable. In fact, the OSTRO® extraction plate involves a five-fold dilution of samples, and as such the actual concentration at the LOD is 0.2ng/mL.

The second, and perhaps most forensically relevant purpose of this study, was to determine whether a given analyte level or analyte level ratio is best suited to distinguish between samples from different exposure patterns. Generally, levels of tramadol were highest in the REP H OD group and lowest in the ACU L group (Figure 3.11). It should be noted that out of all the analytes, TRAM consistently had the largest distribution of RR/m values, including several extreme outliers in the REP H OD group. While the results of the KW tests may differ if these extreme outliers were removed, this practice is not common in the field of forensic toxicology, as the removal of several outliers could exclude important information. These outliers could be resulting from an individual animals' tolerance to the dose of tramadol administered. This is supported by the fact that these extreme outlier points were from animals that overdosed. Metabolite levels were

generally similar in the REP groups, and lower in the ACU L group (Figure 3.12). Comparing the levels of the various metabolites, levels of NDMT were highest, followed by NODMT, ODMT, and lastly TNO, which was only detected in very low amounts, though still greater than the LOD (Figure 3.15). The detection of TNO in low amounts contributes to the extremely large analyte level ratio where TNO is the divisor. Similarly, the aforementioned TRAM extreme outliers contribute to the extremely large analyte level ratios where TRAM is the dividend (Figure 3.16). NDMT being present in the greatest levels may suggest that ODMT, the predominant metabolite of tramadol in humans and rodents,[89] may be more susceptible to degradation post-mortem. As demonstrated in previous studies, the distribution of analyte level ratios shows less variability than the distribution of analyte levels, as can be seen in Figure 3.12 and 3.14. Significant differences (KW, $P < 0.05$) were found in analyte levels and analyte level ratios across the different exposure patterns, as shown in Tables 3.4 and 3.5. The large number of statistical tests performed on the various metrics assessed in this study greatly complicate interpretation of the results. As such, assigning an F_{sig} value greatly simplifies the categorizing of these metrics. Out of the 15 metrics assessed in this study (5 analyte levels and 10 analyte level ratios), only one (TRAM/NDMT) yielded an F_{sig} value greater than 90%. Of particular note is this metrics ability to distinguish between deceased and surviving animals that had received the same dose (REP H OD vs REP H SURV), in all skeletal elements including pooled samples.

The final purpose of this study was to map the relative distribution of both analytes and analyte level ratios across skeletal elements within each of the exposure patterns analyzed. This type of study can provide useful information, such as which skeletal elements may have the highest analyte levels and therefore be may most suitable for sampling. Previously published work in our laboratory using GC-MS has shown that tramadol levels were highest in VRT, followed by SKL,

then PEL, FEM, TIB, and lastly RIB. However, wide variability in response within each skeletal element was also reported.[85] The results of this study also showed wide variability between the various exposure patterns and skeletal elements. In general, TRAM levels were highest in the vertebrae and lowest in the skull. It should be noted that tramadol levels in the vertebrae showed high variation between animal subjects in the REP H OD group. This corresponds to our previously mentioned results, where TRAM showed an extremely high distribution of RR/m values in the REP H OD. Given that the tramadol was administered by intraperitoneal injection, it could be speculated that when the animals overdosed, the drug partitioned first to the vertebral column, given its proximity to the body cavity and its overall size when compared to the other skeletal elements (VRT samples included all vertebrae ranging from the first cervical to the fifth lumbar). Metabolite levels, except for TNO, tended to be greatest in the tibia/fibula and lowest in the skull. TNO levels were greatest in the pelvis and also lowest in the skull. While these findings do not closely correlate with previous work from our laboratory, it indicates that the distribution of a given drug and its analytes throughout the skeletal tissues may be heavily dependent upon a wide variety of factors. These factors could include contact with fluids released during decomposition, the relative proportion of compact to cancellous bone, and the position of the body in which the subject was left post-mortem. This study did not account for these various factors, and as such future work could benefit from a study designed to account for these variables. As mentioned previously, skeletal element was determined to be a significant influence of analyte levels and analyte level ratios within an exposure pattern (in 45/45 KW tests). As such, skeletal element must be accounted for with respect to sampling in cases of toxicological significance.

This work showcases both the analytical power of HPLC-MS/MS in a forensic toxicology context, as well the usefulness of assigning an F_{sig} value to determine the frequency of significant

differences, especially when a large amount of data must be summarized concisely. While similar controlled studies examining the distribution of drugs of abuse and their metabolites in overdosed animal models may be difficult to perform, these studies are still important for the purpose of studying the distribution of these compounds while taking into account external factors that include, but are not limited to, exposure pattern, dose-death interval, microclimate and body position. Future studies should expand the animal model to include pigs, as they share more physiological similarities to humans than rats do. If possible, studies should be conducted on human remains, to examine whether certain drug to metabolite ratios are able to distinguish between different patterns of use. In a medico-legal context, if blood is not readily obtainable for analysis from a cadaver, then skeletal tissues remain one of the few viable alternatives. The ability to potentially determine whether a detected drug was responsible for overdose, or whether the individual was just a recreational user, is enormously important information for a forensic pathologist.

Chapter 5: Conclusion

To the author's knowledge, this is the first study that has examined skeletal drug distribution of tramadol and its metabolites under different exposure conditions using HPLC-MS/MS. Of particular note is this studies' ability to examine the differences in analyte levels and analyte level ratios between overdosed and surviving animals that had received identical doses. Several interesting findings can be reported. First, levels of NDMT were higher than levels of ODMT, which is commonly considered to be tramadol's primary metabolite. This could imply that ODMT is more susceptible to degradation post-mortem, or that NDMT is in fact the primary metabolite in rats at high drug concentrations. Second, both analyte levels and analyte level ratios differ significantly between different dosage patterns and between different skeletal elements. Third, as has been shown in previous work in our laboratory, the assignment of an F_{sig} *score* can simplify interpretation of results and assist in the measurement of a given metrics' analytical value. In this study, the ratio of TRAM/NDMT was able to distinguish between different exposure patterns in over 90% of KW tests performed, including between overdosed and surviving animals that received the same dose.

Future work in this field should focus on the use of F_{sig} scores to determine the effectiveness of a given metric in distinguishing between various factors for a wide array of drugs, and the development of a multivariate statistical analysis approach for predictive modelling of drug exposure patterns. Alternatively, using an additional statistical software program to automate the performance of pairwise comparisons would greatly reduce the amount of labour involved in this study, and would also allow for a larger suite of additional testing to be performed, such as the Bonferroni correction used to compensate for error in multiple comparisons.

Appendix I

Critical *P* Values for Comparison of Exposure Patterns within the Skull

TRAM	p-values:			
		REPHOD	REP H SURV	ACUL
	REPHOD	1	**0.001**	**<0.0001**
	REP H SURV	**0.001**	1	0.277
	ACUL	**<0.0001**	0.277	1

ODMT	p-values:			
		REPHOD	REP H SURV	ACUL
	REPHOD	1	0.452	**0.000**
	REP H SURV	0.452	1	**0.012**
	ACUL	**0.000**	**0.012**	1

NDMT	p-values:			
		REPHOD	REP H SURV	ACUL
	REPHOD	1	0.822	**<0.0001**
	REP H SURV	0.822	1	**<0.0001**
	ACUL	**<0.0001**	**<0.0001**	1

NODMT	p-values:			
		REPHOD	REP H SURV	ACUL
	REPHOD	1	0.261	**0.000**
	REP H SURV	0.261	1	**<0.0001**
	ACUL	**0.000**	**<0.0001**	1

TNO	p-values:			
		REPHOD	REP H SURV	ACUL
	REPHOD	1	0.076	**<0.0001**
	REP H SURV	0.076	1	**0.012**
	ACUL	**<0.0001**	**0.012**	1

TRAM/ODMT	p-values:			
		REPHOD	REP H SURV	ACUL
	REPHOD	1	**0.006**	0.856
	REP H SURV	**0.006**	1	**0.018**
	ACUL	0.856	**0.018**	1

TRAM/NDMT	p-values:			
		REPHOD	REP H SURV	ACUL
	REPHOD	1	**<0.0001**	**0.000**
	REP H SURV	**<0.0001**	1	**<0.0001**
	ACUL	**0.000**	**<0.0001**	1

TRAM/NODMT	p-values:			
		REPHOD	REP H SURV	ACUL
	REPHOD	1	**0.000**	0.594
	REP H SURV	**0.000**	1	**0.016**
	ACUL	0.594	**0.016**	1

TRAM/TNO	p-values:			
		REPHOD	REP H SURV	ACUL
	REPHOD	1	0.394	**0.004**
	REP H SURV	0.394	1	**0.002**
	ACUL	**0.004**	**0.002**	1

ODMT/NDMT	p-values:			
		REPHOD	REP H SURV	ACUL
	REPHOD	1	0.591	**<0.0001**
	REP H SURV	0.591	1	**<0.0001**
	ACUL	**<0.0001**	**<0.0001**	1

ODMT/NODMT	p-values:			
		REPHOD	REP H SURV	ACUL
	REPHOD	1	0.193	0.961
	REP H SURV	0.193	1	0.276
	ACUL	0.961	0.276	1

ODMT/TNO	p-values:			
		REPHOD	REP H SURV	ACUL
	REPHOD	1	0.147	0.087
	REP H SURV	0.147	1	0.747
	ACUL	0.087	0.747	1

NDMT/NODMT	p-values:			
		REPHOD	REP H SURV	ACUL
	REPHOD	1	0.708	**<0.0001**
	REP H SURV	0.708	1	**<0.0001**
	ACUL	**<0.0001**	**<0.0001**	1

NDMT/TNO	p-values:			
		REPHOD	REP H SURV	ACUL
	REPHOD	1	0.200	0.111
	REP H SURV	0.200	1	**0.016**
	ACUL	0.111	**0.016**	1

NODMT/TNO	p-values:			
		REPHOD	REP H SURV	ACUL
	REPHOD	1	0.084	**0.019**
	REP H SURV	0.084	1	0.519
	ACUL	**0.019**	0.519	1

Critical *P* Values for Comparison of Exposure Patterns within the Vertebrae

TRAM p-values:

	REPHOD	REP H SURV	ACUL
REPHOD	1	**<0.0001**	**<0.0001**
REP H SURV	**<0.0001**	1	0.166
ACUL	**<0.0001**	0.166	1

ODMT p-values:

	REPHOD	REP H SURV	ACUL
REPHOD	1	0.086	**<0.0001**
REP H SURV	0.086	1	**0.014**
ACUL	**<0.0001**	**0.014**	1

NDMT p-values:

	REPHOD	REP H SURV	ACUL
REPHOD	1	0.564	**<0.0001**
REP H SURV	0.564	1	**0.000**
ACUL	**<0.0001**	**0.000**	1

NODMT p-values:

	REPHOD	REP H SURV	ACUL
REPHOD	1	0.079	**0.000**
REP H SURV	0.079	1	**0.031**
ACUL	**0.000**	**0.031**	1

TNO p-values:

	REPHOD	REP H SURV	ACUL
REPHOD	1	0.059	**<0.0001**
REP H SURV	0.059	1	**0.004**
ACUL	**<0.0001**	**0.004**	1

TRAM/ODMT p-values:

	REPHOD	REP H SURV	ACUL
REPHOD	1	**0.007**	0.758
REP H SURV	**0.007**	1	0.092
ACUL	0.758	0.092	1

TRAM/NDMT p-values:

	REPHOD	REP H SURV	ACUL
REPHOD	1	**<0.0001**	0.184
REP H SURV	**<0.0001**	1	**<0.0001**
ACUL	0.184	**<0.0001**	1

TRAM/NODMT p-values:

	REPHOD	REP H SURV	ACUL
REPHOD	1	**0.005**	0.326
REP H SURV	**0.005**	1	0.246
ACUL	0.326	0.246	1

TRAM/TNO p-values:

	REPHOD	REP H SURV	ACUL
REPHOD	1	0.319	**0.000**
REP H SURV	0.319	1	**<0.0001**
ACUL	**0.000**	**<0.0001**	1

ODMT/NDMT p-values:

	REPHOD	REP H SURV	ACUL
REPHOD	1	0.710	**0.000**
REP H SURV	0.710	1	**0.000**
ACUL	**0.000**	**0.000**	1

ODMT/NODMT p-values:

	REPHOD	REP H SURV	ACUL
REPHOD	1	0.829	**<0.0001**
REP H SURV	0.829	1	**0.000**
ACUL	**<0.0001**	**0.000**	1

ODMT/TNO p-values:

	REPHOD	REP H SURV	ACUL
REPHOD	1	0.190	**<0.0001**
REP H SURV	0.190	1	**0.010**
ACUL	**<0.0001**	**0.010**	1

NDMT/NODMT	p-values:			
		REPHOD	REP H SURV	ACUL
	REPHOD	1	0.537	**<0.0001**
	REP H SURV	0.537	1	**<0.0001**
	ACUL	**<0.0001**	**<0.0001**	1

NDMT/TNO	p-values:			
		REPHOD	REP H SURV	ACUL
	REPHOD	1	**0.016**	**0.000**
	REP H SURV	**0.016**	1	0.092
	ACUL	**0.000**	0.092	1

NODMT/TNO	p-values:			
		REPHOD	REP H SURV	ACUL
	REPHOD	1	0.201	**<0.0001**
	REP H SURV	0.201	1	**0.004**
	ACUL	**<0.0001**	**0.004**	1

Critical *P* Values for Comparison of Exposure Patterns within the Ribs

TRAM	p-values:			
		REPHOD	REP H SURV	ACUL
	REPHOD	1	**0.003**	**<0.0001**
	REP H SURV	**0.003**	1	0.223
	ACUL	**<0.0001**	0.223	1

ODMT	p-values:			
		REPHOD	REP H SURV	ACUL
	REPHOD	1	0.146	**<0.0001**
	REP H SURV	0.146	1	**0.005**
	ACUL	**<0.0001**	**0.005**	1

NDMT	p-values:			
		REPHOD	REP H SURV	ACUL
	REPHOD	1	0.978	**<0.0001**
	REP H SURV	0.978	1	**<0.0001**
	ACUL	**<0.0001**	**<0.0001**	1

NODMT	p-values:			
		REPHOD	REP H SURV	ACUL
	REPHOD	1	0.199	**<0.0001**
	REP H SURV	0.199	1	**0.009**
	ACUL	**<0.0001**	**0.009**	1

TNO	p-values:			
		REPHOD	REP H SURV	ACUL
	REPHOD	1	0.879	**<0.0001**
	REP H SURV	0.879	1	**0.000**
	ACUL	**<0.0001**	**0.000**	1

TRAM/ODMT	p-values:			
		REPHOD	REP H SURV	ACUL
	REPHOD	1	**0.007**	0.721
	REP H SURV	**0.007**	1	**0.017**
	ACUL	0.721	**0.017**	1

TRAM/NDMT	p-values:			
		REPHOD	REP H SURV	ACUL
	REPHOD	1	**<0.0001**	0.050
	REP H SURV	**<0.0001**	1	**<0.0001**
	ACUL	0.050	**<0.0001**	1

TRAM/NODMT	p-values:			
		REPHOD	REP H SURV	ACUL
	REPHOD	1	**0.012**	0.842
	REP H SURV	**0.012**	1	0.086
	ACUL	0.842	0.086	1

TRAM/TNO	p-values:			
		REPHOD	REP H SURV	ACUL
	REPHOD	1	**0.010**	0.175
	REP H SURV	**0.010**	1	**0.002**
	ACUL	0.175	**0.002**	1

ODMT/NDMT	p-values:			
		REPHOD	REP H SURV	ACUL
	REPHOD	1	0.365	**0.002**
	REP H SURV	0.365	1	**0.001**
	ACUL	**0.002**	**0.001**	1

ODMT/NODMT	p-values:			
		REPHOD	REP H SURV	ACUL
	REPHOD	1	0.868	**0.007**
	REP H SURV	0.868	1	**0.023**
	ACUL	**0.007**	**0.023**	1

ODMT/TNO	p-values:			
		REPHOD	REP H SURV	ACUL
	REPHOD	1	0.796	0.139
	REP H SURV	0.796	1	0.130
	ACUL	0.139	0.130	1

NDMT/NODMT	p-values:			
		REPHOD	REP H SURV	ACUL
	REPHOD	1	0.211	**0.000**
	REP H SURV	0.211	1	**<0.0001**
	ACUL	**0.000**	**<0.0001**	1

NDMT/TNO	p-values:			
		REPHOD	REP H SURV	ACUL
	REPHOD	1	0.949	0.959
	REP H SURV	0.949	1	0.925
	ACUL	0.959	0.925	1

NODMT/TNO	p-values:			
		REPHOD	REP H SURV	ACUL
	REPHOD	1	0.554	0.092
	REP H SURV	0.554	1	0.051
	ACUL	0.092	0.051	1

Critical *P* Values for Comparison of Exposure Patterns within the Pelvis

TRAM	p-values:			
		REPHOD	REP H SURV	ACUL
	REPHOD	1	**0.012**	**<0.0001**
	REP H SURV	**0.012**	1	**0.011**
	ACUL	**<0.0001**	**0.011**	1

ODMT	p-values:			
		REPHOD	REP H SURV	ACUL
	REPHOD	1	0.280	**<0.0001**
	REP H SURV	0.280	1	**0.001**
	ACUL	**<0.0001**	**0.001**	1

NDMT	p-values:			
		REPHOD	REP H SURV	ACUL
	REPHOD	1	0.964	**<0.0001**
	REP H SURV	0.964	1	**<0.0001**
	ACUL	**<0.0001**	**<0.0001**	1

NODMT	p-values:			
		REPHOD	REP H SURV	ACUL
	REPHOD	1	0.348	**<0.0001**
	REP H SURV	0.348	1	**0.002**
	ACUL	**<0.0001**	**0.002**	1

TNO	p-values:			
		REPHOD	REP H SURV	ACUL
	REPHOD	1	0.070	**<0.0001**
	REP H SURV	0.070	1	**0.001**
	ACUL	**<0.0001**	**0.001**	1

TRAM/ODMT	p-values:			
		REPHOD	REP H SURV	ACUL
	REPHOD	1	0.097	0.776
	REP H SURV	0.097	1	0.277
	ACUL	0.776	0.277	1

TRAM/NDMT	p-values:			
		REPHOD	REP H SURV	ACUL
	REPHOD	1	**0.000**	**0.003**
	REP H SURV	**0.000**	1	**<0.0001**
	ACUL	**0.003**	**<0.0001**	1

TRAM/NODMT	p-values:			
		REPHOD	REP H SURV	ACUL
	REPHOD	1	0.139	0.424
	REP H SURV	0.139	1	0.620
	ACUL	0.424	0.620	1

TRAM/TNO	p-values:			
		REPHOD	REP H SURV	ACUL
	REPHOD	1	0.428	**<0.0001**
	REP H SURV	0.428	1	**<0.0001**
	ACUL	**<0.0001**	**<0.0001**	1

ODMT/NDMT	p-values:			
		REPHOD	REP H SURV	ACUL
	REPHOD	1	0.406	**<0.0001**
	REP H SURV	0.406	1	**<0.0001**
	ACUL	**<0.0001**	**<0.0001**	1

ODMT/NODMT	p-values:			
		REPHOD	REP H SURV	ACUL
	REPHOD	1	0.977	**0.001**
	REP H SURV	0.977	1	**0.004**
	ACUL	**0.001**	**0.004**	1

ODMT/TNO	p-values:			
		REPHOD	REP H SURV	ACUL
	REPHOD	1	0.368	**0.000**
	REP H SURV	0.368	1	**0.012**
	ACUL	**0.000**	**0.012**	1

NDMT/NODMT	p-values:			
		REPHOD	REP H SURV	ACUL
	REPHOD	1	0.574	**<0.0001**
	REP H SURV	0.574	1	**<0.0001**
	ACUL	**<0.0001**	**<0.0001**	1

NDMT/TNO	p-values:			
		REPHOD	REP H SURV	ACUL
	REPHOD	1	**0.017**	**0.020**
	REP H SURV	**0.017**	1	0.908
	ACUL	**0.020**	0.908	1

NODMT/TNO	p-values:			
		REPHOD	REP H SURV	ACUL
	REPHOD	1	0.267	**<0.0001**
	REP H SURV	0.267	1	**0.005**
	ACUL	**<0.0001**	**0.005**	1

Critical *P* Values for Comparison of Exposure Patterns within the Femur

TRAM p-values:

	REPHOD	REP H SURV	ACUL
REPHOD	1	0.130	**<0.0001**
REP H SURV	0.130	1	**0.002**
ACUL	**<0.0001**	**0.002**	1

ODMT p-values:

	REPHOD	REP H SURV	ACUL
REPHOD	1	0.331	**<0.0001**
REP H SURV	0.331	1	**<0.0001**
ACUL	**<0.0001**	**<0.0001**	1

NDMT p-values:

	REPHOD	REP H SURV	ACUL
REPHOD	1	0.247	**<0.0001**
REP H SURV	0.247	1	**<0.0001**
ACUL	**<0.0001**	**<0.0001**	1

NODMT p-values:

	REPHOD	REP H SURV	ACUL
REPHOD	1	0.348	**<0.0001**
REP H SURV	0.348	1	**0.002**
ACUL	**<0.0001**	**0.002**	1

TNO p-values:

	REPHOD	REP H SURV	ACUL
REPHOD	1	0.418	**<0.0001**
REP H SURV	0.418	1	**0.000**
ACUL	**<0.0001**	**0.000**	1

TRAM/ODMT p-values:

	REPHOD	REP H SURV	ACUL
REPHOD	1	**0.018**	0.693
REP H SURV	**0.018**	1	**0.025**
ACUL	0.693	**0.025**	1

TRAM/NDMT p-values:

	REPHOD	REP H SURV	ACUL
REPHOD	1	**<0.0001**	**0.001**
REP H SURV	**<0.0001**	1	**<0.0001**
ACUL	**0.001**	**<0.0001**	1

TRAM/NODMT p-values:

	REPHOD	REP H SURV	ACUL
REPHOD	1	**0.010**	0.701
REP H SURV	**0.010**	1	**0.017**
ACUL	0.701	**0.017**	1

TRAM/TNO p-values:

	REPHOD	REP H SURV	ACUL
REPHOD	1	0.888	**<0.0001**
REP H SURV	0.888	1	**0.001**
ACUL	**<0.0001**	**0.001**	1

ODMT/NDMT p-values:

	REPHOD	REP H SURV	ACUL
REPHOD	1	0.592	**0.000**
REP H SURV	0.592	1	**0.013**
ACUL	**0.000**	**0.013**	1

ODMT/NODMT	p-values:			
		REPHOD	REP H SURV	ACUL
	REPHOD	1	0.775	**0.007**
	REP H SURV	0.775	1	**0.013**
	ACUL	**0.007**	**0.013**	1

ODMT/TNO	p-values:			
		REPHOD	REP H SURV	ACUL
	REPHOD	1	0.053	0.068
	REP H SURV	0.053	1	0.966
	ACUL	0.068	0.966	1

NDMT/NODMT	p-values:			
		REPHOD	REP H SURV	ACUL
	REPHOD	1	0.601	**<0.0001**
	REP H SURV	0.601	1	**0.000**
	ACUL	**<0.0001**	**0.000**	1

NDMT/TNO	p-values:			
		REPHOD	REP H SURV	ACUL
	REPHOD	1	**0.002**	0.831
	REP H SURV	**0.002**	1	**0.020**
	ACUL	0.831	**0.020**	1

NODMT/TNO	p-values:			
		REPHOD	REP H SURV	ACUL
	REPHOD	1	**0.022**	**0.007**
	REP H SURV	**0.022**	1	0.676
	ACUL	**0.007**	0.676	1

Critical *P* Values for Comparison of Exposure Patterns within the Tibia and Fibula

TRAM p-values:

	REPHOD	REP H SURV	ACUL
REPHOD	1	0.592	**<0.0001**
REP H SURV	0.592	1	**0.000**
ACUL	**<0.0001**	**0.000**	1

ODMT p-values:

	REPHOD	REP H SURV	ACUL
REPHOD	1	0.105	**0.000**
REP H SURV	0.105	1	**<0.0001**
ACUL	**0.000**	**<0.0001**	1

NDMT p-values:

	REPHOD	REP H SURV	ACUL
REPHOD	1	**0.038**	**<0.0001**
REP H SURV	**0.038**	1	**<0.0001**
ACUL	**<0.0001**	**<0.0001**	1

NODMT p-values:

	REPHOD	REP H SURV	ACUL
REPHOD	1	0.261	**0.000**
REP H SURV	0.261	1	**<0.0001**
ACUL	**0.000**	**<0.0001**	1

TNO p-values:

	REPHOD	REP H SURV	ACUL
REPHOD	1	0.757	**<0.0001**
REP H SURV	0.757	1	**<0.0001**
ACUL	**<0.0001**	**<0.0001**	1

TRAM/ODMT p-values:

	REPHOD	REP H SURV	ACUL
REPHOD	1	**0.006**	0.856
REP H SURV	**0.006**	1	**0.018**
ACUL	0.856	**0.018**	1

TRAM/NDMT p-values:

	REPHOD	REP H SURV	ACUL
REPHOD	1	**<0.0001**	**0.026**
REP H SURV	**<0.0001**	1	**<0.0001**
ACUL	**0.026**	**<0.0001**	1

TRAM/NODMT p-values:

	REPHOD	REP H SURV	ACUL
REPHOD	1	**0.007**	0.269
REP H SURV	**0.007**	1	0.209
ACUL	0.269	0.209	1

TRAM/TNO p-values:

	REPHOD	REP H SURV	ACUL
REPHOD	1	0.838	**<0.0001**
REP H SURV	0.838	1	**<0.0001**
ACUL	**<0.0001**	**<0.0001**	1

ODMT/NDMT p-values:

	REPHOD	REP H SURV	ACUL
REPHOD	1	0.846	**<0.0001**
REP H SURV	0.846	1	**0.002**
ACUL	**<0.0001**	**0.002**	1

ODMT/NODMT p-values:

	REPHOD	REP H SURV	ACUL
REPHOD	1	0.144	**0.000**
REP H SURV	0.144	1	**<0.0001**
ACUL	**0.000**	**<0.0001**	1

ODMT/TNO p-values:

	REPHOD	REP H SURV	ACUL
REPHOD	1	0.074	**<0.0001**
REP H SURV	0.074	1	**0.032**
ACUL	**<0.0001**	**0.032**	1

NDMT/NODMT	p-values:			
		REPHOD	REP H SURV	ACUL
	REPHOD	1	0.876	**<0.0001**
	REP H SURV	0.876	1	**<0.0001**
	ACUL	**<0.0001**	**<0.0001**	1

NDMT/TNO	p-values:			
		REPHOD	REP H SURV	ACUL
	REPHOD	1	**0.018**	**<0.0001**
	REP H SURV	**0.018**	1	0.118
	ACUL	**<0.0001**	0.118	1

NODMT/TNO	p-values:			
		REPHOD	REP H SURV	ACUL
	REPHOD	1	0.128	**<0.0001**
	REP H SURV	0.128	1	**0.007**
	ACUL	**<0.0001**	**0.007**	1

Critical *P* Values for Comparison of Exposure Patterns within Pooled Skeletal Elements

TRAM	p-values:			
		REP H OD	REP H SURV	ACU L
	REP H OD	1	**<0.0001**	**<0.0001**
	REP H SURV	**<0.0001**	1	**<0.0001**
	ACU L	**<0.0001**	**<0.0001**	1

ODMT	p-values:			
		REP H OD	REP H SURV	ACU L
	REP H OD	1	0.227	**<0.0001**
	REP H SURV	0.227	1	**<0.0001**
	ACU L	**<0.0001**	**<0.0001**	1

NDMT	p-values:			
		REP H OD	REP H SURV	ACU L
	REP H OD	1	0.264	**<0.0001**
	REP H SURV	0.264	1	**<0.0001**
	ACU L	**<0.0001**	**<0.0001**	1

NODMT	p-values:			
		REP H OD	REP H SURV	ACU L
	REP H OD	1	0.285	**<0.0001**
	REP H SURV	0.285	1	**<0.0001**
	ACU L	**<0.0001**	**<0.0001**	1

TNO	p-values:			
		REP H OD	REP H SURV	ACU L
	REP H OD	1	**0.015**	**<0.0001**
	REP H SURV	**0.015**	1	**<0.0001**
	ACU L	**<0.0001**	**<0.0001**	1

TRAM/ODMT	p-values:			
		REP H OD	REP H SURV	ACU L
	REP H OD	1	**<0.0001**	0.705
	REP H SURV	**<0.0001**	1	**<0.0001**
	ACU L	0.705	**<0.0001**	1

TRAM/NDMT	p-values:			
		REP H OD	REP H SURV	ACU L
	REP H OD	1	**<0.0001**	**<0.0001**
	REP H SURV	**<0.0001**	1	**<0.0001**
	ACU L	**<0.0001**	**<0.0001**	1

TRAM/NODMT	p-values:			
		REP H OD	REP H SURV	ACU L
	REP H OD	1	**<0.0001**	0.421
	REP H SURV	**<0.0001**	1	**0.000**
	ACU L	0.421	**0.000**	1

TRAM/TNO	p-values:			
		REP H OD	REP H SURV	ACU L
	REP H OD	1	**0.019**	**<0.0001**
	REP H SURV	**0.019**	1	**<0.0001**
	ACU L	**<0.0001**	**<0.0001**	1

ODMT/NDMT	p-values:			
		REP H OD	REP H SURV	ACU L
	REP H OD	1	0.250	**<0.0001**
	REP H SURV	0.250	1	**<0.0001**
	ACU L	**<0.0001**	**<0.0001**	1

ODMT/NODMT	p-values:			
		REP H OD	REP H SURV	ACU L
	REP H OD	1	0.989	**<0.0001**
	REP H SURV	0.989	1	**<0.0001**
	ACU L	**<0.0001**	**<0.0001**	1

ODMT/TNO	p-values:			
		REP H OD	REP H SURV	ACU L
	REP H OD	1	**0.019**	**<0.0001**
	REP H SURV	**0.019**	1	**0.001**
	ACU L	**<0.0001**	**0.001**	1

NDMT/NODMT	p-values:			
		REP H OD	REP H SURV	ACU L
	REP H OD	1	0.174	**<0.0001**
	REP H SURV	0.174	1	**<0.0001**
	ACU L	**<0.0001**	**<0.0001**	1

NDMT/TNO	p-values:			
		REP H OD	REP H SURV	ACU L
	REP H OD	1	**<0.0001**	**0.001**
	REP H SURV	**<0.0001**	1	0.649
	ACU L	**0.001**	0.649	1

NODMT/TNO	p-values:			
		REP H OD	REP H SURV	ACU L
	REP H OD	1	**0.048**	**<0.0001**
	REP H SURV	**0.048**	1	**0.000**
	ACU L	**<0.0001**	**0.000**	1

Appendix II

Critical *P* Values for Comparison of Skeletal Elements within REP H OD Exposure Pattern

TRAM	p-values:						
		SKL	VRT	RIB	PEL	FEM	TIB/FIB
	SKL	1	<0.0001	0.529	<0.0001	<0.0001	<0.0001
	VRT	<0.0001	1	<0.0001	0.137	0.101	0.319
	RIB	0.529	<0.0001	1	<0.0001	<0.0001	<0.0001
	PEL	<0.0001	0.137	<0.0001	1	0.880	0.624
	FEM	<0.0001	0.101	<0.0001	0.880	1	0.521
	TIB/FIB	<0.0001	0.319	<0.0001	0.624	0.521	1
ODMT	p-values:						
		SKL	VRT	RIB	PEL	FEM	TIB/FIB
	SKL	1	<0.0001	0.344	0.009	0.581	<0.0001
	VRT	<0.0001	1	<0.0001	0.000	<0.0001	0.740
	RIB	0.344	<0.0001	1	0.106	0.684	<0.0001
	PEL	0.009	0.000	0.106	1	0.038	0.001
	FEM	0.581	<0.0001	0.684	0.038	1	<0.0001
	TIB/FIB	<0.0001	0.740	<0.0001	0.001	<0.0001	1
NDMT	p-values:						
		SKL	VRT	RIB	PEL	FEM	TIB/FIB
	SKL	1	<0.0001	0.204	0.011	0.022	0.001
	VRT	<0.0001	1	<0.0001	0.036	0.018	0.146
	RIB	0.204	<0.0001	1	0.000	0.000	<0.0001
	PEL	0.011	0.036	0.000	1	0.795	0.517
	FEM	0.022	0.018	0.000	0.795	1	0.364
	TIB/FIB	0.001	0.146	<0.0001	0.517	0.364	1
NODMT	p-values:						
		SKL	VRT	RIB	PEL	FEM	TIB/FIB
	SKL	1	<0.0001	0.008	0.052	0.976	<0.0001
	VRT	<0.0001	1	<0.0001	<0.0001	<0.0001	0.829
	RIB	0.008	<0.0001	1	0.458	0.008	0.000
	PEL	0.052	<0.0001	0.458	1	0.049	<0.0001
	FEM	0.976	<0.0001	0.008	0.049	1	<0.0001
	TIB/FIB	<0.0001	0.829	0.000	<0.0001	<0.0001	1
TNO	p-values:						
		SKL	VRT	RIB	PEL	FEM	TIB/FIB
	SKL	1	<0.0001	0.017	<0.0001	<0.0001	<0.0001
	VRT	<0.0001	1	0.000	0.040	0.470	0.096
	RIB	0.017	0.000	1	<0.0001	<0.0001	0.059
	PEL	<0.0001	0.040	<0.0001	1	0.183	0.000
	FEM	<0.0001	0.470	<0.0001	0.183	1	0.017
	TIB/FIB	<0.0001	0.096	0.059	0.000	0.017	1

TRAM/ODMT	p-values:						
		SKL	VRT	RIB	PEL	FEM	TIB/FIB
	SKL	1	0.865	0.375	**0.008**	**<0.0001**	**0.019**
	VRT	0.865	1	0.470	**0.005**	**<0.0001**	**0.029**
	RIB	0.375	0.470	1	**0.000**	**<0.0001**	0.159
	PEL	**0.008**	**0.005**	**0.000**	1	**0.045**	**<0.0001**
	FEM	**<0.0001**	**<0.0001**	**<0.0001**	**0.045**	1	**<0.0001**
	TIB/FIB	**0.019**	**0.029**	0.159	**<0.0001**	**<0.0001**	1
TRAM/NDMT	p-values:						
		SKL	VRT	RIB	PEL	FEM	TIB/FIB
	SKL	1	**0.003**	**0.007**	**<0.0001**	**0.000**	**0.000**
	VRT	**0.003**	1	0.797	0.207	0.391	0.566
	RIB	**0.007**	0.797	1	0.136	0.274	0.414
	PEL	**<0.0001**	0.207	0.136	1	0.685	0.491
	FEM	**0.000**	0.391	0.274	0.685	1	0.777
	TIB/FIB	**0.000**	0.566	0.414	0.491	0.777	1
TRAM/NODMT	p-values:						
		SKL	VRT	RIB	PEL	FEM	TIB/FIB
	SKL	1	**0.014**	**0.003**	**0.031**	**0.000**	**0.000**
	VRT	**0.014**	1	0.554	**<0.0001**	**<0.0001**	0.256
	RIB	**0.003**	0.554	1	**<0.0001**	**<0.0001**	0.605
	PEL	**0.031**	**<0.0001**	**<0.0001**	1	0.136	**<0.0001**
	FEM	**0.000**	**<0.0001**	**<0.0001**	0.136	1	**<0.0001**
	TIB/FIB	**0.000**	0.256	0.605	**<0.0001**	**<0.0001**	1
TRAM/TNO	p-values:						
		SKL	VRT	RIB	PEL	FEM	TIB/FIB
	SKL	1	**0.028**	**0.016**	**<0.0001**	**<0.0001**	0.330
	VRT	**0.028**	1	0.787	**<0.0001**	**0.006**	0.220
	RIB	**0.016**	0.787	1	**0.000**	**0.016**	0.142
	PEL	**<0.0001**	**<0.0001**	**0.000**	1	0.200	**<0.0001**
	FEM	**<0.0001**	**0.006**	**0.016**	0.200	1	**<0.0001**
	TIB/FIB	0.330	0.220	0.142	**<0.0001**	**<0.0001**	1
ODMT/NDMT	p-values:						
		SKL	VRT	RIB	PEL	FEM	TIB/FIB
	SKL	1	**0.000**	**<0.0001**	0.197	0.181	**<0.0001**
	VRT	**0.000**	1	0.418	**0.010**	**<0.0001**	**0.014**
	RIB	**<0.0001**	0.418	1	**0.001**	**<0.0001**	0.113
	PEL	0.197	**0.010**	**0.001**	1	**0.009**	**<0.0001**
	FEM	0.181	**<0.0001**	**<0.0001**	**0.009**	1	**<0.0001**
	TIB/FIB	**<0.0001**	**0.014**	0.113	**<0.0001**	**<0.0001**	1

ODMT/NODMT	p-values:						
		SKL	VRT	RIB	PEL	FEM	TIB/FIB
	SKL	1	**<0.0001**	**<0.0001**	0.474	0.347	**0.000**
	VRT	**<0.0001**	1	0.473	**<0.0001**	**<0.0001**	0.219
	RIB	**<0.0001**	0.473	1	**<0.0001**	**<0.0001**	0.055
	PEL	0.474	**<0.0001**	**<0.0001**	1	0.822	**<0.0001**
	FEM	0.347	**<0.0001**	**<0.0001**	0.822	1	**<0.0001**
	TIB/FIB	**0.000**	0.219	0.055	**<0.0001**	**<0.0001**	1
ODMT/TNO	p-values:						
		SKL	VRT	RIB	PEL	FEM	TIB/FIB
	SKL	1	0.091	0.073	**<0.0001**	**<0.0001**	0.861
	VRT	0.091	1	0.885	**<0.0001**	**<0.0001**	0.063
	RIB	0.073	0.885	1	**<0.0001**	**<0.0001**	**0.050**
	PEL	**<0.0001**	**<0.0001**	**<0.0001**	1	0.908	**<0.0001**
	FEM	**<0.0001**	**<0.0001**	**<0.0001**	0.908	1	**<0.0001**
	TIB/FIB	0.861	0.063	**0.050**	**<0.0001**	**<0.0001**	1
NDMT/NODMT	p-values:						
		SKL	VRT	RIB	PEL	FEM	TIB/FIB
	SKL	1	**<0.0001**	**<0.0001**	0.936	0.087	**<0.0001**
	VRT	**<0.0001**	1	0.349	**<0.0001**	**<0.0001**	0.260
	RIB	**<0.0001**	0.349	1	**<0.0001**	**<0.0001**	0.871
	PEL	0.936	**<0.0001**	**<0.0001**	1	0.073	**<0.0001**
	FEM	0.087	**<0.0001**	**<0.0001**	0.073	1	**<0.0001**
	TIB/FIB	**<0.0001**	0.260	0.871	**<0.0001**	**<0.0001**	1
NDMT/TNO	p-values:						
		SKL	VRT	RIB	PEL	FEM	TIB/FIB
	SKL	1	**0.000**	**<0.0001**	**<0.0001**	**<0.0001**	**0.009**
	VRT	**0.000**	1	0.738	**<0.0001**	**0.005**	0.231
	RIB	**<0.0001**	0.738	1	**0.000**	**0.016**	0.133
	PEL	**<0.0001**	**<0.0001**	**0.000**	1	0.174	**<0.0001**
	FEM	**<0.0001**	**0.005**	**0.016**	0.174	1	**<0.0001**
	TIB/FIB	**0.009**	0.231	0.133	**<0.0001**	**<0.0001**	1
NODMT/TNO	p-values:						
		SKL	VRT	RIB	PEL	FEM	TIB/FIB
	SKL	1	0.829	0.968	**<0.0001**	**<0.0001**	0.280
	VRT	0.829	1	0.865	**<0.0001**	**<0.0001**	0.195
	RIB	0.968	0.865	1	**<0.0001**	**<0.0001**	0.274
	PEL	**<0.0001**	**<0.0001**	**<0.0001**	1	0.983	**<0.0001**
	FEM	**<0.0001**	**<0.0001**	**<0.0001**	0.983	1	**<0.0001**
	TIB/FIB	0.280	0.195	0.274	**<0.0001**	**<0.0001**	1

Critical *P* Values for Comparison of Skeletal Elements within REP H SURV Exposure Pattern

TRAM	p-values:						
		SKL	VRT	RIB	PEL	FEM	TIB/FIB
	SKL	1	0.086	0.953	0.064	**0.016**	**0.000**
	VRT	0.086	1	0.081	0.915	0.457	**0.034**
	RIB	0.953	0.081	1	0.060	**0.015**	**0.000**
	PEL	0.064	0.915	0.060	1	0.513	**0.040**
	FEM	**0.016**	0.457	**0.015**	0.513	1	0.184
	TIB/FIB	**0.000**	**0.034**	**0.000**	**0.040**	0.184	1
ODMT	p-values:						
		SKL	VRT	RIB	PEL	FEM	TIB/FIB
	SKL	1	**0.048**	0.887	0.366	0.155	**<0.0001**
	VRT	**0.048**	1	**0.037**	0.275	0.637	**0.015**
	RIB	0.887	**0.037**	1	0.303	0.125	**<0.0001**
	PEL	0.366	0.275	0.303	1	0.569	**0.000**
	FEM	0.155	0.637	0.125	0.569	1	**0.005**
	TIB/FIB	**<0.0001**	**0.015**	**<0.0001**	**0.000**	**0.005**	1
NDMT	p-values:						
		SKL	VRT	RIB	PEL	FEM	TIB/FIB
	SKL	1	**0.030**	0.994	0.147	**0.025**	**<0.0001**
	VRT	**0.030**	1	**0.033**	0.455	0.877	**0.025**
	RIB	0.994	**0.033**	1	0.157	**0.028**	**<0.0001**
	PEL	0.147	0.455	0.157	1	0.382	**0.003**
	FEM	**0.025**	0.877	**0.028**	0.382	1	**0.045**
	TIB/FIB	**<0.0001**	**0.025**	**<0.0001**	**0.003**	**0.045**	1
NODMT	p-values:						
		SKL	VRT	RIB	PEL	FEM	TIB/FIB
	SKL	1	**0.013**	0.475	0.550	0.340	**<0.0001**
	VRT	**0.013**	1	0.082	0.058	0.160	0.050
	RIB	0.475	0.082	1	0.899	0.792	**0.000**
	PEL	0.550	0.058	0.899	1	0.696	**0.000**
	FEM	0.340	0.160	0.792	0.696	1	**0.001**
	TIB/FIB	**<0.0001**	0.050	**0.000**	**0.000**	**0.001**	1
TNO	p-values:						
		SKL	VRT	RIB	PEL	FEM	TIB/FIB
	SKL	1	**0.040**	0.063	**<0.0001**	**0.005**	**0.007**
	VRT	**0.040**	1	0.849	0.059	0.409	0.467
	RIB	0.063	0.849	1	**0.037**	0.313	0.362
	PEL	**<0.0001**	0.059	**0.037**	1	0.329	0.282
	FEM	**0.005**	0.409	0.313	0.329	1	0.925
	TIB/FIB	**0.007**	0.467	0.362	0.282	0.925	1

TRAM/ODMT	p-values:						
		SKL	VRT	RIB	PEL	FEM	TIB/FIB
	SKL	1	0.847	0.640	0.090	0.066	0.232
	VRT	0.847	1	0.787	0.141	0.103	0.174
	RIB	0.640	0.787	1	0.231	0.170	0.106
	PEL	0.090	0.141	0.231	1	0.807	**0.005**
	FEM	0.066	0.103	0.170	0.807	1	**0.004**
	TIB/FIB	0.232	0.174	0.106	**0.005**	**0.004**	1
TRAM/NDMT	p-values:						
		SKL	VRT	RIB	PEL	FEM	TIB/FIB
	SKL	1	0.244	0.347	**0.038**	0.087	0.687
	VRT	0.244	1	0.824	**0.001**	**0.005**	0.134
	RIB	0.347	0.824	1	**0.003**	**0.010**	0.199
	PEL	**0.038**	**0.001**	**0.003**	1	0.811	0.121
	FEM	0.087	**0.005**	**0.010**	0.811	1	0.214
	TIB/FIB	0.687	0.134	0.199	0.121	0.214	1
TRAM/NODMT	p-values:						
		SKL	VRT	RIB	PEL	FEM	TIB/FIB
	SKL	1	0.106	0.277	0.656	**0.048**	**0.026**
	VRT	0.106	1	0.593	**0.044**	**0.001**	0.682
	RIB	0.277	0.593	1	0.134	**0.004**	0.317
	PEL	0.656	**0.044**	0.134	1	0.122	**0.008**
	FEM	**0.048**	**0.001**	**0.004**	0.122	1	**<0.0001**
	TIB/FIB	**0.026**	0.682	0.317	**0.008**	**<0.0001**	1
TRAM/TNO	p-values:						
		SKL	VRT	RIB	PEL	FEM	TIB/FIB
	SKL	1	0.264	**0.004**	**0.002**	0.129	0.970
	VRT	0.264	1	0.081	0.053	0.659	0.309
	RIB	**0.004**	0.081	1	0.874	0.216	**0.007**
	PEL	**0.002**	0.053	0.874	1	0.159	**0.004**
	FEM	0.129	0.659	0.216	0.159	1	0.160
	TIB/FIB	0.970	0.309	**0.007**	**0.004**	0.160	1
ODMT/NDMT	p-values:						
		SKL	VRT	RIB	PEL	FEM	TIB/FIB
	SKL	1	0.546	0.730	0.515	0.397	0.062
	VRT	0.546	1	0.800	0.214	0.160	0.206
	RIB	0.730	0.800	1	0.325	0.246	0.131
	PEL	0.515	0.214	0.325	1	0.816	**0.013**
	FEM	0.397	0.160	0.246	0.816	1	**0.010**
	TIB/FIB	0.062	0.206	0.131	**0.013**	**0.010**	1

ODMT/NODMT	p-values:						
		SKL	VRT	RIB	PEL	FEM	TIB/FIB
	SKL	1	**0.004**	**0.001**	0.133	0.123	0.420
	VRT	**0.004**	1	0.595	**<0.0001**	**<0.0001**	0.055
	RIB	**0.001**	0.595	1	**<0.0001**	**<0.0001**	**0.015**
	PEL	0.133	**<0.0001**	**<0.0001**	1	0.899	**0.026**
	FEM	0.123	**<0.0001**	**<0.0001**	0.899	1	**0.026**
	TIB/FIB	0.420	0.055	**0.015**	**0.026**	**0.026**	1
ODMT/TNO	p-values:						
		SKL	VRT	RIB	PEL	FEM	TIB/FIB
	SKL	1	0.541	0.107	**0.004**	0.066	0.590
	VRT	0.541	1	0.325	**0.026**	0.218	0.268
	RIB	0.107	0.325	1	0.223	0.775	**0.040**
	PEL	**0.004**	**0.026**	0.223	1	0.379	**0.001**
	FEM	0.066	0.218	0.775	0.379	1	**0.024**
	TIB/FIB	0.590	0.268	**0.040**	**0.001**	**0.024**	1
NDMT/NODMT	p-values:						
		SKL	VRT	RIB	PEL	FEM	TIB/FIB
	SKL	1	0.288	0.278	0.430	0.246	0.059
	VRT	0.288	1	0.981	0.066	**0.032**	0.394
	RIB	0.278	0.981	1	0.063	**0.030**	0.407
	PEL	0.430	0.066	0.063	1	0.678	**0.009**
	FEM	0.246	**0.032**	**0.030**	0.678	1	**0.004**
	TIB/FIB	0.059	0.394	0.407	**0.009**	**0.004**	1
NDMT/TNO	p-values:						
		SKL	VRT	RIB	PEL	FEM	TIB/FIB
	SKL	1	0.307	**0.005**	**0.000**	**0.032**	0.907
	VRT	0.307	1	0.084	**0.007**	0.253	0.395
	RIB	**0.005**	0.084	1	0.344	0.603	**0.012**
	PEL	**0.000**	**0.007**	0.344	1	0.151	**0.001**
	FEM	**0.032**	0.253	0.603	0.151	1	0.055
	TIB/FIB	0.907	0.395	**0.012**	**0.001**	0.055	1
NODMT/TNO	p-values:						
		SKL	VRT	RIB	PEL	FEM	TIB/FIB
	SKL	1	0.869	0.261	**0.005**	0.058	0.528
	VRT	0.869	1	0.345	**0.010**	0.087	0.438
	RIB	0.261	0.345	1	0.106	0.420	0.092
	PEL	**0.005**	**0.010**	0.106	1	0.464	**0.001**
	FEM	0.058	0.087	0.420	0.464	1	**0.016**
	TIB/FIB	0.528	0.438	0.092	**0.001**	**0.016**	1

Critical *P* Values for Comparison of Skeletal Elements within ACU L Exposure Pattern

TRAM	p-values:						
		SKL	VRT	RIB	PEL	FEM	TIB/FIB
	SKL	1	0.103	0.408	0.504	0.435	0.122
	VRT	0.103	1	**0.023**	0.303	**0.021**	0.834
	RIB	0.408	**0.023**	1	0.148	0.931	**0.024**
	PEL	0.504	0.303	0.148	1	0.151	0.371
	FEM	0.435	**0.021**	0.931	0.151	1	**0.023**
	TIB/FIB	0.122	0.834	**0.024**	0.371	**0.023**	1
ODMT	p-values:						
		SKL	VRT	RIB	PEL	FEM	TIB/FIB
	SKL	1	0.498	0.419	0.806	**0.029**	0.295
	VRT	0.498	1	0.171	0.370	**0.009**	0.783
	RIB	0.419	0.171	1	0.561	0.216	0.078
	PEL	0.806	0.370	0.561	1	0.052	0.198
	FEM	**0.029**	**0.009**	0.216	0.052	1	**0.002**
	TIB/FIB	0.295	0.783	0.078	0.198	**0.002**	1
NDMT	p-values:						
		SKL	VRT	RIB	PEL	FEM	TIB/FIB
	SKL	1	0.428	0.282	0.449	0.079	0.667
	VRT	0.428	1	0.085	0.142	**0.019**	0.696
	RIB	0.282	0.085	1	0.708	0.565	0.146
	PEL	0.449	0.142	0.708	1	0.310	0.241
	FEM	0.079	**0.019**	0.565	0.310	1	**0.032**
	TIB/FIB	0.667	0.696	0.146	0.241	**0.032**	1
NODMT	p-values:						
		SKL	VRT	RIB	PEL	FEM	TIB/FIB
	SKL	1	**0.031**	0.536	0.964	**0.039**	**0.019**
	VRT	**0.031**	1	0.142	**0.028**	**<0.0001**	0.989
	RIB	0.536	0.142	1	0.509	**0.012**	0.115
	PEL	0.964	**0.028**	0.509	1	**0.044**	**0.017**
	FEM	**0.039**	**<0.0001**	**0.012**	**0.044**	1	**<0.0001**
	TIB/FIB	**0.019**	0.989	0.115	**0.017**	**<0.0001**	1
TNO	p-values:						
		SKL	VRT	RIB	PEL	FEM	TIB/FIB
	SKL	1	0.063	0.400	0.080	0.144	**0.001**
	VRT	0.063	1	**0.012**	**0.001**	**0.002**	0.226
	RIB	0.400	**0.012**	1	0.437	0.595	**<0.0001**
	PEL	0.080	**0.001**	0.437	1	0.805	**<0.0001**
	FEM	0.144	**0.002**	0.595	0.805	1	**<0.0001**
	TIB/FIB	**0.001**	0.226	**<0.0001**	**<0.0001**	**<0.0001**	1

TRAM/ODMT	p-values:						
		SKL	VRT	RIB	PEL	FEM	TIB/FIB
	SKL	1	0.877	0.918	0.548	0.069	0.291
	VRT	0.877	1	0.811	0.489	0.074	0.426
	RIB	0.918	0.811	1	0.650	0.112	0.280
	PEL	0.548	0.489	0.650	1	0.218	0.100
	FEM	0.069	0.074	0.112	0.218	1	**0.005**
	TIB/FIB	0.291	0.426	0.280	0.100	**0.005**	1
TRAM/NDMT	p-values:						
		SKL	VRT	RIB	PEL	FEM	TIB/FIB
	SKL	1	0.449	0.821	0.242	0.151	0.792
	VRT	0.449	1	0.613	0.071	**0.042**	0.612
	RIB	0.821	0.613	1	0.190	0.120	0.982
	PEL	0.242	0.071	0.190	1	0.770	0.159
	FEM	0.151	**0.042**	0.120	0.770	1	0.096
	TIB/FIB	0.792	0.612	0.982	0.159	0.096	1
TRAM/NODMT	p-values:						
		SKL	VRT	RIB	PEL	FEM	TIB/FIB
	SKL	1	0.106	0.277	0.656	**0.048**	**0.026**
	VRT	0.106	1	0.593	**0.044**	**0.001**	0.682
	RIB	0.277	0.593	1	0.134	**0.004**	0.317
	PEL	0.656	**0.044**	0.134	1	0.122	**0.008**
	FEM	**0.048**	**0.001**	**0.004**	0.122	1	**<0.0001**
	TIB/FIB	**0.026**	0.682	0.317	**0.008**	**<0.0001**	1
TRAM/TNO	p-values:						
		SKL	VRT	RIB	PEL	FEM	TIB/FIB
	SKL	1	**0.025**	0.182	0.193	0.135	**0.000**
	VRT	**0.025**	1	**0.001**	**0.001**	**0.000**	0.350
	RIB	0.182	**0.001**	1	0.899	0.937	**<0.0001**
	PEL	0.193	**0.001**	0.899	1	0.827	**<0.0001**
	FEM	0.135	**0.000**	0.937	0.827	1	**<0.0001**
	TIB/FIB	**0.000**	0.350	**<0.0001**	**<0.0001**	**<0.0001**	1
ODMT/NDMT	p-values:						
		SKL	VRT	RIB	PEL	FEM	TIB/FIB
	SKL	1	0.534	0.768	0.585	0.061	**0.008**
	VRT	0.534	1	0.752	0.893	**0.022**	0.075
	RIB	0.768	0.752	1	0.834	**0.042**	**0.029**
	PEL	0.585	0.893	0.834	1	**0.016**	**0.033**
	FEM	0.061	**0.022**	**0.042**	**0.016**	1	**<0.0001**
	TIB/FIB	**0.008**	0.075	**0.029**	**0.033**	**<0.0001**	1

ODMT/NODMT	p-values:						
		SKL	VRT	RIB	PEL	FEM	TIB/FIB
	SKL	1	**<0.0001**	**0.000**	0.585	0.559	**0.003**
	VRT	**<0.0001**	1	0.709	**0.001**	**0.001**	0.229
	RIB	**0.000**	0.709	1	**0.002**	**0.002**	0.401
	PEL	0.585	**0.001**	**0.002**	1	0.960	**0.016**
	FEM	0.559	**0.001**	**0.002**	0.960	1	**0.021**
	TIB/FIB	**0.003**	0.229	0.401	**0.016**	**0.021**	1
ODMT/TNO	p-values:						
		SKL	VRT	RIB	PEL	FEM	TIB/FIB
	SKL	1	**0.031**	0.408	0.229	**0.040**	**0.002**
	VRT	**0.031**	1	**0.005**	**0.001**	**<0.0001**	0.481
	RIB	0.408	**0.005**	1	0.775	**0.273**	**0.000**
	PEL	0.229	**0.001**	0.775	1	0.379	**<0.0001**
	FEM	**0.040**	**<0.0001**	**0.273**	0.379	1	**<0.0001**
	TIB/FIB	**0.002**	0.481	**0.000**	**<0.0001**	**<0.0001**	1
NDMT/NODMT	p-values:						
		SKL	VRT	RIB	PEL	FEM	TIB/FIB
	SKL	1	**0.001**	**0.005**	0.306	0.154	**<0.0001**
	VRT	**0.001**	1	0.607	**0.019**	**<0.0001**	0.486
	RIB	**0.005**	0.607	1	**0.062**	**<0.0001**	0.202
	PEL	0.306	**0.019**	**0.062**	1	**0.015**	**0.001**
	FEM	0.154	**<0.0001**	**<0.0001**	**0.015**	1	**<0.0001**
	TIB/FIB	**<0.0001**	0.486	0.202	**0.001**	**<0.0001**	1
NDMT/TNO	p-values:						
		SKL	VRT	RIB	PEL	FEM	TIB/FIB
	SKL	1	**0.033**	0.288	0.119	**0.050**	**0.004**
	VRT	**0.033**	1	**0.003**	**0.000**	**0.000**	0.603
	RIB	0.288	**0.003**	1	0.703	0.436	**0.000**
	PEL	0.119	**0.000**	0.703	1	0.662	**<0.0001**
	FEM	**0.050**	**0.000**	0.436	0.662	1	**<0.0001**
	TIB/FIB	**0.004**	0.603	**0.000**	**<0.0001**	**<0.0001**	1
NODMT/TNO	p-values:						
		SKL	VRT	RIB	PEL	FEM	TIB/FIB
	SKL	1	**0.003**	0.826	0.404	0.045	**0.000**
	VRT	**0.003**	1	0.010	**0.000**	**<0.0001**	0.723
	RIB	0.826	0.010	1	**0.321**	**0.038**	**0.002**
	PEL	0.404	**0.000**	**0.321**	1	0.237	**<0.0001**
	FEM	0.045	**<0.0001**	**0.038**	0.237	1	**<0.0001**
	TIB/FIB	**0.000**	0.723	**0.002**	**<0.0001**	**<0.0001**	1

References

[1] Strømgaard, K., Krogsgaard-Larsen, P., Madsen, U. (2009). Textbook of Drug Design and Discovery, Fourth Edition, CRC Press.

[2] Hemmings, H.C., Egan, T.D. (2013). Pharmacology and Physiology for Anesthesia: Foundations and Clinical Application: Expert Consult – Onine and Print. Elsevier Health Sciences, p. 253.

[3] Narcotic Drugs Estimated World Requirements for 2008, Statistics for 2006. New York: United Nations Pubns. 2008 p. 77.

[4] Triggle, D.J. (2006). Morphine. New York: Chelsea House Publishers. p. 20-1.

[5] Drug Facts: Prescription Opioids. NIDA. June 2019.

[6] Miller, N.S., Dackis, C.A., Gold, M.S. (1987). The Relationship of Addiction, Tolerance, and Dependence to Alcohol and Drugs: A Neurochemical Approach. *J Subst Abuse Treat*, 197-207.

[7] Webster, L.R. (2017). Risk Factors for Opioid-Use Disorder and Overdose. *Anesthesia and Analgesia*, 1741-8.

[8] Bruneau, J., Ahamad, K., Goyer, M.E., Poulin, G., Selby, P., Fischer, B., Wild, T.C., Wood, E. (2018). Management of Opioid Use Disorders: A National Clinical Practice Guideline. *CMAJ*, 247-57.

[9] Scholl, L. Seth, P., Kariisa, M., Wilson, N., Baldwin, G. (2018). Drug and Opioid-Involved Deaths – United States, 2013-2017. *Morb Mortal Wkly Rep, 1419-27.*

[10] Hedegaard, H., Minino, A.M., Warner, M. (2020). Drug Overdose Deaths in the United States, 1999-2018. NCHS data brief no. 356. Hyattsville, MD: US Department of Health and Human Services, CDC, National Centre for Health Statistics.

[11] O'Donnell, J., Gladden, R.M., Goldberger, B.A., Mattson, C.L., Kariisa, M. (2020). Notes from the Field: Opioid-Involved Overdose Deaths with Fentanyl or Fentanyl Analogs Detected – United States, July 2016-December 2018. *Morb Mortal Wkly Rep*, 271-3.

[12] Abdesselam, K., Dann, M.J., Alwis, R., Laroche, J., Ileka-Priouzeau, S. (2018). At-a-glance – Opioid Surveillance: Monitoring and Responding to the Evolving Crisis. *Health Promot Chronic Dis Prev Can*, 312-316.

[13] National Science and Technology Council. (2016). Strengthening the Medicolegal-Death-Investigation System: improving data systems.

[14] Armenian, P., Vo, K., Barr-Walker, J,, Lynch, K. (2017) Fentanyl, Fentanyl Analogues and Novel Synthetic Opioids: A Comprehensive Review. *UCSF*.

[15] Drug Enforcement Agency (DEA). Counterfeit Prescription Pills Containing Fentanyls: a Global Threat (2016).

[16] Stogner, J.M. (2014). The Potential Threat of Acetyl Fentanyl: Legal Issues, Contaminated Heroin, and Acetyl Fentanyl 'Disguised' as other Opioids. *Ann Emerg Med*, 637-9.

[17] Ruangyuttikarn, W., Law, M.Y., Rollins, D.E., Moody, D.E. (1990). Detection of fentanyl and its analogues by enzyme-linked immunosorbent assay. *J Anal Tox*, 160-4.

[18] Salomone, A., Palamar, J.J., Bigiarini, R,. Gerace, E., Di Corcia, D., Vincenti, M. (2019). Detection of Fentanyl Analogues and Synthetic Opioids in Real Hair Samples. *J Anal Tox*, 259-65.

[19] Mallama, C.A., Trinidad, J.P., Swain, R.S., Zhao, Y., Woods, C., McAnich, J.K. (2019). A Comparison of Opioid-Involved Fatalities Captured in the National Poison Data System to Data Derived from US Death Certificate Literal Text. *Pharamacoepidemiology and Drug Safety*, 1377-85.

[20] Hawton, K., Ferrey, A., Casey, D., Wells, C., Fuller, A., Bankhead, C., Clements, C., Ness, J., Gunnell, D., Kapur, N., Geulayov, G. (2019). Relative toxicity of Analgesics Commonly Used for Intentional Self-Poisoning: A Study of Case Fatality Based on Fatal and Non-Fatal Overdoses. *J Affective Disorders*, 814-9.

[21] Souza, M.J., Cox, S.K. (2011). Tramadol Use in Zoologic Medicine. *Vet Clin North Am Exot Anim Pract*, 117-30.

[22] Schenck, E.G., Arend, A. (1978). The Effect of Tramadol in an Open Clinical Trial. *Arzneimittelforschung,* 209-12.

[23] Lintz, W., Barth, H., Becker, R., Frankus, E., Schmidt-Bothelt, E. (1998). Pharmacokinetics of Tramadol and Bioavailability of Enteral Tramadol Formulations. 2nd communication: Drops with Ethanol. *Arzneimittelforschung*, 436-45.

[24] Lintz, W., Barth, H., Osterloh, G., Schmidt-Bothelt, E. (1986). Bioavailability of Enteral Tramadol Formulation. 1st communication: Capsules. *Arzneimittel Forschung, 1278-83.*

[25] Raffa, R.B., Nayak, R.K., Liao, S., Minn, F.L. (1995). The Mechanism of Action and Pharmacokinetics of Tramadol Hydrochloride. *Rev Contemp Pharmacother*, 485-97.

[26] Lee, C.R., McTavish, D., Sorkin, E.M. (1993). Tramadol: a Preliminary Review of its Pharmacodynamic and Pharmacokinetic Properties, and Therapeutic Potential in Acute and Chronic Pain States. *Drugs,* 313-40.

[27] Bamigbade, T.A., Langford, R.M. (1998). The Clinical Use of Tramadol Hydrochloride. *Pain Rev*, 155-82.

[28] Tao, Q., Stone, D.J., Borenstein, M.R., Codd, E.E., Coogan, T.P., Desai-Krieger, D., Liao, S., Raffa, R.B. (2002). Differential Tramadol and O-desmethyl Metabolite Levels in Brain vs Plasma of Mice and Rats Administered Tramadol Hydrochloride Orally. *J Clin Pharm Ther,* 99-106.

[29] Liao, S., Hill, J.F., Nayak, R.K. (1992). Pharmacokinetics of Tramadol Following Single and Multiple Oral Doses in Man. *Pharm Res*, 308.

[30] Lintz, W., Erlacin, S., Frankus, E., Uragg, H. (1981). Biotransformation of Tramadol in Man and Animal. *Arzneimittelforschung,* 1932-43.

[31] Raffa, R.B., Haslego, M.L., Maryanoff, C.A., Villani, F.J., Codd, E.E., Connelly, C.D., Martinez, R.P., Schupsky, J.J., Buben, J.A., Wu, W.N., Takacs, A.N., Mckown, L.A. (1996). Unexpected Antinociceptive Effect of the N-oxide of Tramadol Hydrochloride. *J Pharmacol Exp Ther,* 1098-104.

[32] Paar, W.D., Frankus, P., Dengler, H.J. (1992). The Metabolism of Tramadol by Human Liver Microsomes. *Clin Invest*, 708-10.

[33] Subrahmanyam, V., Renwick, A.B., Walters, D.G., Young, P.J., Price, R.J., Tonelli, A.P., Lake, B.G. (2001). Identification of Cytochrome P450 Isoforms Responsible for cis-Tramadol Metabolism in Human Liver Microsomes. *Drug Metab Dispos*, 1146-55.

[34] Lavasani, H., Sheikholelami, B., Ardakani, Y.H., Abdollahi, M., Hakemi, L., Rouini, M.R. (2013). Study of the Pharmacokinetic Changes of Tramadol in Diabetic Rats. *Daru*, 1-13.

[35] Grond, S., Sablotzki, A. (2004). Clinical Pharmacology of Tramadol. *Clin Pharmacokinet*, 879-923.

[36] Frink, M.C., Hennies, H.H., Englberger, W., Haurand, M., Wilffert, B. (1996). Influence of Tramadol on Neurotransmitter Systems of the Rat Brain. *Arzneimittelforschung*, 1029-36.

[37] Raffa, R.B., Friderichs, E., Reimann, W., Shank, R.P., Codd, E.E., Vaught, J.L. (1992). Opioid and Nonopioid Components Independently Contribute to the Mechanism of Action of Tramadol, an "Atypical" Opioid Analgesic. *J Pharmacol Exp Ther,* 275-85.

[38] Driessen, B., Reimann, W. (1992). Interaction of the Central Analgesic, Tramadol, with the Uptake and Release of 5-hydroxy-tryptamine in the Rat Brain *in vitro*. *Br J Pharmacol*, 147-51.

[39] Halfpenny, D.M., Callado, L.F., Hopwood, S.E., Bamigbade, T.A., Langford, R.M., Stamford, J.A. (1999). Effects of Tramadol Stereoisomers on Norepinephrine Efflux and Uptake in the Rat Locus Coeruleus Measured by Real Time Voltammetry. *Br J Anaesth*, 909-15.

[40] Raffa, R.B., Friderichs, E. (1996). The Basic Science Aspect of Tramadol Hydrochloride. *Pain Rev*, 249-71.

[41] Grond, S., Meuser, T., Zech, D., Hennig, U., Lehmann, K.A. (1995). Analgesic Efficacy and Safety of Tramadol Enantiomers in Comparison with the Racemate: a Randomised, Double-Blind study with Gynaecological Patients using Intravenous Patient-Controlled Analgesia. *Anaesthesist,* 387-94.

[42] Collart, L., Luthy, C., Favario-Constantin, C., Dayer, P. (1993). Duality of the Analgesic Effect of Tramadol in Humans, *Schweiz Med Wochenschr*, 2241-3.

[43] Goeringer, K.E., Logan, B.K., Christian, G.D. (1997). Identification of Tramadol and its Metabolites in Blood from Drug-Related Deaths and Drug-Impaired drivers. *J Anal Toxicol,* 529-37.

[44] Watterson, J. (2006). Challenges in Forensic Toxicology of Skeletonized Human Remains. *Analyst*, 961-5.

[45] Caplan, Y.H., Levine, B. (1990). Vitreous Humour in the Evaluation of Postmortem Blood Ethanol Concentrations. *J Anal Toxicol*, 305-7.

[46] Wyman, J., Bultman, S. (2004). Postmortem Distribution of Heroin Metabolites in Femoral Blood, Liver, Cerebrospinal Fluid, and Vitreous Humour. *J Anal Toxicol*, 260-3.

[47] Sims, D.N., Lokan, R.J., James, R.A., Felgate, P.D., Gardiner, J., Vozzo, D.C. (1999). Putrefactive Pleural Effusions as an Alternative Sample for Drug Quantification. *Am J Forensic Med Pathol*, 343-6.

[48] McIntyre, L.M., King, C.V., Boratto, M., Drummer, O.H. (2000). Post-mortem Drug Analyses in Bone and Bone Marrow. *Ther Drug Monit*, 79-83.

[49] Noguchi, T.T., Nakamura, G.R., Griesemer, E.C. (1978). Drug Analyses of Skeletonizing Remains. *J Forensic Sci*, 490-2.

[50] Majda, A., Mrochem, K., Wietecha-Posluzsky, R., Zapotoczny, S., Zawadzki, M. (2020). Fast and Efficient Analyses of the Postmortem Human Blood and Bone Marrow using DI-SPME/LC-TOFMS Method for Forensic Medicine Purposes. *Talanta*, 209*, 120533.*

[51] Raikos, N., Tsoukali, H., Njau, S.N. (2001). Determination of Opiates in Postmortem Bone and Bone Marrow. *Forensic Sci Int*, 140-1.

[52] Horak, E.L., Jenkins, A.J. (2005). Postmortem Tissue Distribution of Olanzapine and Citalopram in a Drug Intoxication. *J Forensic Sci*, 679-81.

[53] Kudo, K., Sugie, H., Syoui, N., Kurihara, K., Jitsufuchi, N., Imamura, T., Ikeda, N. (1997). Detection of Triazolam in Skeletal Remains Buried for 4 years. *Int J Legal Med*, 281-3.

[54] Gorczynski, L.Y., Melbye, F.J. (2001). Detection of Benzodiazepines in Different Tissues, Including Bone, Using a Quantitative ELISA Assay. *J Forensic Sci*, 916-8.

[55] Guillot, E., de Mazancourt, P., Durigon, M., Alvarez, J.C. (2007). Morphine and 6-acetylmorphine Concentrations in Blood, Brain, Spinal Cord, Bone Marrow and Bone after Lethal Acute or Chronic Diacetylmorphine Administration to Mice. *Forensic Sci Int*, 139-44.

[56] Kojima, T., Okamoto, I., Miyazaki, T., Chikasue, F., Yashiki, M., Nakamura, K. (1986). Detection of Methamphetamine and Amphetamine in a Skeletonized Body Buried for 5 Years. *Forensic Sci Int*, 93-102.

[57] Winek, C.L., Costantino, A.G., Wahba, W.W., Collom, W.D. (1985). Blood versus Bone Marrow Pentobarbital Concentrations. *Forensic Sci Int*, 15-24.

[58] Benko, A. (1985). Toxicological Analysis of Amobarbital and Glutethimide from Bone Tissue. *J Forensic Sci*, 708-14.

[59] Winek, C.L., Matejczyk, R.J., Buddie, E.G. (1983). Blood, Bone Marrow and Eye Fluid Ethanol Concentrations in Putrefied Rabbits. *Forensic Sci Int*, 151-9.

[60] Winek, C.L., Morris, E.M., Wahba, W.W. (1993). The Use of Bone Marrow in the Study of Postmortem Redistribution of Nortriptyline. *J Anal Toxicol*, 93-8.

[61] Watterson, J.H., VandenBoer, T.C. (2008). Effects of Tissue Type and the Dose-Death Interval on the Detetion of Acute Ketamine Exposure in Bone and Marrow with Solid-Phase Extraction and ELISA with Liquid Chromatography – Tandem Mass Spectrometry Confirmation. *J Anal Toxicol*, 631-8.

[62] Cornthwaite, H.M., McDonald, C.S., Watterson, J.H. (2019). Analysis of Dextromethorphan and Three Metabolites in Decomposed Skeletal Tissues by UPLC-QTOF-MS: Comparison of Acute and Repeated Drug Exposures. *J Anal Toxicol*, 726-33.

[63] Desrosiers, N.A., Watterson, J.H., Dean, D., Wyman, J.F. (2012). Detection of Amitriptyline, Citalopram, and Metabolites in Porcine Bones Following Extended Outdoor Decomposition. *J Forensic Sci,* 544-9.

[64] Orfanidis, A., Gika, H., Mastrogianni, O., Krokos, A., Theodoridis, G., Zaggelidou, E., Raikos, N. (2018). Determination of Drugs of Abuse and Pharmaceuticals in Skeletal Tissue by UHPLC-MS/MS. *For Sci Int*, 137-45.

[65] Srikanth, C.H., Joshi, P., Bikkasani, A.K., Porwal, K., Gayen, J.R. (2014). Bone Distribution Study of Anti-Leprotic Drug Clofamizine in Rat Bone Marrow Cells by a Sensitive Reverse Phase Liquid Chromatography Method. *J Chromatogr B Analyt Technol Biomed Life Sci*, 82-6.

[66] Delabarde, T., Keyser, C., Tracqui, A., Charabidze, D., Ludes, B. (2013). The Potential of Forensic Analysis on Human Bones Found in Riverine Environment. *For Sci Int*, e1-e5.

[67] Vandenbosch, M., Somers, T., Cuypers, E. (2018). Distribution of Methadone and Metabolites in Skeletal Tissues. *J Anal Toxicol*, 400-8.

[68] Wiart, J. Hakim, F., Andry, A., Eiden, C., Drevin, G., Lelievre, B., Rouge-Maillart, C., Decourcelle, M., Lemaire-Hurtel, A., Allorge, D., Gaulier, J. (2020). Pitfalls of Toxicological Investigations in Hair, Bones, and Nails in Extensively Decomposed Bodies: Illustration with Two Cases. *Int J Leg Med*.

[69] Engvall, E. (1972). Enzyme-Linked Immunosorbent Assay, ELISA. *J Immunology*, 129-35.

[70] Levine, B. Principles of Forensic Toxicology. Washington, DC: American Association for Clinical Chemistry Press. 2013.

[71] Dewar, R.A., McWilliam, I.G. (1958). Flame Ionization Detector for Gas Chromatography. *Nature*, 760.

[72] Ho, CS; Chan, M.H.M., Cheung, R.C.K., Law, L.K., Lit, L.C.W., Ng, K.F., Suen, M.W.M., Tai, H.L. (2003). Electrospray Ionization Mass Spectrometry: Principles and Clinical Applications. *Clin Biochem Rev*., 3-12.

[73] Wu, A.H., Gerona, R., Armenian, P., French, D., Petrie, M., Lynch, K.L. (2012). Role of Liquid Chromatography-High-Resolution Mass Spectrometry (LC-HR/MS) in Clinical Toxicology. *Clin Toxicol*, 733-42.

[74] Polettini, A., Gottardo, R., Pascali, J.P., Tagliaro, F. (2008). Implementation and Performance Evaluation of a Database of Chemical Formulas for the Screening of Pharmaco/Toxicologically Relevant Compounds in Biological Samples using Electrospray Ionization-Time-of-Flight Mass Spectrometry. *Anal Chem*, 3050-57.

[75] Ferrer, I., Thurman, E.M. (2003). Liquid Chromatography/Time-of-Flight/Mass Spectrometry (LC/TOF/MS) for the Analysis of Emerging Contaminants. *Trends Anal Chem*, 750-6.

[76] Gosselin, M., Fernandez, M.R., Wille, S.R., Samya, N., de Boeck, G., Bourel, B. (2010). Quantification of Methadone and its Metabolite 2-ethylidene-1,5-dimethyl-3,3-dephenylpyrolidine in Third Instar Larvae of *lucilia sericata* (Diptera: Calliphoridae) using Liquid Chromatography-Tandem Mass Spectrometry. *J Anal Toxicol*, 1-7.

[77] Cornthwaite, H.M., Watterson, J.H. (2014). The Influence of Body Position and Microclimate on Ketamine and Metabolite Distribution in Decomposed Skeletal Remains. *J Anal Tox*, 548-54.

[78] Watterson, J.H., Desrosiers, N.A., Betit, C.C., Dean, D. Wyman, J.F. (2010). Relative Distribution of Drugs in Decomposed Skeletal Tissue. *J Anal Toxicol*, 510-5.

[79] Unger, K.A., Watterson, J.H. (2016). Analysis of Dextromethorphan and Dextrorphan in Skeletal Remains Following Decomposition in Different Microclimate Conditions. *J Anal Toxicol*,

[80] Watterson, J.H., Desrosiers, N.A. (2011). Examination of the Effect of Dose-Death Interval Detection of Meperidine Exposure in Decomposed Skeletal Tissues Using Microwave-Assisted Extraction. *For Sci Int*, 40-5.

[81] Watterson, J.H., Donohue, J.P., Betit, C.C. (2012). Comparison of Relative Dstribution of Ketamine and Norketamine in Decomposed Skeletal Tissues Following Single and Repeated Exposures. *J Anal Toxicol*, 429-33.

[82] Watterson, J.H., Botman, J.E. (2009). Detection of Acute Diazepam Exposure in Bone and Marrow: Influence of Tissue Type and the Dose-Death Interval on Sensitivity of Detection by ELISA with Liquid Chromatography Tandem Mass Spectrometry Confirmation. *J For Sci*, 708-14.

[83] Lafrenière, N.M., Watterson, J.H. (2009). Detection of Acute Fentanyl Exposure in Fresh and Decomposed Skeletal tissues. *For Sci Int*, 100-6.

[84] Imfeld, A.B., Watterson, J.H. (2016). Influence of Dose-Death Interval on Colchicine and Metabolite Distribution in Decomposed Skeletal Tissues. *Int J Leg Med*, 371-9.

[85] Wiebe, T.R., Watterson, J.H. (2014). Analysis of Tramadol and O-desmethyltramadol in Decomposed Skeletal Tissues Following Acute and Repeated Tramadol Exposure by Gas Chromatography Mass Spectrometry. *For Sci Int*, 261-5.

[86] Scientific Working Group for Forensic Toxicology (SWGTOX) Standard Practices for Method Validation in Forensic Toxicology (2013). *J Anal Toxicol*, 452-74.

[87] Cornthwaite, H.M., Labine, L., Watterson, J.H. (2018). Semi-Quantitative Analysis of Tramadol, Dextromethorphan, and Metabolites in Decomposed Skeletal Tissues by Ultra-Performance Liquid Chromatography Quadrupole Time of Flight Mass Spectrometry. *Drug Test Anal*, 961-7.

[88] ANSI/ASB Standard 036, Standard Practices for Method Validation in Forensic Toxicology, First Edition, 2019.

[89] Parasrampuria, R., Vuppugalla, R., Elliott, K., Mehvar, R. (2007). Route-Dependent Stereoselective Pharmacokinetics of Tramadol and its Active O-demethylated Metabolite in Rats. *Chirality*, 190-6.